REPUBLIC OF TURKEY

YILDIZ TECHNICAL UNIVERSITY

GRADUATE SCHOOL OF NATURAL AND APPLIED SCIENCES

DEFINITION AND VALIDATION OF AN ELASTOMER USING FINITE ELEMENT HYPERELASTIC MODELS

Faisal AHMED

MSc. THESIS

Department of Civil Engineering

Civil Engineering (English) Program

Supervisor

Assist. Prof. Fatih ALEMDAR

December, 2021

REPUBLIC OF TURKEY

YILDIZ TECHNICAL UNIVERSITY

GRADUATE SCHOOL OF NATURAL AND APPLIED SCIENCES

DEFINITION AND VALIDATION OF AN ELASTOMER USING FINITE ELEMENT HYPERELASTIC MODELS

A thesis submitted by Faisal AHMED in partial fulfillment of the requirements for the degree of MASTER OF SCIENCE is approved by the committee on 27.12.2021 in Department of Civil Engineering, Civil Engineering (English) Program.

Assist. Prof. Fatih ALEMDAR

Yıldız Technical University

Supervisor

Approved By the Examining Committee

Assist. Prof. Fatih ALEMDAR, Supervisor
Yıldız Technical University _____

Assoc. Prof. Murat Serdar KIRÇIL, Member
Yıldız Technical University _____

Assoc. Prof. Hasan ÖZKAYNAK, Member
Beykent University _____

I hereby declare that I have obtained the required legal permissions during data collection and exploitation procedures, that I have made the in-text citations and cited the references properly, that I haven't falsified and/or fabricated research data and results of the study and that I have abided by the principles of the scientific research and ethics during my Thesis Study under the title of Location Analysis of The Emergency Service Centers Of a Case Company supervised by my supervisor, Assist. Prof. Dr. Fatih ALEMDAR. In the case of a discovery of false statement, I am to acknowledge any legal consequence.

Faisal AHMED

Signature

Dedicated to my parents, my siblings

and my best friends

ACKNOWLEDGEMENTS

I would like to express my gratitude and appreciation for my supervisor Dr. Fatih ALEMDAR whose guidance, support, and encouragement have been invaluable throughout this study. I have benefited greatly from your wealth of knowledge and meticulous editing. And my biggest thanks to my family for all the support you have shown me through this research, the culmination of three years of learning. With many thanks to my sister Dr. Safiya Ahmed for her guidance throughout this study. Finally, I wish to thank Arsan Kauçuk company who supported us with the essential material for this project.

Faisal AHMED

TABLE OF CONTENTS

LIST OF SYMBOLS

υ	Poisons Ratio
U	Strain Energy Per Unit Volume
Δ	Change
M	The Initial Shear Modulus
N	A Material Parameter
$\bar{I}_i$	The Deviatoric Strain Invariants

LIST OF ABBREVIATIONS

FE	Finite Element
SEF	Strain Energy Function
SPEF	Strain Potential Energy Function
GHG	Greenhouse Gas
CIA	Computer Aid Analysis

LIST OF FIGURES

LIST OF TABLES

ABSTRACT

Definition and Validation of Hyperelastic Material Using Finite Element Hyperelastic Models

Faisal AHMED

Department of Civil Engineering

MSc. Thesis

Supervisor: Assist. Prof. Fatih ALEMDAR

Elastomers are a commonly used material in various industries, constructions are one of the industries that use elastomers in different structural elements. Physical tests on hyperelastic elements generally required time and special types of equipment, therefore it will be more practical to create digital models for this type of element. To study these elements' behavior under different loads, a correct strain potential energy function (SPEF) should be selected to predict the nonlinear hyperelastic behavior accurately.

This research aims to define and select the most accurate hyperelastic model for rubber elastomer used in an elastomeric bearing sample, which is originally used on structure foundation to resist seismic horizontal forces. The required experiments to define hyperelastic models were performed, Finite element software was used to evaluate strain energy function for different hyperelastic models. Comparisons were made

between six hyperelastic models to find the best model that can fit this type of rubber. Curve fitting method was used to select the accurate model. Multiple models gave an accurate prediction of this element behavior.

Two physical validation tests (Double Shear) were also performed on elastomeric double shear specimens to check the validity of simulation prediction under these different behaviors. Polynomial and Ogden models were selected to simulate and validate the double shear test since both had the best curve fit with the experimental result. Polynomial form was the best choice to model double shear test and the finite element simulation showed an accurate prediction for specimen behavior in terms of curve fitting and error percentage.

Keywords: Elastomer, bearing, finite element, hyperelastic, polynomial, seismic isolators, civil engineering

ÖZET

Sonlu Eleman Hiperelastik Modeller Kullanılarak Elastomerin Tanımlanması ve Doğrulanması

Faisal AHMED

İnşaat Mühendisliği Anabilim Dalı

Yüksek Lisans Tezi

Danışman: Dr. Öğretim Üyesi Fatih ALEMDAR

Elastomerler, çeşitli endüstrilerde yaygın olarak kullanılan bir malzeme olup inşaat, elastomerleri farklı yapı elemanlarında kullanan endüstrilerden biridir. Hiperelastik elemanlar üzerinde yapılan fiziksel testler genellikle zaman ve özel ekipman gerektirir, bu nedenle bu tip elemanlar için sonlu eleman modeller oluşturmak daha pratik olacaktır. Bu elemanların farklı yükler altındaki davranışlarını incelemek için, doğrusal olmayan hiperelastik davranışı doğru bir şekilde tahmin etmek için doğru bir gerinim potansiyel enerji fonksiyonu (SPEF) seçilmelidir.

Bu araştırma, sismik yatay kuvvetlere direnmek için orijinal olarak yapı temelinde kullanılan elastomerik yatak numunesinde kullanılan kauçuk elastomer için en doğru hiperelastik modeli tanımlamayı ve seçmeyi amaçlamaktadır. Hiperelastik modelleri tanımlamak için gerekli olan deneyler yapıldı ve farklı hiperelastik modeller için gerinim enerjisi fonksiyonunu değerlendirmek için Sonlu elemanlar

yazılımı kullanıldı. Bu tip kauçuğa uyan en iyi modeli bulmak için altı farklı hiperelastik model arasında karşılaştırmalar yapılmıştır. Doğru modeli seçmek için eğri uydurma yöntemi kullanıldı. Birden fazla modelle bu öğe davranışının doğru bir tahminini verdi.

Bu farklı davranışlar altında simülasyon tahmininin geçerliliğini kontrol etmek için elastomerik çift tesirli kesme numuneleri üzerinde iki fiziksel doğrulama testi (Çift tesirli kesme) de gerçekleştirilmiştir. Her ikisi de deneysel sonuçla en iyi eğri uyumuna sahip olduğundan, çift tesirli kesme testini simüle etmek ve doğrulamak için polinom ve Ogden modelleri seçilmiştir. Polinom formu, çift tesirli kesme testi modellemek için en doğru seçim olup ve sonlu eleman simülasyonu, eğri uydurma ve hata yüzdesi açısından numune davranışını en doğru tahmin ettiği görülmüştür.

Anahtar Kelimeler: Elastomer, mesnet, sonlu eleman, hiperelastik, polinom, sismik izolatörler, inşaat mühendisliğ

1
INTRODUCTION

A hyperelastic material "is a type of inherent model for ideally elastic material for which the stress-strain relationship derives from a strain energy density function." [1]. Elastomers are an ideal example of a hyperelastic material. An elastomer is a polymer with viscoelasticity (i.e., both viscosity and elasticity) and has very weak intermolecular forces (Intermolecular forces (or secondary forces) are the forces which mediate interaction between atoms), generally low Young's modulus E (mechanical property that measures the tensile stiffness of a solid material) and high failure strain compared with other materials. The behavior of unfilled, vulcanized elastomers often conforms closely to the hyperelastic ideal. [2]. Elastomers can experience at least 300% elongation of their original length and get back their initial shape after the load is removed. It can go more than 600% of its initial length. Extendibility can reach approximately 800 to 1,000% elongation at breaking point compared to a few percent for metal [3].

Stress-Strain behavior of hyperelastic material is highly non-linear, and a simple modulus of elasticity is no longer sufficient. Therefore, it's crucial to characterize this material to understand behavior.

1.1 History of Using Hyperelastic Materials

The original material in this family is natural rubber. It has entered the field of study at the end of the 18^{th} century. Its use started to increase during the 19^{th} century, mainly due to the development of the rubber hardening technique (vulcanization). This material in civil engineering applications was limited for many reasons, including high gas penetrability, positively affected by oils and solvents, and sensitivity to age growing. Therefore, it was necessary to be treated with additives, making it little interest in this area. The development of manufactured elastomers began around the middle of the 20^{th} century. The previous weakness points and difficulty in meeting market

requirements due to geopolitical factors made the development of manufactured elastomers that reached real success in the late 50s. After the development of synthetic elastomers. After this time, researchers helped to create a perfect polymer related to this family, classified depending on their use (e.g., heat resistance, aging, and elastic properties). The enhanced properties of synthetic elastomers and keeping natural rubber's interesting features allowed it to add good usage in the civil engineering field [3].

As mentioned before rubber's main feature is the unusual elasticity that allows it to have two different behaviors, the stability of solids and the high deformability of liquids. These features allow it to stretch several times from its original length. Without getting any damage. Therefore, rubber can be determined as a bridge between solid and liquid states.

Today we have a vast collection of elastomers due to additives included in the rubber mixture during production, which results in this collection of different materials with wide domain properties.

1.2 Examples for Elastomers

The ingredients used in manufacturing elastomers were used to create several types of rubbers. The main types of elastomers are listed as follow:

The ingredients that were previously mentioned were used to create several types of rubbers. There are two main types of elastomers which are unsaturated rubber and saturated rubber. Each type includes several kinds as follow:

1.2.1 Unsaturated Rubbers

- Natural polyisoprene (natural rubber NR)
- Synthetic polyisoprene
- Polybutadiene
- Chloroprene rubber (CR), polychloroprene, Neoprene, Baypren etc.
- Butyl rubber
- Styrene-butadiene rubber

- Nitrile rubber

1.2.2 Saturated Rubbers

- EPM Ethylene Propylene Rubber,
- Epichlorohydrin rubber
- Polyacrylic rubber
- Silicone rubber
- Fluoro silicone rubber
- Fluoro elastomers; Viton, Tecnoflon, Fluorel, Aflas and Dai-El
- Perfluoro elastomers; Tecnoflon PFR, Kalrez, Chemraz, Perlast
- Polyether block amides
- Chlorosulfonated polyethylene
- Ethylene-vinyl acetate

1.3 Elastomers in Civil Engineering

Elastomers have plenty of uses in different industries, even in civil engineering, the use of rubber is not limited. Here are the most comment uses for this material listed below.

1.3.1 Elastomeric Bearings

Bearing is an element that translates stresses between structure elements while allowing an absolute degree of freedom. A bridge bearing is usually the element that connects the deck and supports. Bearings are also used for horizontal energy absorption in structure foundations to reduce seismic force in areas that have strong earthquakes. Also, it can be used to reduce the impact of collision between the neighboring structures [4].

Bearings are elastomeric material reinforced with steel layers, the rubber has thick layers and is bonded with thin steel layers Figure 1.1 below shows the design of bearings. The distribution and thickness depend on this element's use. These layers have the ability to absorb lateral force, rotation flexibility as shown in Figure 1.1 below.

Figure 1.1 An elastomeric bearing

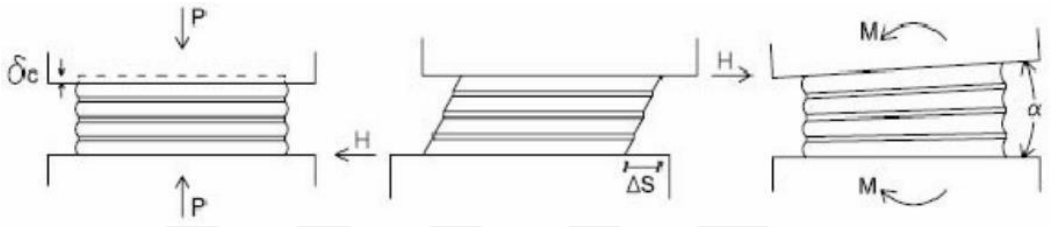

Figure 1.2 Elastomeric bearing under different loading conditions

Elastomer's viscosity depends on the type of material and use, therefore there are high and low damping elements. Low damping bearing has a smother displacement curve which makes it closer to linear force-displacement behavior.

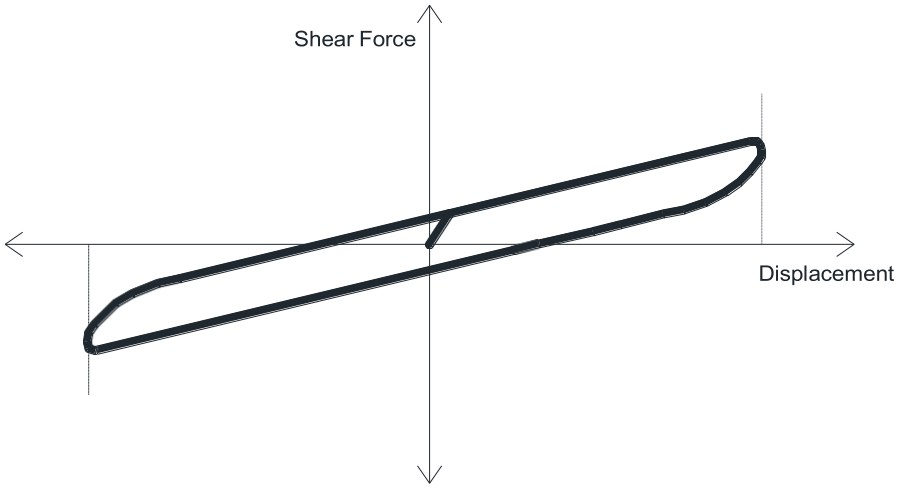

Figure 1.3 Load damping elastomeric bearings stress-strain

However, high damping bearings have a much more superior damping factor and the nonlinear behavior will increase.

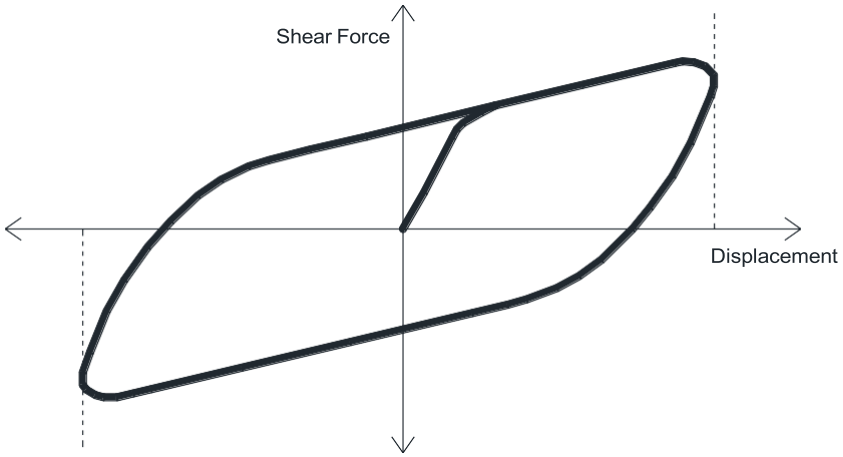

Figure 1.4 High Damping elastomeric bearing stress-strain

In this research, rubber material and bearing samples were cut from an elastomeric bearing to define and validate all hyperelastic models.

1.3.2 Expansion Joints

Expansion joints devices must be installed at the connection parts of two structure parts as changes in the length due to expansion of the whole structure. These joints allow specific movement of elements on each side of these structural elements. In bridges, expansion joints can be installed at each end of bridge girders or parts. It can allow dilatation and movement of parts freely, resist traffic, give road surface continuity, keep low noise or vibration, and ensure standing against water.

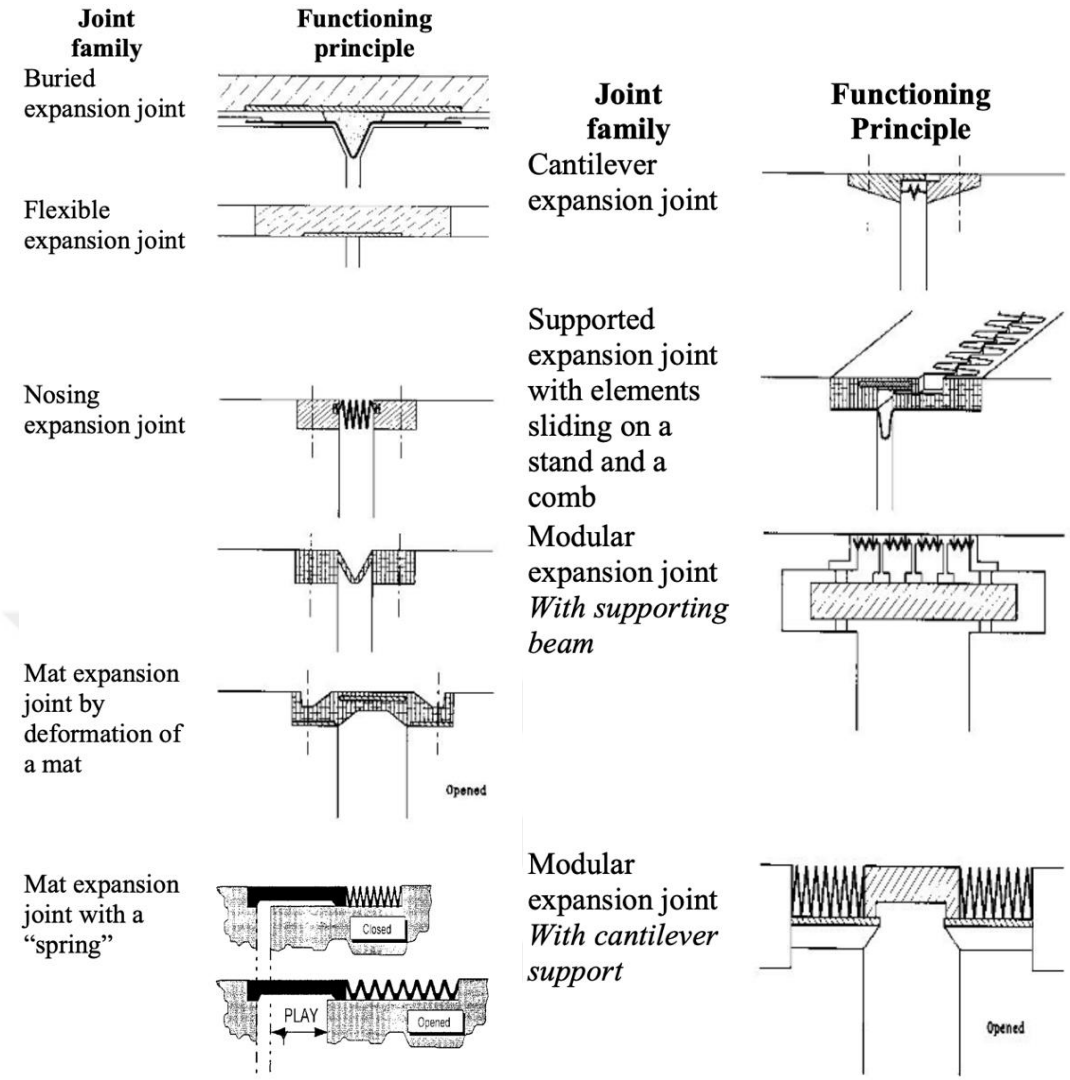

Figure 1.5 Several types of expansion joints

1.3.3 Sealing Joints

Sealing joints are used to reduce surface water and insoluble materials into a joint system between two parts of a structure. It can save dowel bars from corrosion by reducing the penetration of de-icing chemicals. Sealing joints can be found between concrete elements, drainage pipes, gutter cornice, or even retaining walls that are generally underwater table level. The figure below explains how sealing joints are used inside

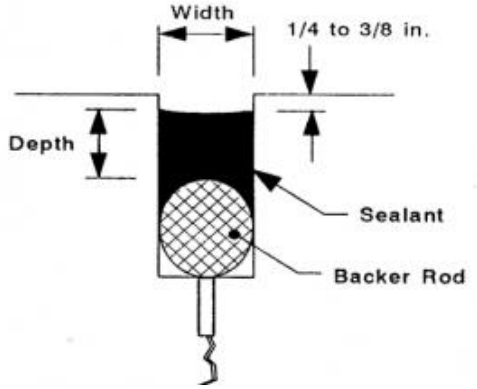

Figure 1.6 Sealing joint

The joint sealant aims to minimize infiltration of surface water and incompressible material into the joint system. Sealants can also reduce dowel bar corrosion potential by reducing the entrance of de-icing chemicals.

1.3.4 Bridges Deck Waterproofing

Structures are sensitive to water action because they can dissolve some concrete components or corrupt reinforcement elements. Civil engineers added to the structures and bridges design some types of waterproofing elastomers to protect these structures from the surrounding environment from years ago.

1.3.5 Earthquake Devices

Elastomers are found in this specific field of dynamic actions, seismic areas, and extension in the field of road restraint systems. These fields represent some elastomers properties, which allow some flexibility in the horizontal direction and reduce vibration frequencies.

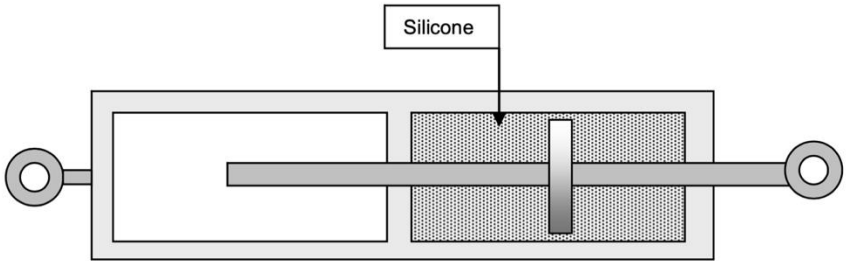

Figure 1.7 Seismic device using the properties of silicone *[3]*

1.4 Hyperelastic in Sustainable Development

The production of an elastomer has relatively little by-product greenhouse gas (GHG) emission to the environment, but it requires a lot of energy to manufacture it. These points can make elastomers fabrication not so much environmentally friendly. As mentioned from elastomers properties, it can resist fatigue and has satisfactory durability. Also, high resistance to environmental conditions.

At the end of the elastomer's life cycle, it becomes a hard process to recycle this material. When elastomers are used with other materials (steel reinforced elastomer), it becomes very difficult to separate elastomers from the other material. Despite these difficulties, there are two ways to recycle this material.

- Mechanical Action: Transform elastomer to powder by grinding it using special devices. This powder can be reused in used elastomer formulation, also it can be used to improve some properties in bitumen. It has also many uses in fields other than civil engineering.
- Regenerate action: Chemical agents can be used to break the bonds for elastomer particles, the result can be used in other rubber fabrication.

Although this material cannot be considered a pollution agent at the end of its life cycle, it's still considered waste.

2
LITERATURE REVIEW

2.1 Background

Earthquake isolation resistance systems have become an important part of structures in Turkey due to the country's location, it lies at one of the most active earthquake zones called Mediterranean-Alpine-Himalayan. Between 1900 and 2005, the number of earthquakes between the magnitudes 5-5.9 is 1170, 6-6.9 is 155, and 7-8 is 34 [5] [6]. These earthquakes have caused significant loss of life and great damage to human-made structures. Therefore, the concept of seismic isolation began to gain prominence, especially after the 1999 Marmara Earthquake [5]. Hyperelastic materials are one of the materials used in these isolation systems to resist seismic forces. Characterization is required to understand the nonlinear behavior of this material.

Hyperelastic material such as elastomers is a widely used material in various industries, and it has multiple applications [7]. The main mechanical feature of the elastomer family is the extraordinary elasticity. When a load is applied on an elastomer, it can experience significant elongation from its original length and get back to the initial shape after the load is removed. Therefore, elastomers consider as unique materials in civil engineering. The behavior of the elastomeric material is highly nonlinear, and a simple modulus of elasticity that can be predicted from the stress-strain curve is no longer sufficient. Therefore, it is essential to characterize this material to understand its behavior. To study this material behavior under different loads, a correct strain energy function should be selected to predict the nonlinear hyperelastic behavior accurately.

The appropriate experiments to define a hyperelastic material are not yet clearly defined by national or international standards organizations [8]. This difficulty derives from the complicated mathematical models required to represent both the nonlinear and nearly incompressible elastomers' properties [8]. Therefore, the evolution of using this material required trial and error rather than basic equations.

Hyperelastic materials are more complex to model compared to other materials, which needs a few attributes to define. Rubber has a highly nonlinear behavior. It can also be more affected by temperature, environment, stress rate and strain values, and many other factors. The evolution of using this material required trial and error rather than basic equations. These models are called hyperelastic material models [9].

Experimental testing of elastomers to achieve curve fitting in finite element analysis needs multiple strain moods through experiments under special loading conditions. Models' limitations and specifications should also be considered when performing experiments. [8]. There are several behaviors for elastomers when a load is applied to them. Each behavior can be defined in a different method. The most important response to be defined is the strain potential energy which can predict the material's behavior.

2.2 Hyperelastic Model

Several hyperelastic models are available to predict the stress-strain behavior of hyperelastic, these models required experimental tests to determine its coefficients. The physical tests usually performed on elastomers are compression and tension. For a homogeneous material, homogeneous deformation modes suffice to characterize the material constants.

Hyperelastic models mostly share the same input requirements values from test data. Generally, nominal stress and strain data sets are generated by elongation of the elastomer in multiple modes and "fitted" to define suitable variables in the material model. Typically, three sets of stress-strain curves are needed for input for fitting, as shown in the figure below [9].

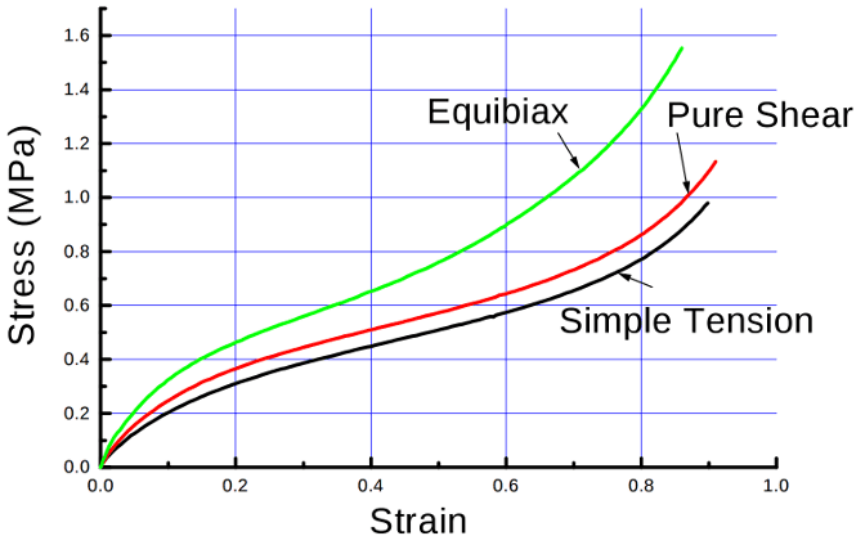

Figure 2.1 Stress-strain curves example for a hyperelastic material [10]

The purpose of the test described here is to define and meet the input requirements of mathematical object models in structure, nonlinear finite element analysis software [8].

Defining hyperelastic material in FE usually required testing rubber in different modes. FE software documentation gave recommendations for the appropriate way to perform the required tests to get better input data [11]. Four types of deformation modes are required to define this material:

2.2.1 Uniaxial Tension

The uniaxial test is done by stretching or compressing a specimen from two sides. However, pure compression is generally hard to achieve because of the friction between specimen and the test device.

2.2.2 Biaxial Tension

An equal tensile force is applied to all specimen sides. The biaxial machine is not commonly available due to high prices and low uses. Therefore, several researchers developed custom fixtures to use a uniaxial test machine in performing this test [12] [13] [14].

2.2.3 Planar Tension

To achieve pure shear, the stretching should also be from the wider two sides; the specimen should have more width than the height. In fact, the width should be at least ten times more than the height of the specimen [8].

2.2.4 Volumetric Compression

A volumetric test is used to evaluate bulk modulus and compressibility. Force is applied to a fully confined specimen to measure Bulk modulus, which is usually 2-3 greater than the shear modulus [8].

2.3 Mechanical Models

Researches also created more simple models to predict the shear behavior of elastomeric material. Generally mechanical models are simpler than hyperelastic models. One of the mechanical model's examples is Koh and Kelly model [4], which represents a simple mechanical model (Hariingx column) with two degrees of freedom to represent the shear and flexural deformation of elastomeric bearings. Mainly, this model was first found to estimate stiffness and compressibility of a bearing element, then it has been developed to evaluate dynamic effect and damping factor of the rubber material. The general function is shown below.

$$P = GA_s \frac{(1 + 4p_e\theta \cot\theta)^{1/2} - 1}{2\cos\theta} \tag{1.1}$$

P compression load

G shear modulus

A_s Shear area

p_e Euler buckling load/GA_s

θ Rotation

2.4 Viscoelastic Model

Viscoelastic behavior is represented in the material that has both viscosity and elasticity. The result accuracy and reliability in modeling a rubber material can be affected by the viscoelastic response. Viscoelastic behavior should be included when time should be considered, such as the determination of cyclic loading when energy is dissipated at unloading step. The models that combine the hyperelastic and viscoelastic are called hyper-viscoelastic models. Viscoelastic effect required time-dependent tests for estimating the relaxation time. [15] created multiple Visco-Hyperelastic models, result example can be shown in **Figure 2.2** below.

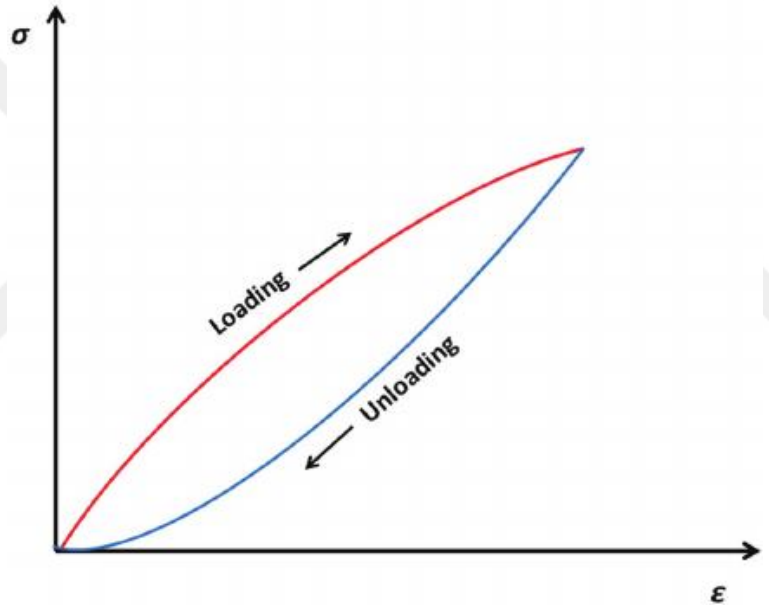

Figure 2.2 Viscoelastic effect curring loading and unloading states [15]

2.5 Mullins Effect [16]

Rubber materials can experience some changes in their mechanical properties through the loading and unloading process. This phenomenon is referred to as Mullin's effect [16] (Damage effect). Few studies considered Mullin's effect in the application and modeling of rubber material. [8] Mentioned that the first load cycle has a unique load result, this can be explained by Mullins effect. This effect can be fixed by loading and

unloading specimens three times before testing the sample [17], Figure below shows the change in stress-strain behavior through multiple cycles tests on the same specimen.

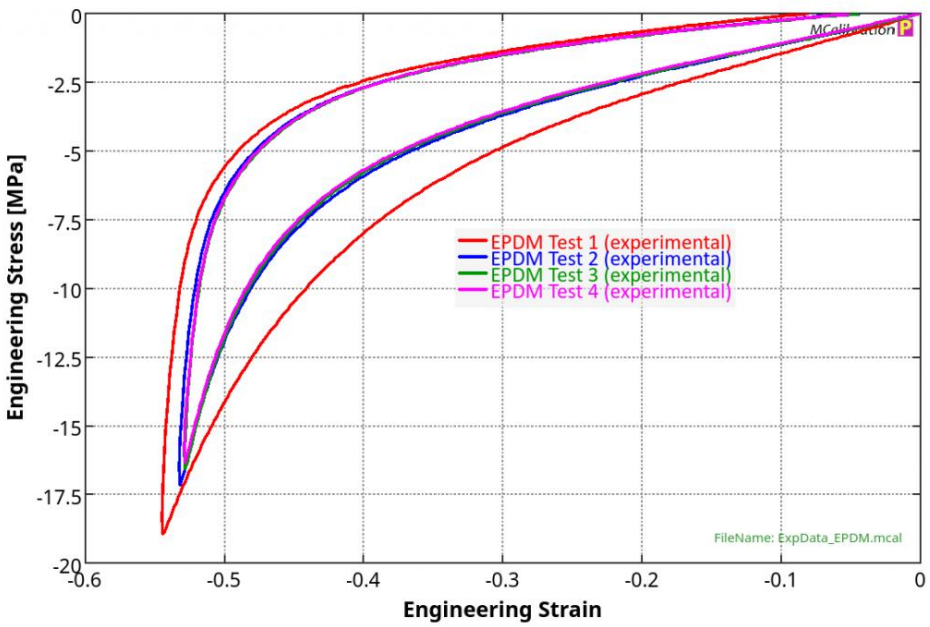

Figure 2.3 Stress-strain behavior through multiple cycles (Mullins effect) [18]

2.6 Problem Statement

Rubber material is used in various kinds of industries, The high demand for this material required a better understanding and prediction of this material behavior. The appropriate experiments to define a hyperelastic material are not yet clearly defined and documented by national or international standards organizations [8]. Also, there is a lack of studies in the literature about rubber modeling. This difficulty derives from the complicated mathematical models required to represent both the nonlinear and nearly incompressible elastomers' properties [8]. Therefore, the evolution of using this material required trial and error rather than basic equations.

Rubber modeling does not depend on hyperelastic models only, it also depends on Viscoelasticity and material damage. All these aspects required investigation to accurately predict this material behavior. however, this research is focusing on defining the non-leaner behavior using hyperelastic models

2.7 Objective

Finding a suitable strain potential energy function (SPEF) and choosing the best model to characterize Hyperelastic for elastomeric material used in elastomeric bearing. The best-fitted model will be used to simulate several tests on an elastomeric bearing, It should be able to predict the different behaviors correctly.

2.8 Scope

To define the most sufficient strain potential energy function (SPEF), at least one of the four experimental tests should be made (Uniaxial, Biaxial, Planar, and Volumetric) and the result will become input data to determine coefficients for finite element functions. FEM simulation model will be used to validate experimental results by remodeling three physical tests made on elastomeric bearing samples. The results will be compared with physical tests data. The closest Strain potential energy curves from tests should fit the mathematically calculated curves.

3
METHODOLOGY

In this chapter, the required tests will be performed on elastomeric rubber specimens to define hyperelastic material behavior. To predict the behavior of elastomeric material in finite element, several models are available to characterize it, these models share the same input requirements. Tests must be performed in a different stretching mode for the elastomeric samples. Nominal stress and strain values should be evaluated and used as input data to evaluate the parameters of all FE models. At least one of the three shear tests is required in order to characterize a hyperelastic material, the combination of all four tests can give a good prediction of this material behavior. After performing hyperelastic tests, bearing experiments will be followed up to validate the defined hyperelastic models. Three tests with different modes were made on a sample of elastomeric bearing, the result data will be compared with digital models later.

After finishing hyperelastic models, validation tests will be followed up to analyze and compare them with Computer aid analysis (CIA) models. Three experimental tests were performed on elastomeric bearing samples; Compression test, shear test, and shear under compression test.

3.1 The Required Tests

Defining hyperelastic material in FE usually required testing rubber in different modes. [19] documentation gave recommendations for the appropriate way to perform the required tests to get better input data. Four types of deformation modes are required to define this material:

- **Uniaxial tension:** the uniaxial test is done by stretching or compressing a specimen from two sides. However, pure compression is generally hard to achieve because of the friction between specimen and the test device [8].

- **Equibiaxial tension:** this test is done by applying an equal tensile force to specimen's sides. The biaxial machine is not commonly available due to high prices and low uses. Therefore, several researchers developed custom fixtures to use a uniaxial test machine in performing this test [12] [13] [14].
- **Planar tension:** to achieve pure shear, the stretching should also be from the wider two sides; the specimen should have more width than length. In fact, the width should be at least ten times more than the length of the specimen.
- **Volumetric compression:** Volumetric test is used to evaluate bulk modulus and compressibility. Force applied to a totally confined specimen to measure Bulk modulus, which is usually 2-3 greater than the shear modulus [8].

The most commonly performed experiments are uniaxial tension, uniaxial compression, and planar tension. These modes are illustrated schematically in **Figure 3.1**. For ideal incompressible hyperelastic material, the following test modes have become identical: uniaxial tension with biaxial compression, uniaxial compression with biaxial tension, and planar tension with planar compression. With these corresponding test modes, only three independent deformations are required to be evaluated. Therefore, most of the available researches depend on the tension mode of these tests except for volumetric.

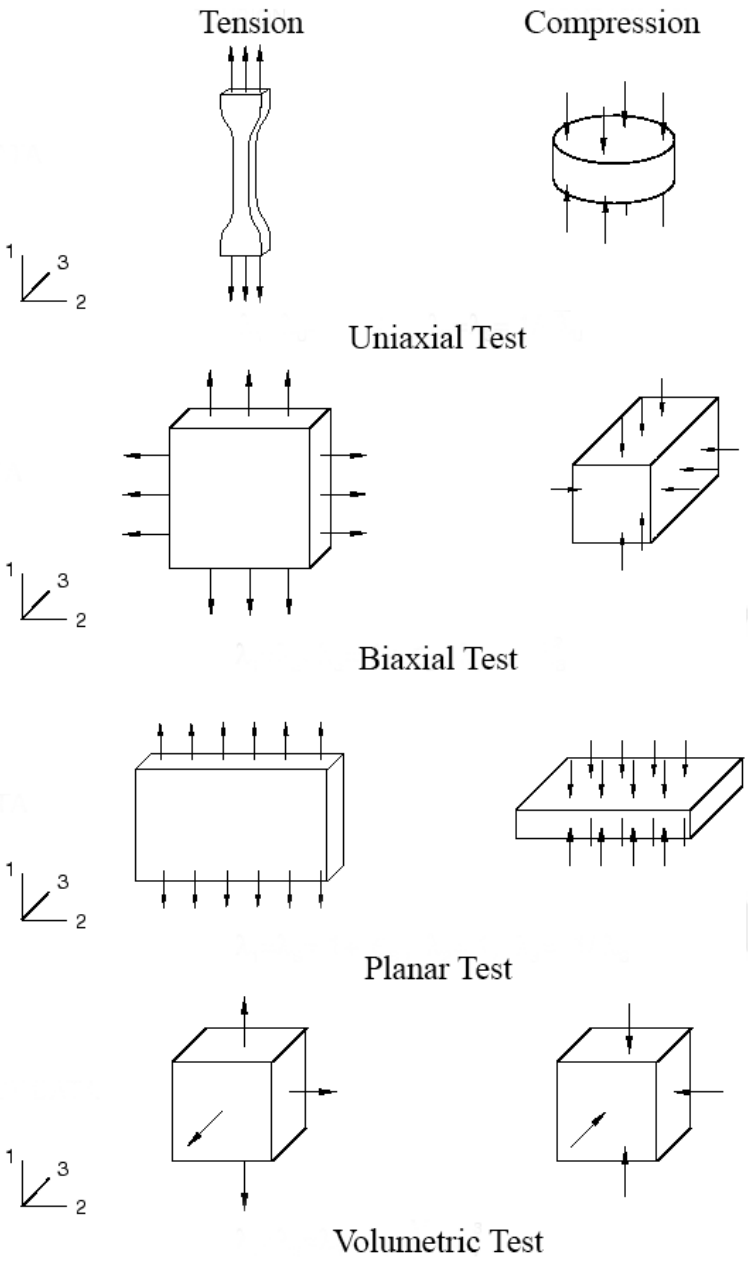

Figure 3.1 Required tests for hyperelastic material

Although there are six different experimental tests conditions, after applying pressure, the following modes become identical: Uniaxial tension and Biaxial compression, uniaxial compression and Equibiaxial tension, planar tension, and planar compression. With these corresponding tests modes, there are only three independent deformation modes to get their data.

A typical set of 3 stress-strain curves appropriate for input into fitting routines. Appropriate experimental loading sequences and realistic strain levels are needed to capture the elastomer behavior that applies in the analysis.

3.2 Testing Machine

The main machine Instron 8872 Servohydraulic fatigue testing system which is used in performing uniaxial and planar tests. The device can perform static and dynamic tests on materials with a load up to 25 KN. **Figure 3.2** below shows more details about the testing machine.

Figure 3.2 Instron 8872 fatigue testing system

Device Features:

- Double-acting (Tension and compression) with force capacity up to ±25 KN (±5620 lbf)

- High-stiffness, precision-aligned load frame with twin columns and actuator in upper crosshead
- 100 mm (4 in) of usable stroke
- Designed for both dynamic and static testing on a variety of materials and components
- Choice of hydraulic configuration and dynamic performance to suit application

With these features, the device can give highly precise test results data. The second machine is Instron 5982 which is used for volumetric test, this machine has a force capacity of 100 MPa and vertical space of 1430 mm. The device is shown in **Figure 3.3**

Figure 3.3 Instron 5982 testing system

3.3 Strain Measuring

Extensometer and digital camera Strain and displacement are the most important parameters in these experiments, due to high rate of displacement it becomes difficult to estimate strain through normal strain measuring devices like LVDT, etc. therefore,

Digital image correlation (DIC) is used to find strain from these experiments. High-resolution camera used with frame rate.

3.4 Material Properties

Two sets of rubber mix are used in definition tests, the first set is natural rubber and the second is Chloroprene as shown in table 1 below,

Table 3.1 Test specimens material types

Type	Material (based mix)	Shore-A
H100044	Natural Rubber (NR)	60 ± 5 Class-A
H400010	Chloroprene CR (CR)	60 ± 5 Class-A

3.5 Uniaxial Tensile Test

Test performed on a dog-bone-shaped specimen using ASTM D638 Type I standards, the required state of this test is to achieve pure tensile strain state in the long direction of the specimen. Extensometer device were attached with the specimen to evaluate the strain camera device was used to estimate the strain in the sample. More than 100% strain was applied to the specimen and a loading rate of 7.5 mm/min. Stress-strain results from stretching specimens in one direction are shown in the figure below.

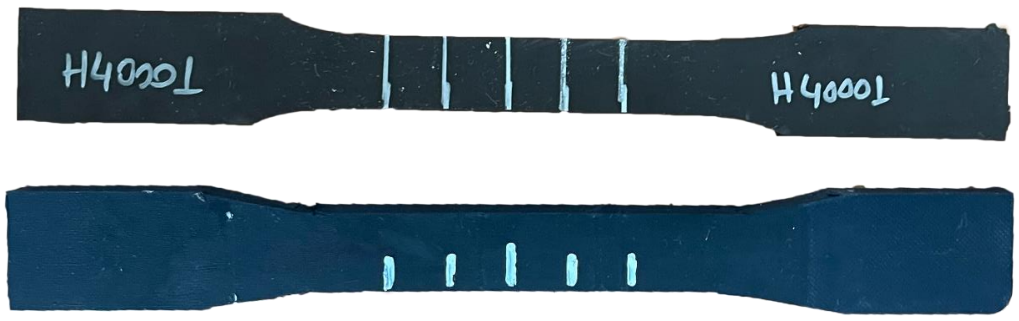

Figure 3.4 Uniaxial test specimen

Figure 3.5 Uniaxial test setup

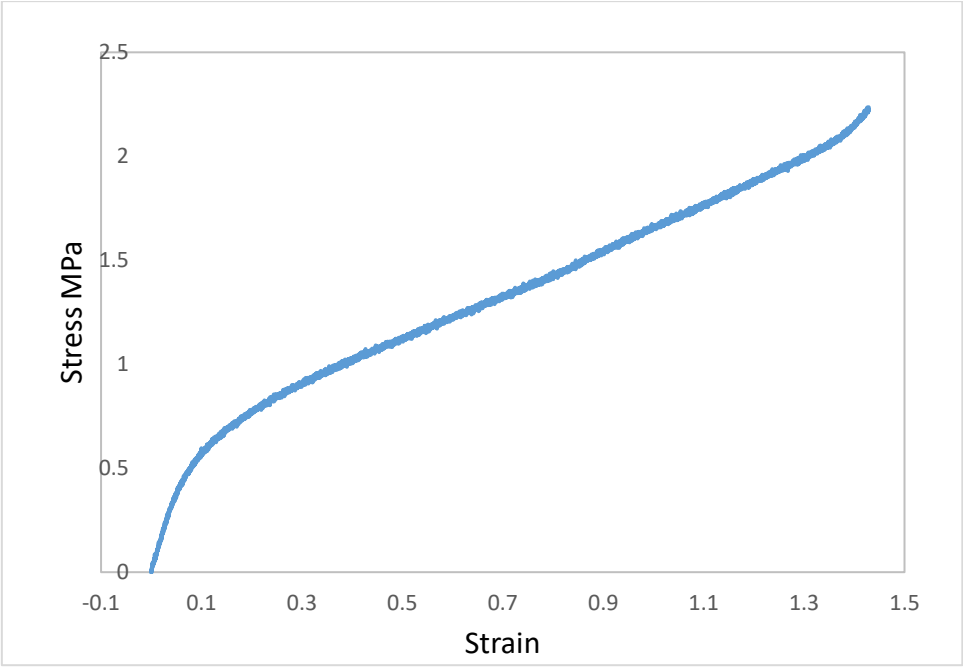

Figure 3.6 Uniaxial test result for H100044 specimen

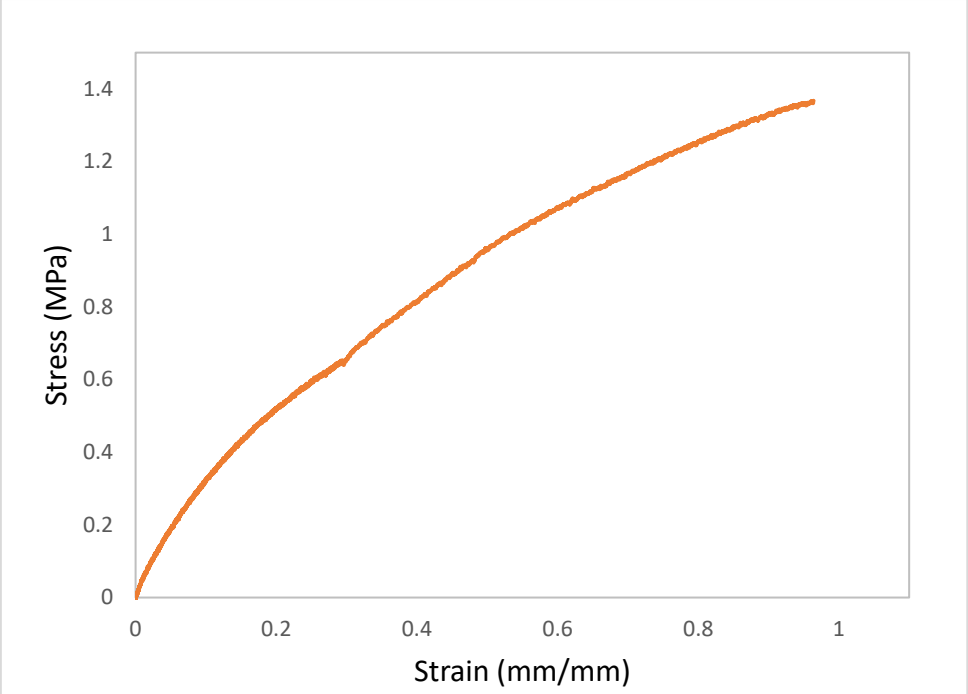

Figure 3.7 Uniaxial test result for H400010 specimen

3.6 Biaxial Test

Biaxial is one of the tests that can be used as input data to define hyperelastic material for evaluating potential energy and characterizing rubber material. Due to the unavailability and high prices for biaxial machines, also the most used testing machine is uniaxial machine, therefore a biaxial fixture was developed to be used with uniaxial test machine. The fixture design was inspired by [20]. The model was selected from many other options as its more suitable for our specimen and design simplicity. Unfortunately for technical issue in our testing machine Instron 8803 and lack of time, this test couldn't be done. But the device information and its modeling process will be described in the next paragraphs.

The fixture mechanism is a symmetrically jointed arm that is designed to test specimens by stretching it from four sides. The arms are connected with a pin connection that allows rotation and displacement freely. Arms transfer the load from top and bottom pieces to the specimen handles, the fixture designed in a way that does not allow handle rotation through test performing which was possible in the original design. A small analysis was made to check fixture validity through finite element molding. [14] also

analyzed several biaxial fixtures for checking their validity in test machine, the research confirms the results we got in device behavior when analyzing mechanism as mentioned: "The analysis shows an irregular behavior. During the test, the fixture appears to have a proper function until reaching a rotation in the wrong direction of the parts that hold the specimen" [14]. Therefore, modification has been made to the original design to fix these issues and fit our specimen test requirements. Compression load is applied to the top and bottom plates are distributed to four sides equally through arms, each side gets 25% of the pressure.

The first step was sketching parts of the fixture then a CAD model was created for the complete design and the final stage, finite element model was created and analysis was made to validate the final design. The model shows very stable results and it can fit our test requirements.

3.6.1 Description of The Device

The fixture consists of three main parts (arms, top-bottom holders, and specimen handles). Arms are part that connects all fixture parts as shown, dimensions of each piece are (35, 4, 1) centimeter for width, height, and thickness respectively. **Figure 3.8** below shows all details for this part.

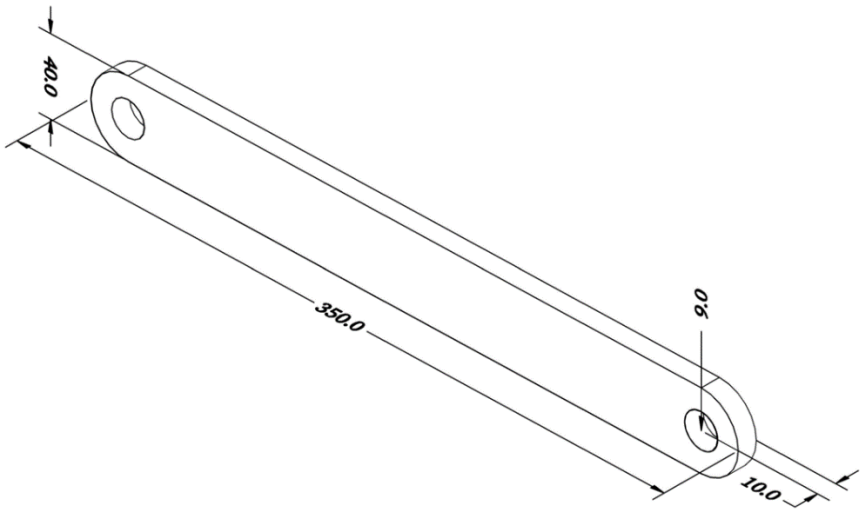

Figure 3.8 Fixture arm, dimensions in mm

Top-Bottom holders are the parts that transfer and distribute the load to the connected arm, bolt connectors are welded with the top plate. The dimensions of this piece are described in **Figure 3.9**.

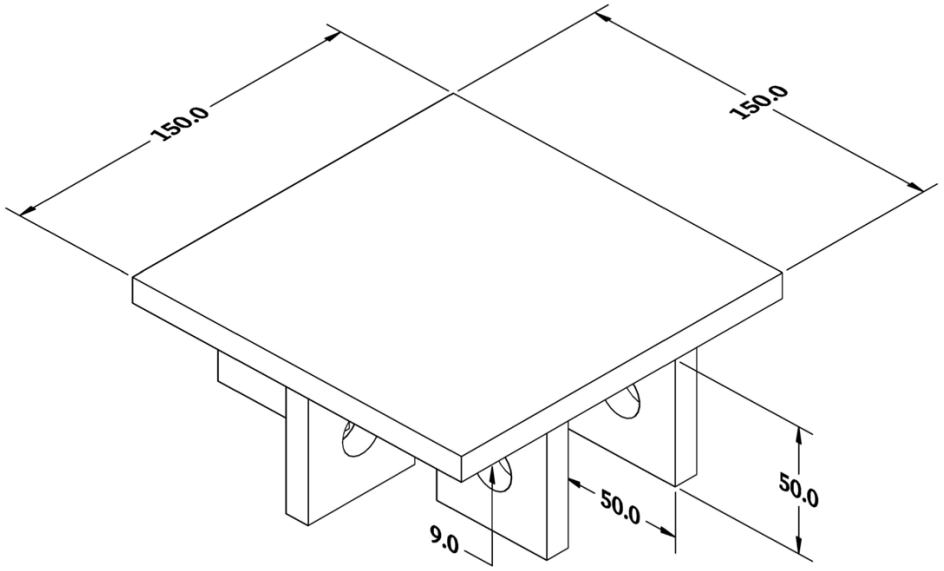

Figure 3.9 Top-bottom part, all dimensions in mm

The final major piece is handled which transfers load from arms to specimen, this fixture has four handles connected with arms with 18mm diameter bolts. Each handle is connected with one bolt only so it will not allow rotation of specimen through test and keep is horizontally aligned. **Figure 3.10** below shows all details for this part. Clear shape for all parts connected is described below.

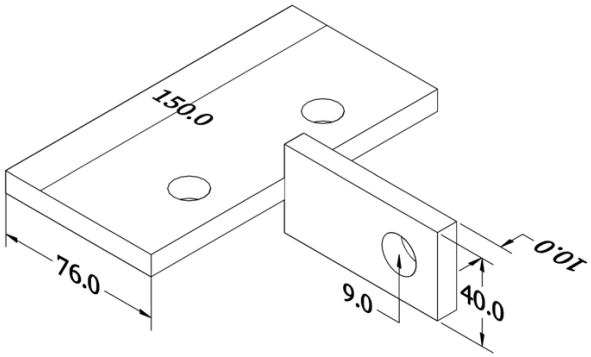

Figure 3.10 Handle part, dimensions in mm

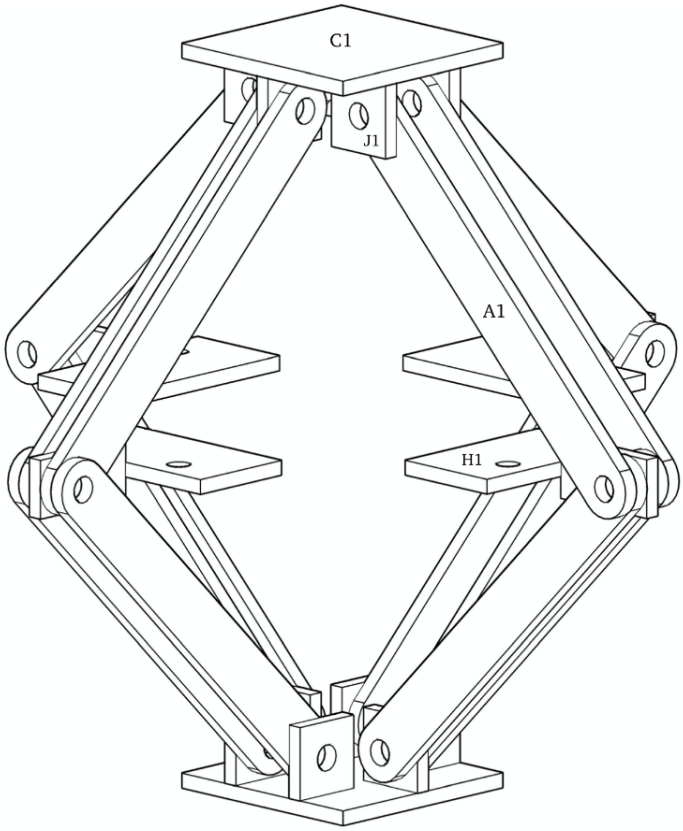

Figure 3.11 Final design for the fixture

3.6.2 FE Analysis for The Fixture

After completing the final design finite element analysis was required before manufacturing the fixture. Abaqus software was used to create the model, the simulation showed very stable results with successfully fixing original design errors, and it is ready to be manufactured. The figure below shows results from FEA model simulation.

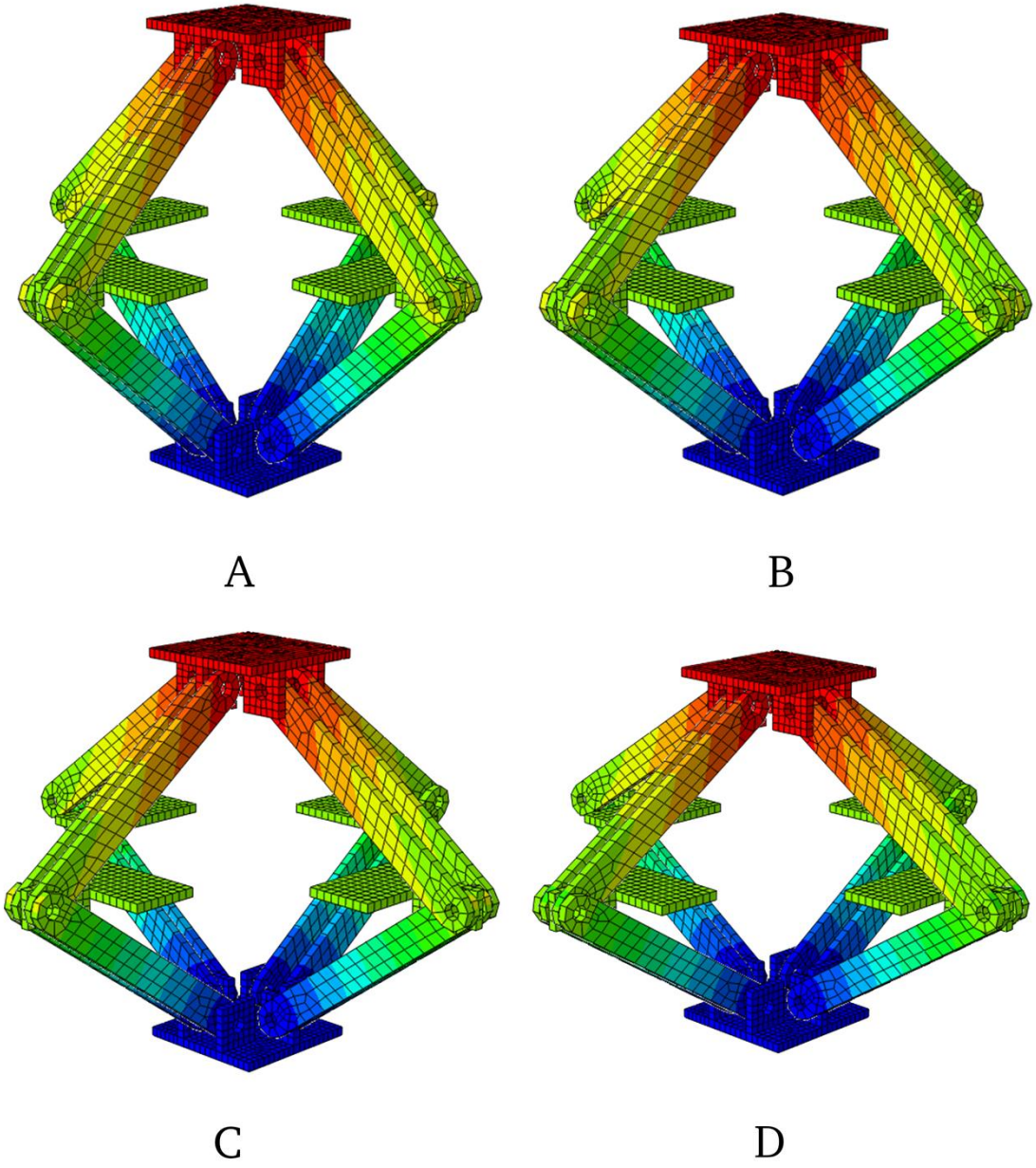

Figure 3.12 Finite element model for biaxial fixture

As we discussed biaxial test is very important for characterizing a hyperelastic material, although biaxial testing machines are commercially available, they are very expensive compared with uniaxial ones. In particular, testing of unidirectional specimens under transverse biaxial loading is especially interesting for the study of hyperelastic, a mechanism of damage that has already been numerically studied.

Figure 3.13 Manufactured biaxial test fixture

As mentioned before, this fixture should be used for biaxial and planar tests. However, due to a technical problem with our testing machine and lack of time, biaxial test couldn't be done. But the fixture is still ready to be used for any similar test.

3.7 Pure Shear Planar Test

This test can represent the actual shear behavior of the rubber, it's required that the specimen dimension in the loading direction must be less than the width. The idea is to create a perfectly fixed side direction such that the rubber thinning can only occur in the thickness direction. Specimen dimensions were 30 mm in height, 100 mm in width, and 6 mm in thickness **Figure 3.14**. Handles from biaxial fixture are used to grab planar specimen from both sides as shown in **Figure 3.15**. Two specimens were used one for each material type, stress-strain results from planar test are shown in **Figure 3.16** and **Figure 3.17** below.

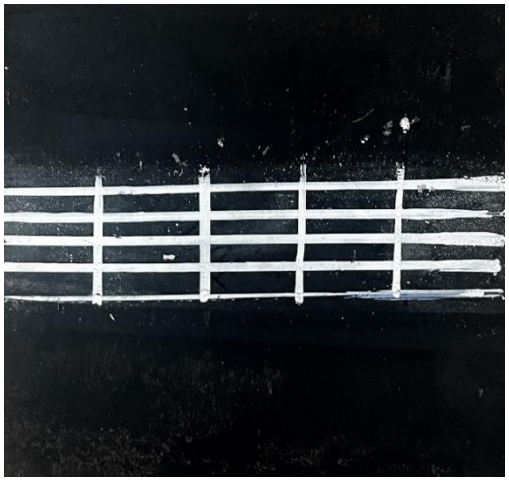

Figure 3.14 Specimen for planar test

Figure 3.15 Specimen setup in testing machiene

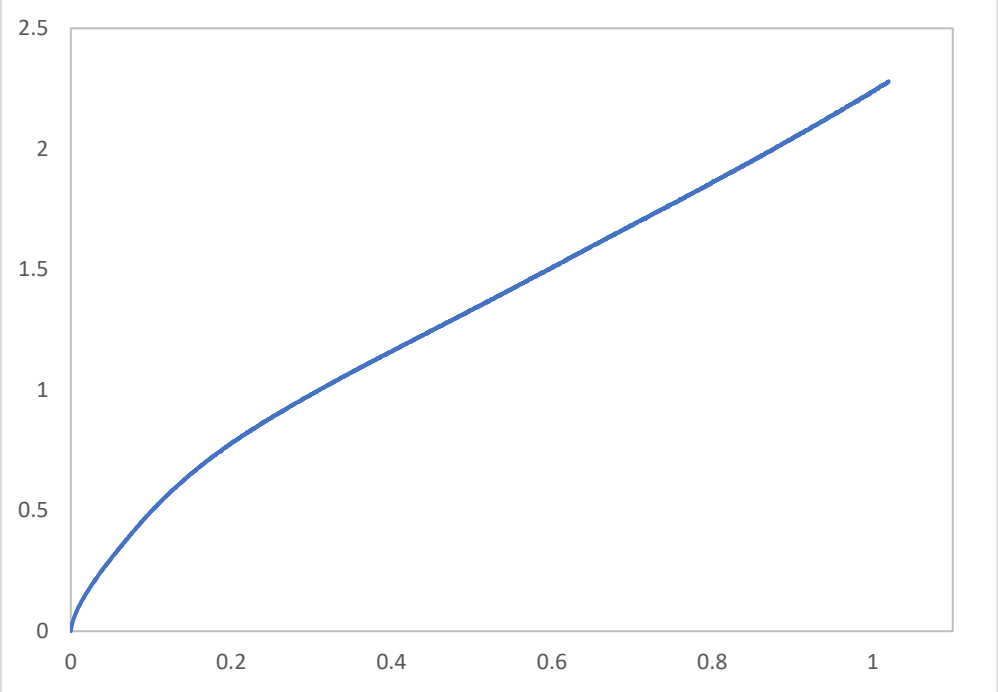

Figure 3.16 Planar results for H100044

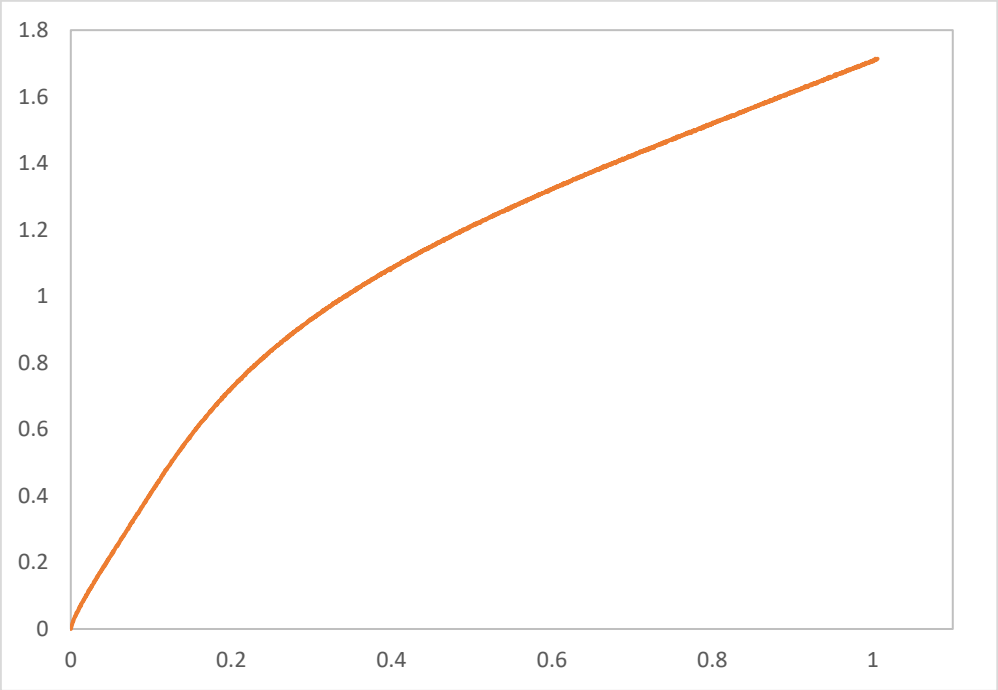

Figure 3.17 Planar results for H400010

3.8 Volumetric Test

Volumetric test is used to evaluate bulk modulus and compressibility. Bulk modulus is usually 2-3 greater than the shear modulus. The mold used contains a cylindrical shape hole with a 28.24 mm diameter, the mold has complemented bar with the same diameter that can fit in the hole completely and allow vertical movement only, this results in a volumetric load applied to all sides in specimen. Specimen dimensions are shown in **Figure 3.18**.

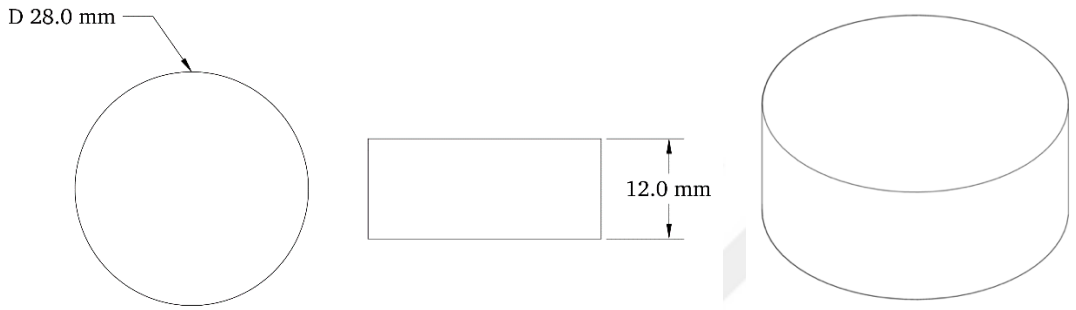

Figure 3.18 2D and 3D Representation for volumetric test specimen

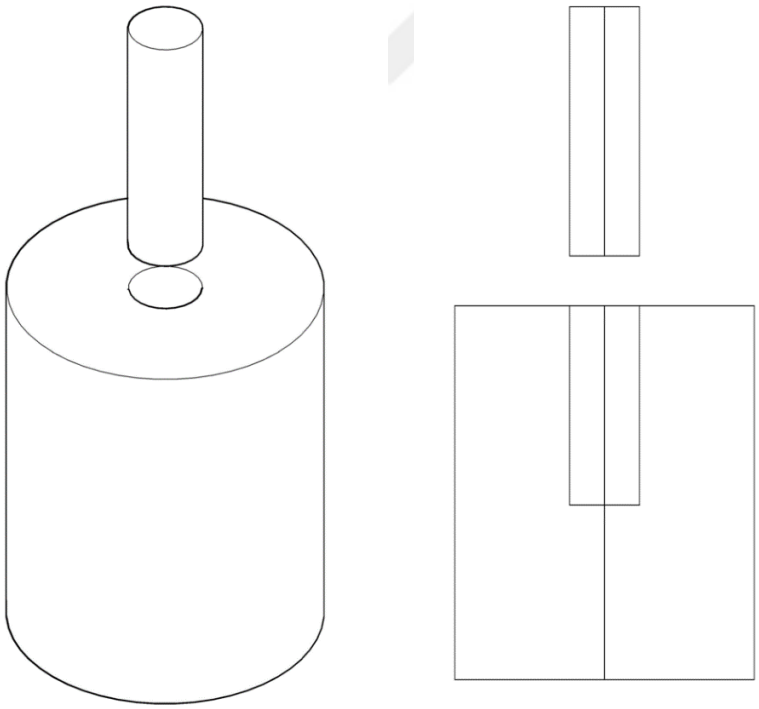

Figure 3.19 Volumetric test representation

Figure 3.20 Volumetric test fixture

The required values to estimate in the volumetric test are pressure and volume ratio. Volume ratio can be evaluated by dividing the volume change over the total volume using equation 2 below, results are shown in **Figure 3.21** and **Figure 3.22** below.

$$\text{Volume Ratio} = \frac{\Delta V}{V} \tag{3.1}$$

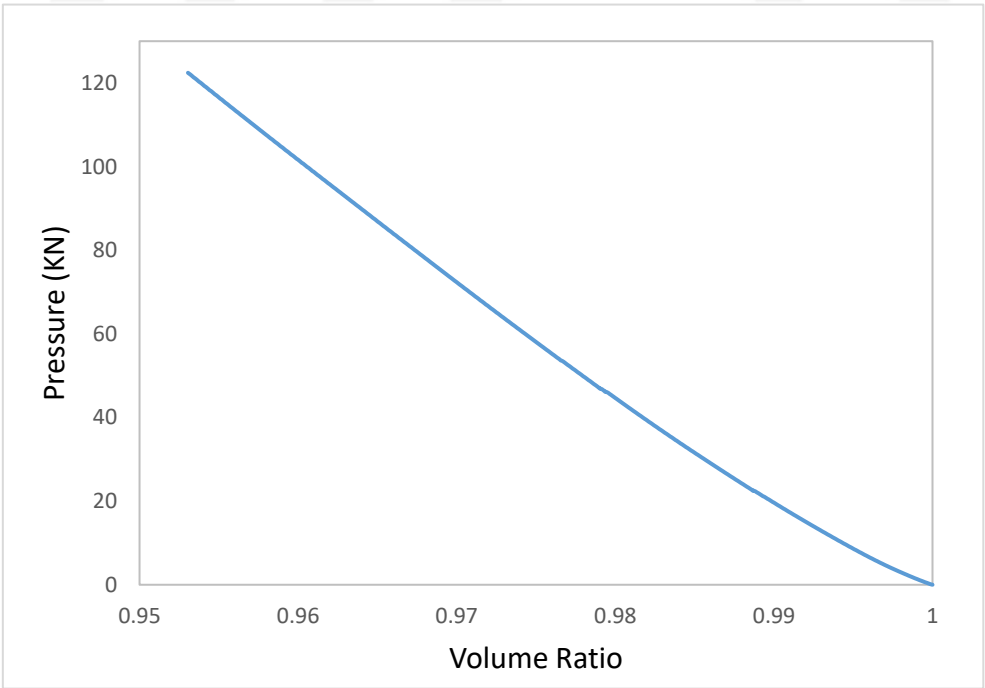

Figure 3.21 Volumetric test results for H100044

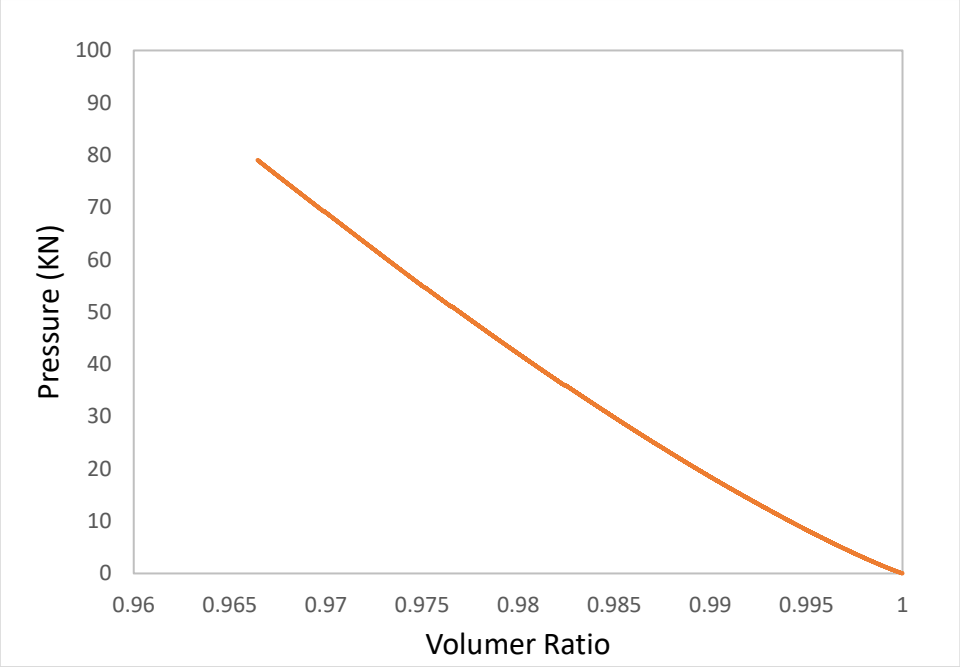

Figure 3.22 Volumetric test result for H400010

3.9 Validation Tests

The previous tests will be used to calculate the potential strain energy function U. To ensure the model used is can predict different behaviors of the material, two physical tests for elastomeric element made from the same material will be simulated in finite element. The result from the simulation must be close to the physical test. Curve fitting and calculating error will be used to validate different models. Double shear specimens for both material types were used to validate the selected models.

3.9.1 Double Shear Test

The double shear (quadlap) specimen consists of four rubber layers set between steel plates connected by heat as shown in **Figure 3.23** and **Figure 3.24**. Rubber layers are square with 40 mm side dimension and 10 mm thickness. Rubber layer thickness is less than the other two dimensions to reduce bending effects [7]. Two specimens were tested, one for H100044 and the other for H400010. Each specimen will be simulated in finite element to compare it with physical tests results. Up to six cycles were applied to each specimen with a total displacement of ±100 mm, loading speed was 60 mm/min and max load applied is 2 Mpa. Stress-strain results for double shear test are shown in **Figure 3.25** and **Figure 3.26** below.

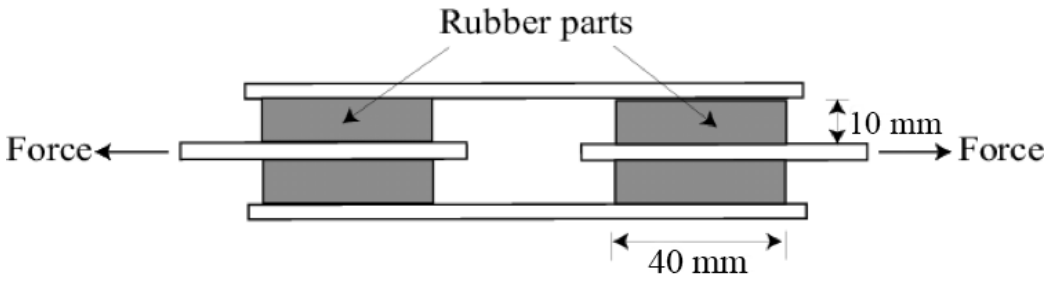

Figure 3.23 2D sketch for double shear specimen

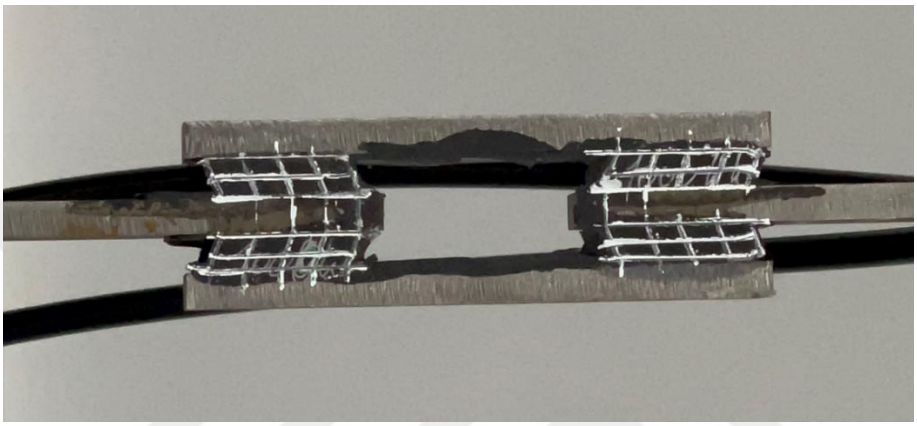

Figure 3.24 Double shear specimen

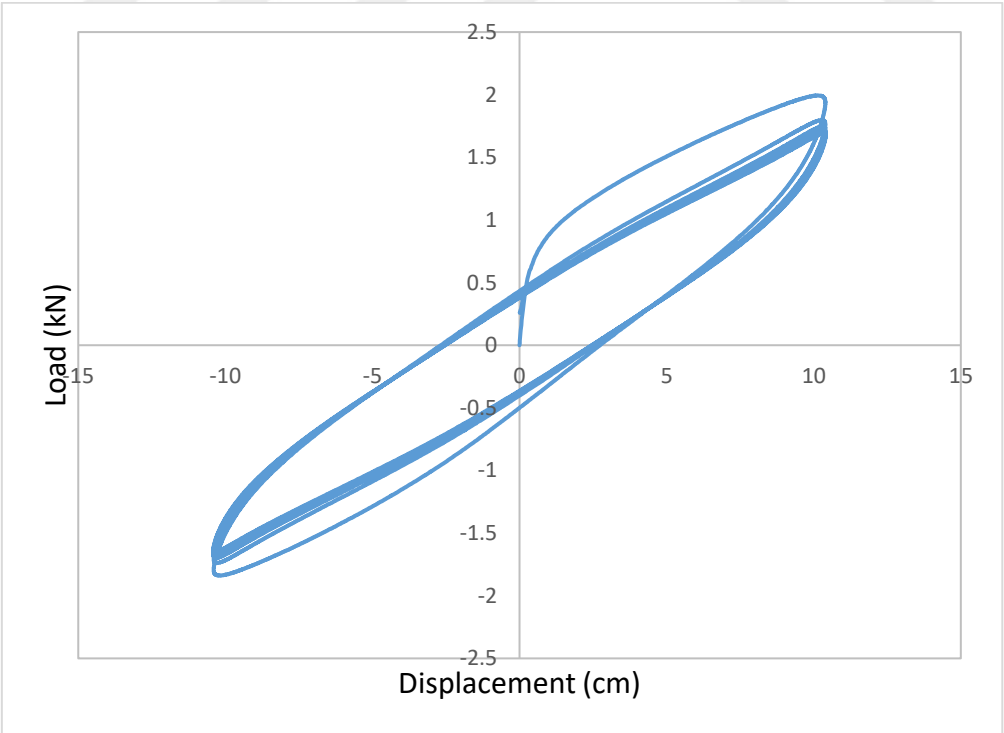

Figure 3.25 Double shear test for H100044 specimen

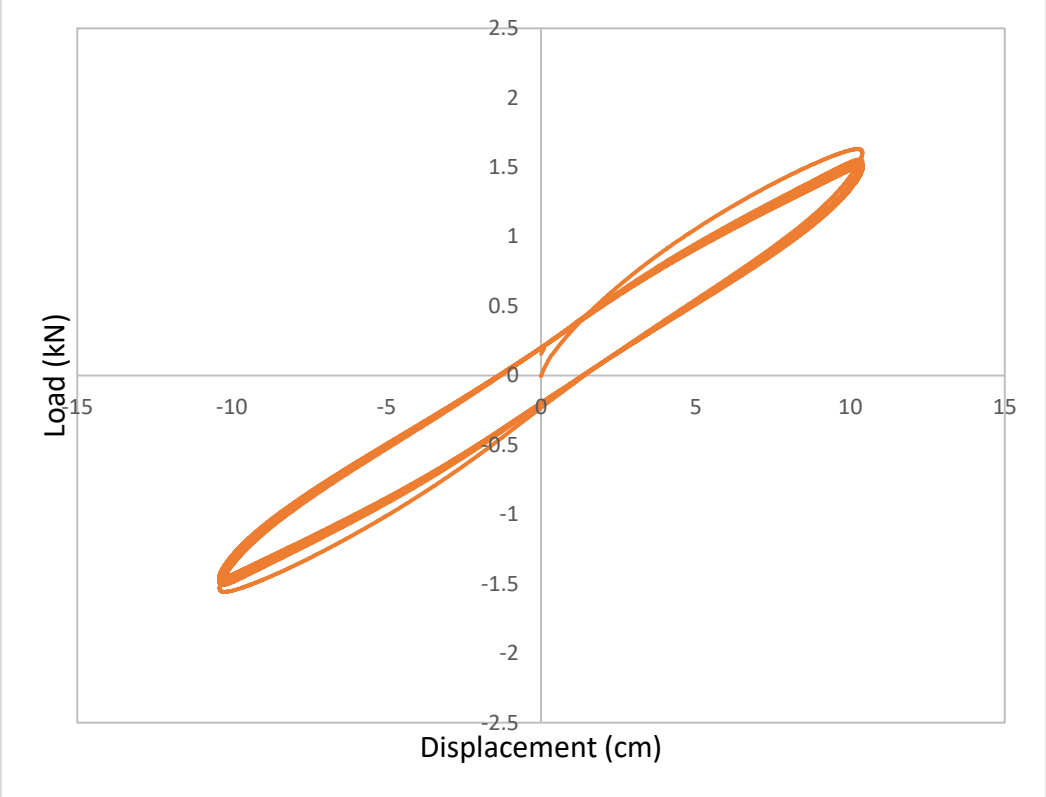

Figure 3.26 Double shear test for H400010 specimen

4
FINITE ELEMENT MODELING

Physical experimental studies are executed with limited loads, directions, and boundary conditions. Every experiment preparation can take a long time, also it may require special types of equipment that might be financially not available. Computer-Aided analysis using finite element can give a precise idea about the material's behavior.

From the previously explained tests, nominal stress and strain values are evaluated and used as input data to evaluate strain energy functions. Curve fitting was used to compare different models and select the model that gives the best representation for the material. To validate the results of energy functions, Finite element model will be created from tests data using digital software. Curve fitting method will be used to validate FE models.

Finite element validation aims to find the best model to define this material and fit the experimental results. After finding the most suitable model, the other behaviors of this structural element can be predicted. ABAQUS CAE 2017 software was used in evaluating coefficients for all models and the modeling process [11]. There is several finite element software that can solve and model a hyperelastic material. ABAQUS software is one of the best programs that can be used in FE modeling. All of the hyperelastic models used to define strain energy function (SEF) to characterize the material behavior are pre-defined in the software. These hyperelastic models mostly share the exact input requirements. As discussed before, these inputs should be obtained from the stress-strain data taken from experimental test.

4.1 Hyperelastic Models

Finite element models have two main groups of models in terms of defining the strain energy function. The first group of models depends on the phenomenological hypothesis, which solves the problem from the aspect of continuum mechanics [21]

[22] [23] [24]. The second type of solution depends on the microscopic structure to characterize the behavior, the material reaction is considered from the aspect of microstructure [25] [26]. All hyperelastic models share the same input requirements [11].

The model is isotropic and nonlinear. Although Elastomers have very small compressibility compared to their shear flexibility, it should model correctly to gain precise results, especially wherein applications where the material is completely confined. In the implementation where the model is not highly confined, compressibility is not very crucial. The relative compressibility of a material by the ratio of initial bulk modulus K_0, to its initial shear modulus, μ_0. This ratio can also represent Poisson's ratio υ,

$$\upsilon = \frac{3\,K_0/\mu_0 - 2}{6\,K_0/\mu_0 + 2} \tag{4.1}$$

In Abaqus, there are two types of solutions to find potential energy, standard and explicit solutions

4.1.1 Abaqus Standard

Standard solution is recommended for almost incompressible hyperelastic materials. Initial Poisson's ratio is greater than 0.495 (the ratio of K_0/μ_0 greater than 100). Except for elastomeric foam which is elastic but very compressible material.

4.1.2 Abaqus Explicit

The material is considered to be fully incompressible with Abaqus/Explicit solution as the program has no mechanism for imposing such a constraint at each material calculation point.

4.1.3 Strain Energy Potentials

Hyperelastic material can be characterized in terms of "strain energy potential" U(e), the definition of this term is "the strain energy stored in the material per unit of reference volume (volume in the initial configuration) as a function of the strain at that point in the material". There are various functions forms of strain energy potentials available in Abaqus to model this material: the Arruda-Boyce form, the Marlow form,

the Mooney-Rivlin form, the neo-Hookean form, the Ogden form, the polynomial form, the reduced polynomial form, the Yeoh form, and the Van der Waals form.

4.2 Evaluating Hyperelastic Materials

There are several hyperelastic models available to use in Abaqus. To evaluate hyperelastic material in Abaqus, from the property section new material are created, this material will be used generally to evaluate all models. In the mechanical properties of the material creation window, hyperelastic material should be selected from elastic section. After this property is selected test data will be added from test data choice, four tests available as discussed before, and the strain energy function should be set as unknown in order to evaluate the required models as shown in the figure below. Abaqus also gives the ability to apply smoothing points to test data, experimental tests can contain some noise in results data which can affect the quality of the strain energy derived function.

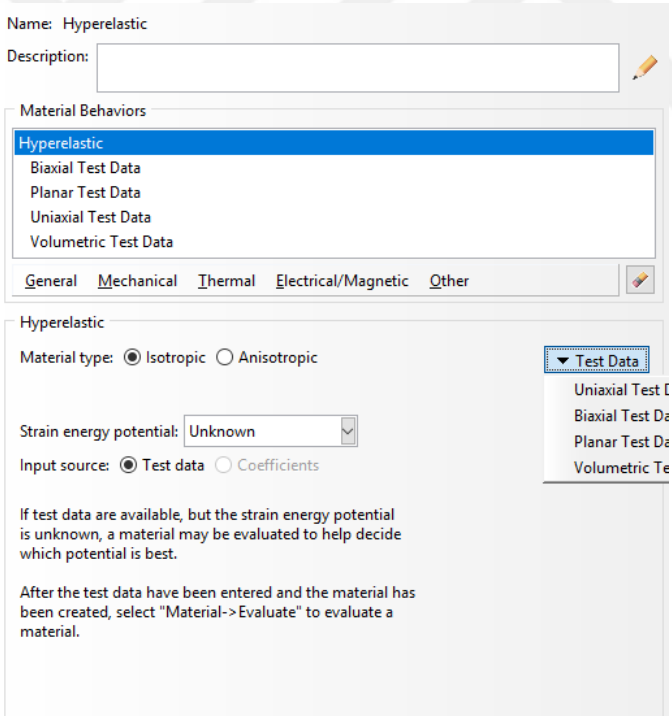

Figure 4.1 Hyperelastic material definition with test data

The final step will be evaluating all models, from material then evaluate choice new window will be shown, specific tests data can be selected in the evaluation process. Minimum and maximum strain values should be set for each test, the best value is to

add physical experiments strain values in order to get the best fitting curves. Abaqus gives the ability to simulate simple shear test to compare it with experimental result if there is any. Ogden model accepts only one of the three shear tests besides volumetric test.

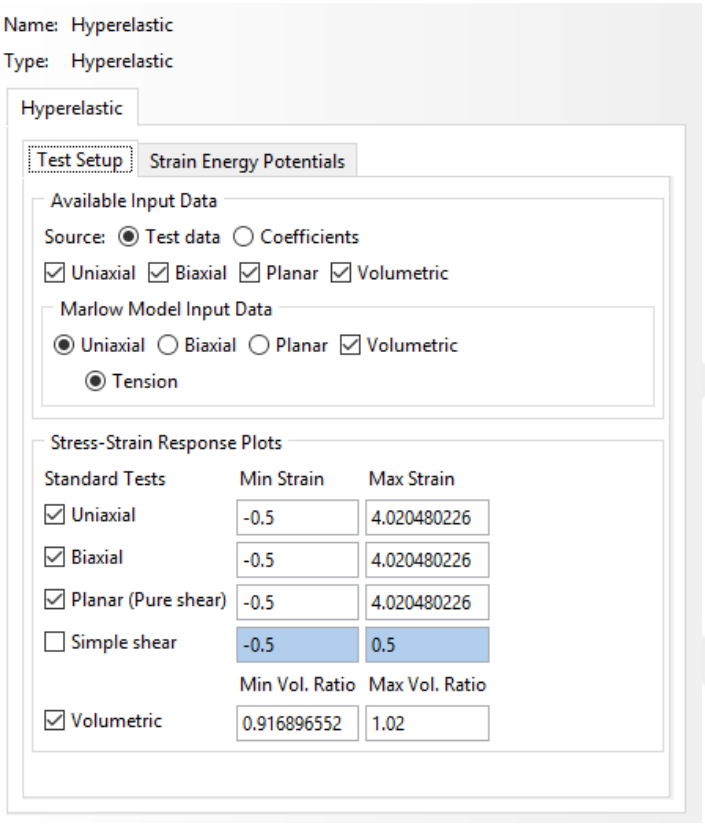

Figure 4.2 Evaluation setup for hyperelastic models

After finishing all settings Abaqus will evaluate all models coefficients for every model, also it will give information for each test if the model is stable in simulating the test as shown in **Figure 4.3** below.

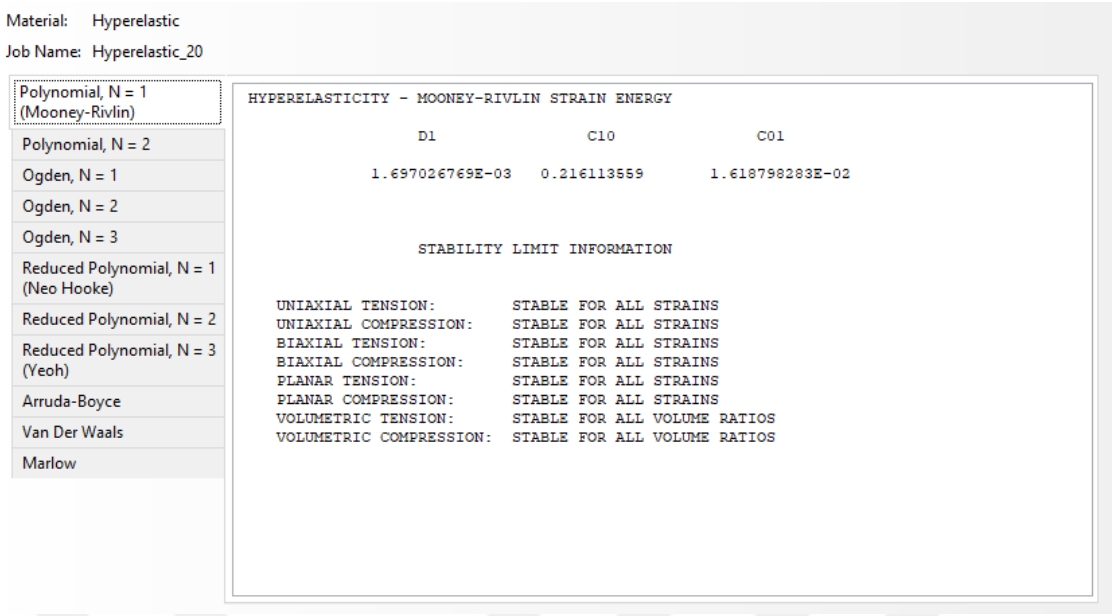

Figure 4.3 Evaluation results for different hyperelastic models

Strain energy potentials can be added directly to create response curves. Experimental test data can be imported and this software will evaluate the optimal strain energy potential. At least one of the three shear tests should be provided to evaluate potential energy for the available models. When data from several tests are available, results are more accurate in fitting experimental results. The coefficients can be added in a new material or the potential energy function of the same evaluation material can be changed to the required model. Each model description and evaluation will be followed up in the next sections.

Evaluating hyperelastic models from test data can be unstable at specific strain values. Abaqus makes a stability check and during models evaluation to determine the strain magnitudes that give an unstable prediction, unstable models will be marked with a warning message [11]. Solution convergence may not occur for simulation if the stability limit is exceeded.

4.2.1 Arruda-Boyce Model

The first model selected in this research depends on three parameters which are μ, λ_m and D, it was developed by [25]. The general form is shown in the equation below. This form also assumes the model is incompressible. The general form is represented in the equation below:

$$U = \mu \left[\frac{1}{2}\left(\bar{I}_1 - 3\right) + \frac{1}{20\lambda_m^2}\left(\bar{I}_1^2 - 9\right) + + \frac{1}{1050\lambda_m^4}\left(\bar{I}_1^3 - 27\right)\right] + \frac{1}{D}\left(\frac{J_{e\ell}^2 - 1}{2} - ln J_{e\ell}\right) \quad (4.2)$$

U is the strain energy per unit volume;

μ, λ_m and D: Temperature-dependent material parameters;

$\bar{I}_1$: The first deviatoric strain invariant.

These parameter values were calculated as shown in the tables below, Curve fitting graphs for both material and tests are shown in the figures below.

Table 4.1 Arruda-Boyce parameters for H100044

μ	1.04156857
λ_m	3281.16456
D	9.723752396E-04

Table 4.2 Arruda-Boyce parameters for H40001

μ	0.953310266
λ_m	3404.83209
D	1.060178162E-03

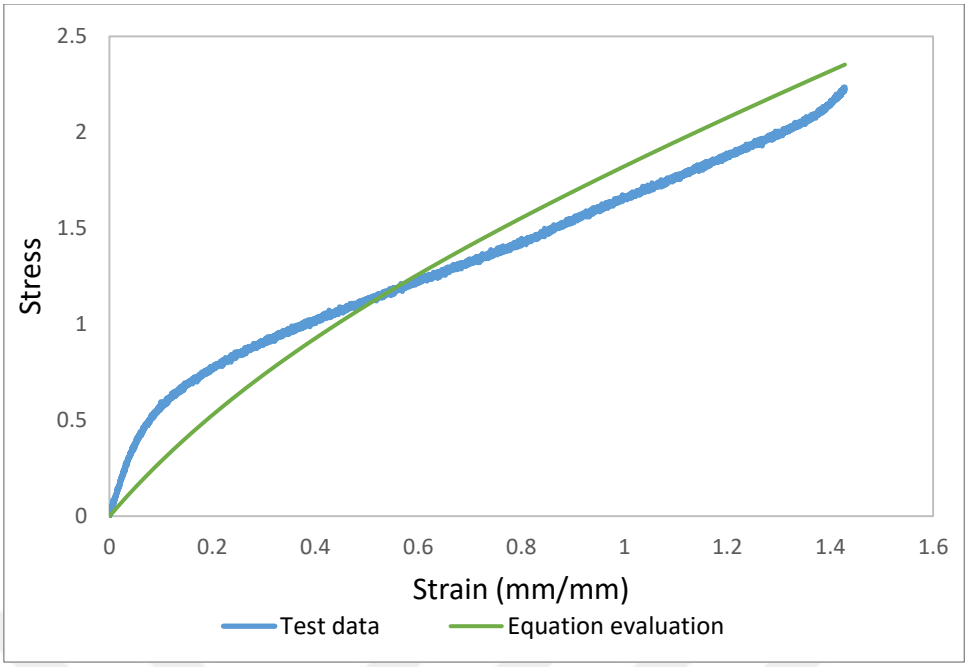

Figure 4.4 Arruda Boyce uniaxial modeling for 100044

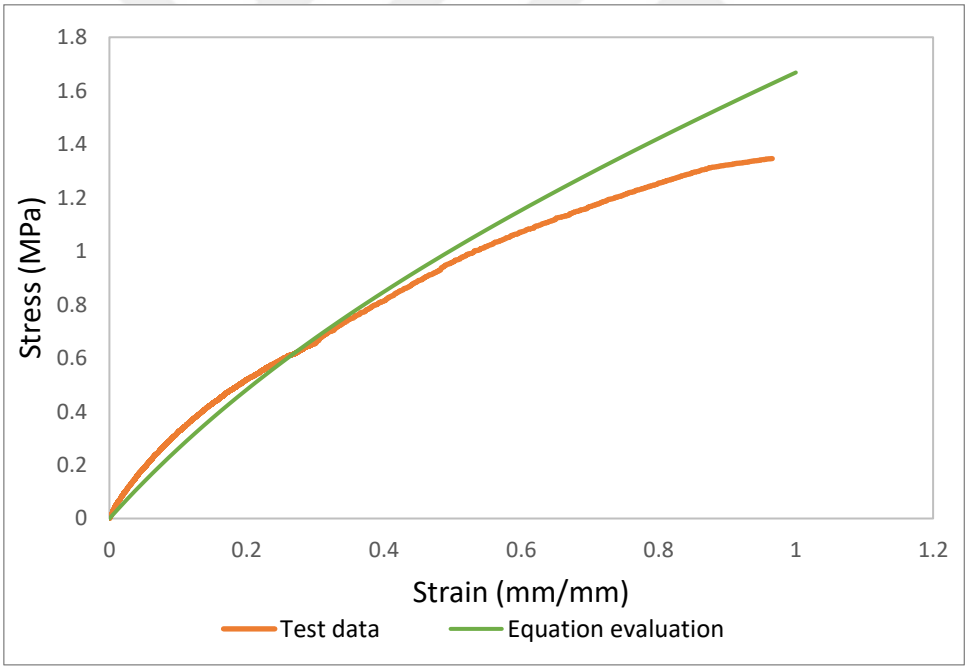

Figure 4.5 Arruda Boyce uniaxial modeling for 400010

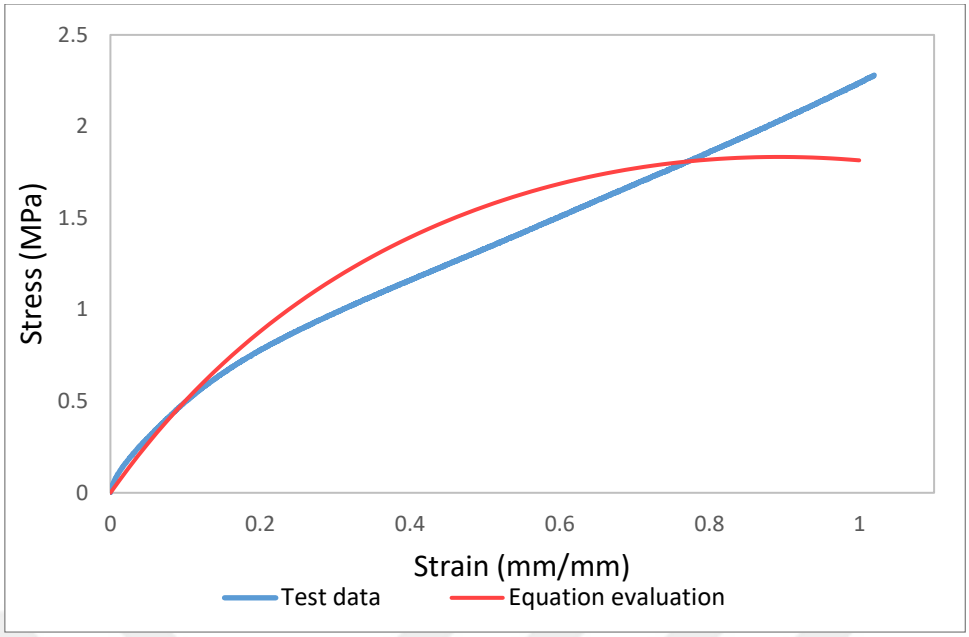

Figure 4.6 Arruda-Boyce planar results for 100044

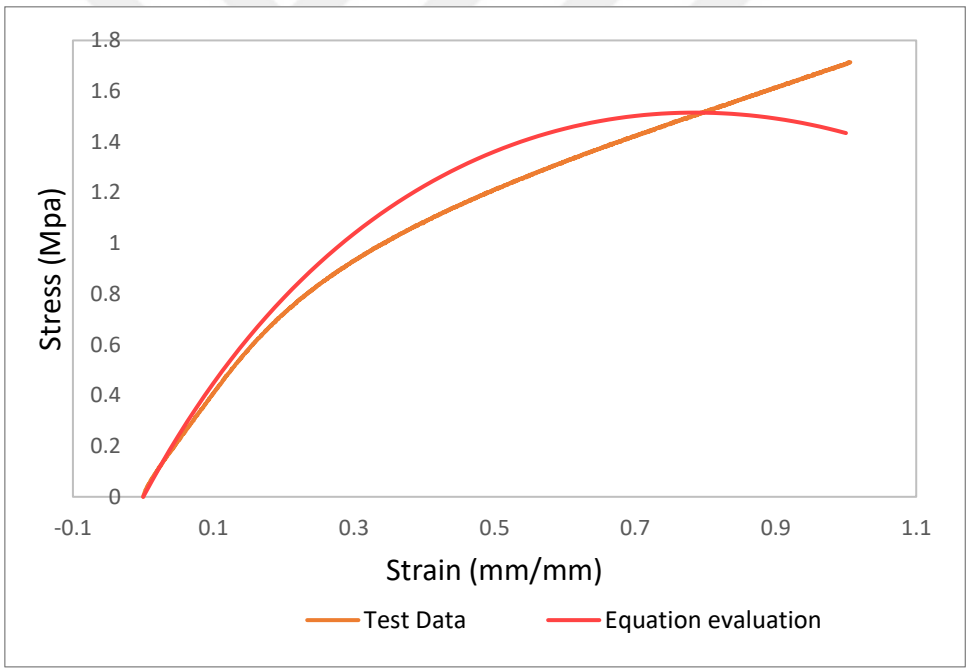

Figure 4.7 Arruda-Boyce planar results for 400010

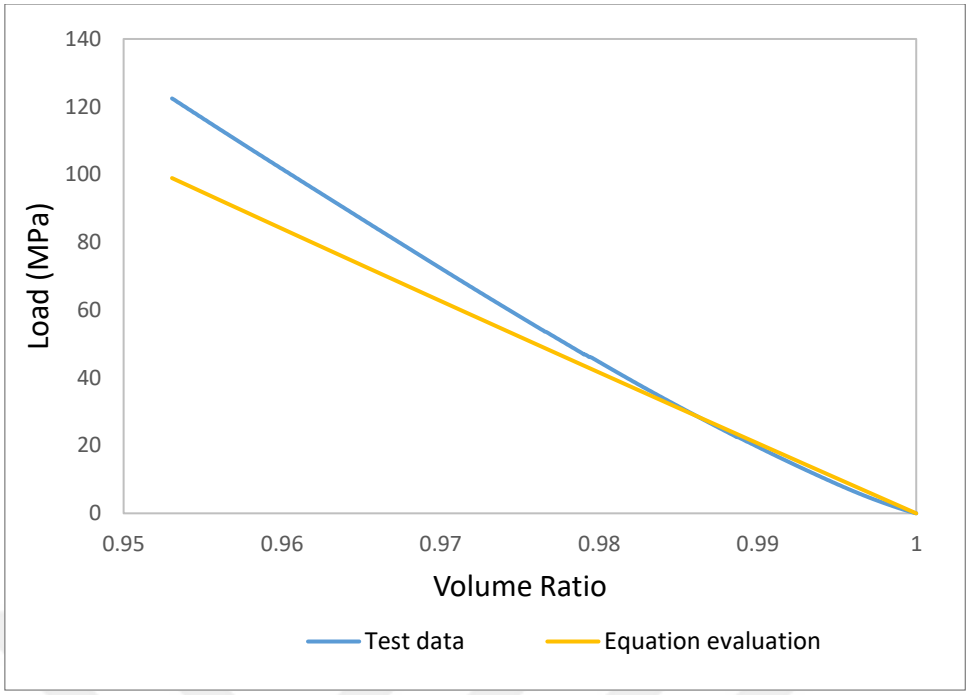

Figure 4.8 Arruda-Boyce Volumetric modeling for 100044

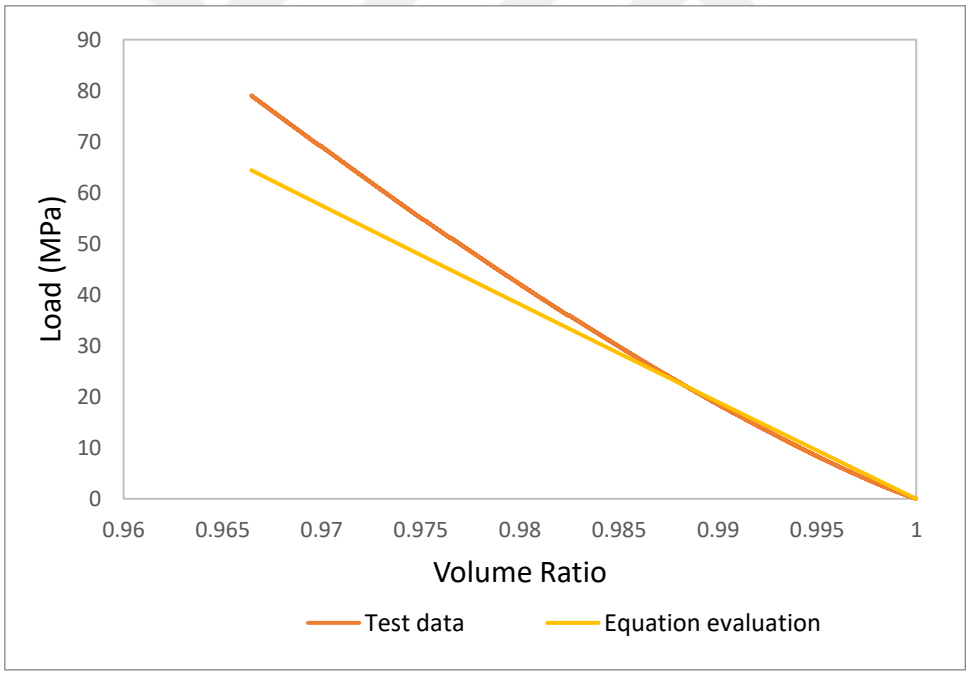

Figure 4.9 Arruda-Boyce Volumetric modeling for 400010

4.2.2 Full Polynomial Model

The Polynomial model can be represented in equation 4.3 below for compressible and isotropic elastomer. In this solution analysis, the second order is used to evaluate

material, coefficients are listed as shown in the table below. Stress-strain for curve fitting is represented in the figures below.

$$U = \sum_{i+j=1}^{N} C_{ij} \left(\bar{I}_1 - 3\right)^i \left(\bar{I}_2 - 3\right)^j + \sum_{i=1}^{N} \frac{1}{D_1} \left(J^{e\ell} - 1\right)^{2i} \quad (4.3)$$

U is the strain energy per unit volume;

N is a material parameter;

C_{ij} *and* D_i: are temperature-dependent material parameters, it can be determined from uniaxial, biaxial, and planar tests.

$\bar{I}_1$, $\bar{I}_2$ are the first and second deviatoric strain invariants.

Table 4.3 Polynomial model parameters for H10001

C01	6.40985839
C02	3.77451741
C11	-1.90281959
C10	-4.90135135
C20	0.432701930
D1	1.118516108E-03
D2	7.666966787E-06

Table 4.4 Polynomial model parameters for H40001

C01	3.05559860
C02	3.21196669
C11	-2.19403792

Table 4.4 Polynomial model parameters for H40001 (continued)

C10	-2.25191890
C20	0.507766036
D1	1.202042733E-03
D2	4.951202068E-06

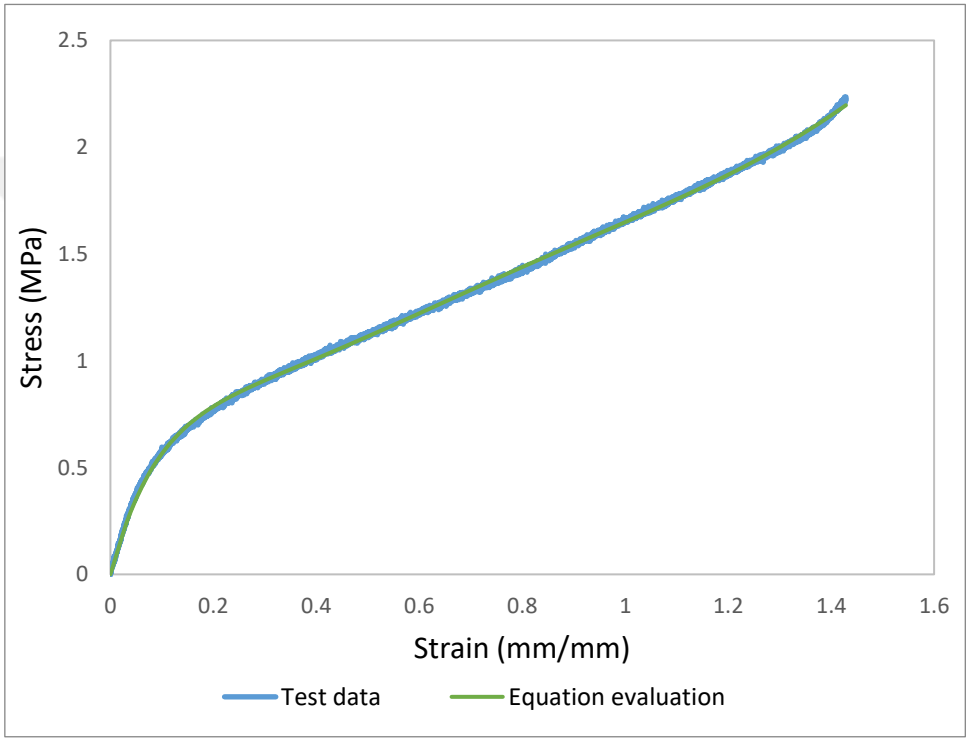

Figure 4.10 Polynomial uniaxial test result for H100044 specimen

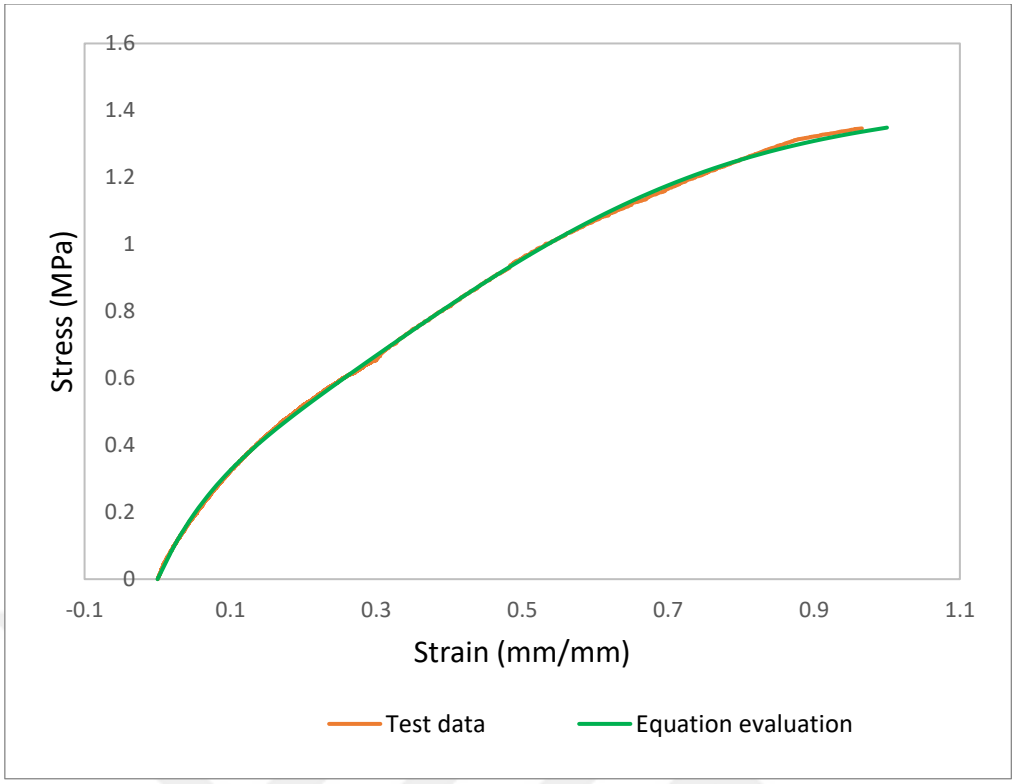

Figure 4.11 Polynomial uniaxial test result for H400010 specimen

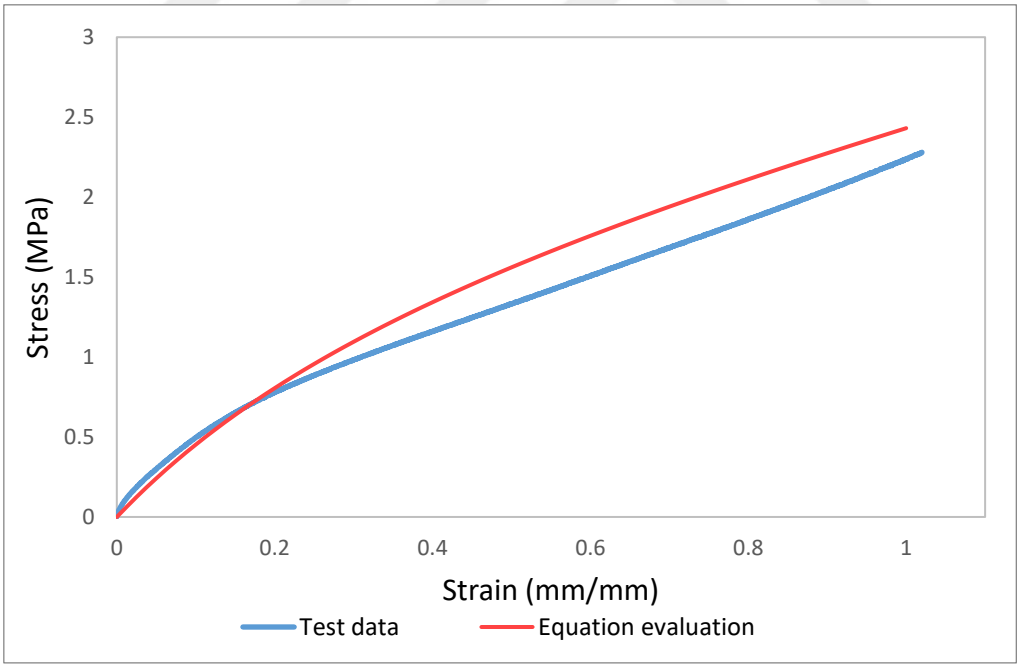

Figure 4.12 Planar results for H100044

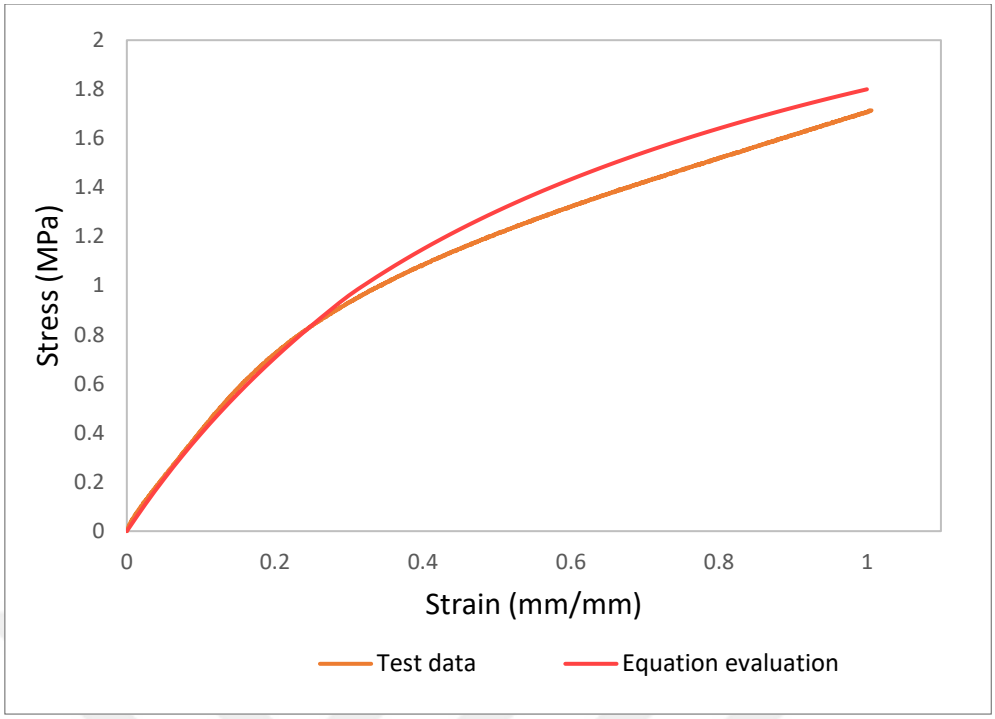

Figure 4.13 Planar results for H400010

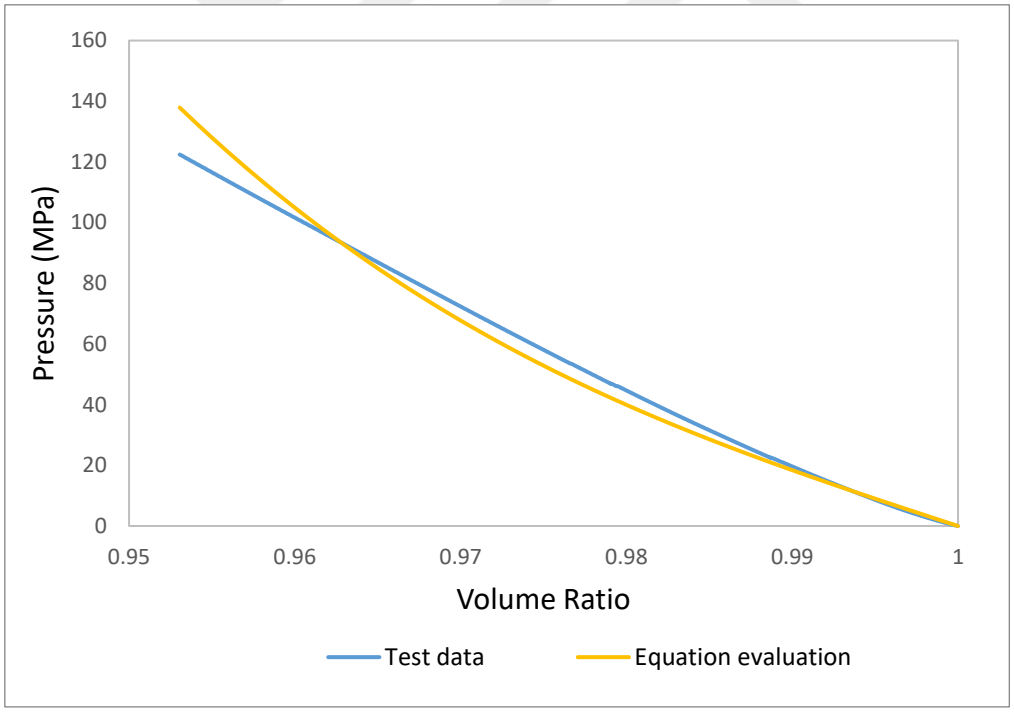

Figure 4.14 Polynomial volumetric test result for H100044 specimen

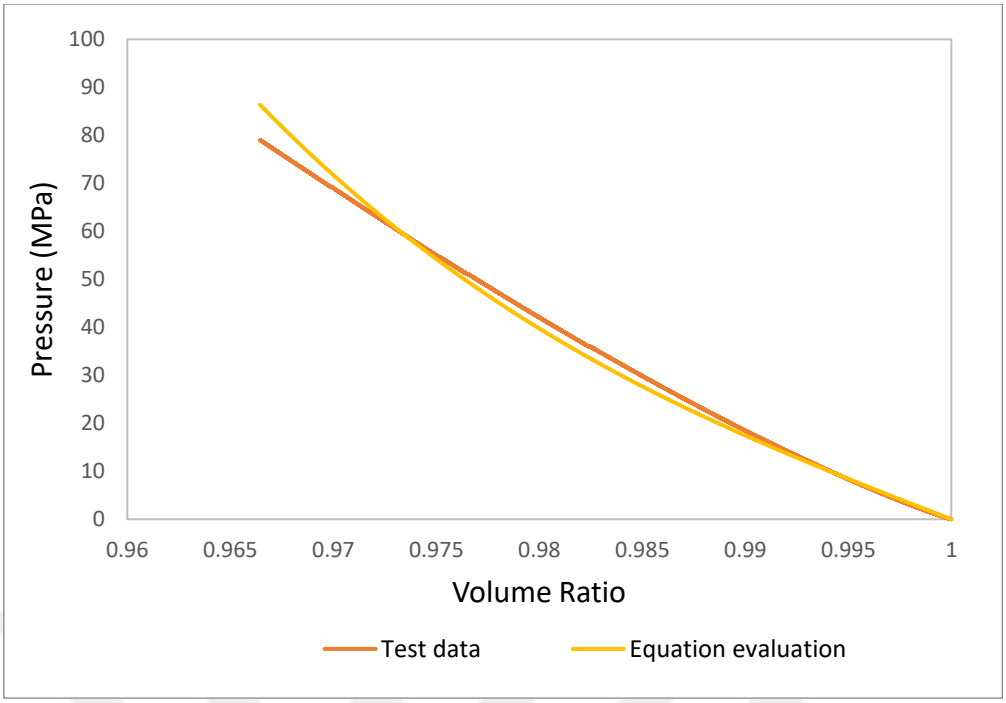

Figure 4.15 Polynomial volumetric test result for H400010 specimen

4.2.3 Moony-Rivlin Model

Moony-Rivlin is the first order of polynomial model, it is derived by [21] [22], the model equation is shown below:

$$U = C_{10}\left(\bar{I}_1 - 3\right) + C_{01}\left(\bar{I}_2 - 3\right) + \frac{1}{D_1}\left(J^{el} - 1\right)^2 \qquad (4.4)$$

U is the strain energy per unit volume;

C_{10}, C_{01} *and* D_1: Temperature-dependent material parameters;

$\bar{I}_1$: The first deviatoric strain invariant

Table 4.5 Mooney-Rivlin parameters for H100044

C01	0.737112984
C10	0.103860912
D1	9.642244687E-04

Table 4.6 Mooney-Rivlin parameters for H400010

$C01$	0.499477352
C10	0.125155808
D1	1.053436549E-03

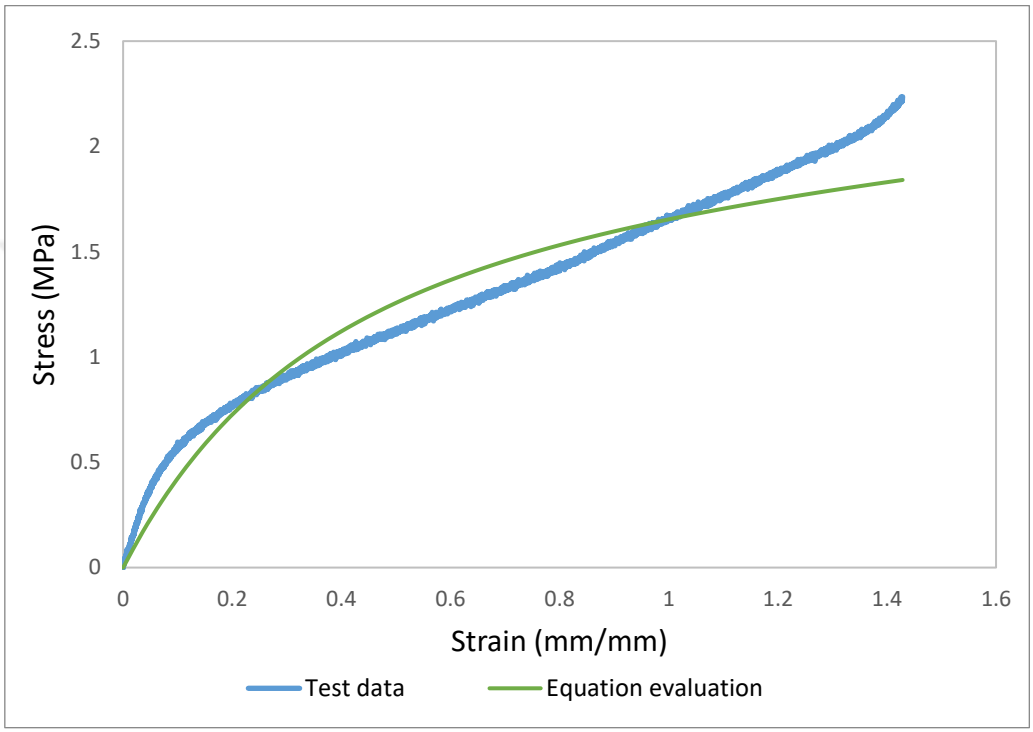

Figure 4.16 Moony-Rivlin uniaxial test result for H100044 specimen

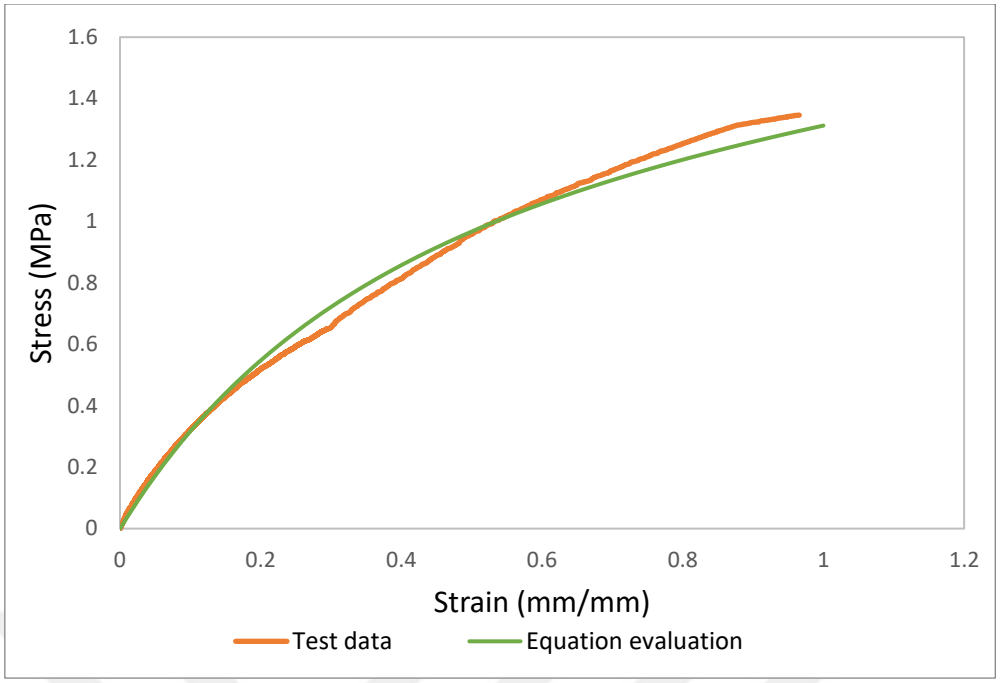

Figure 4.17 Moony-Rivlin uniaxial test result for H400010 specimen

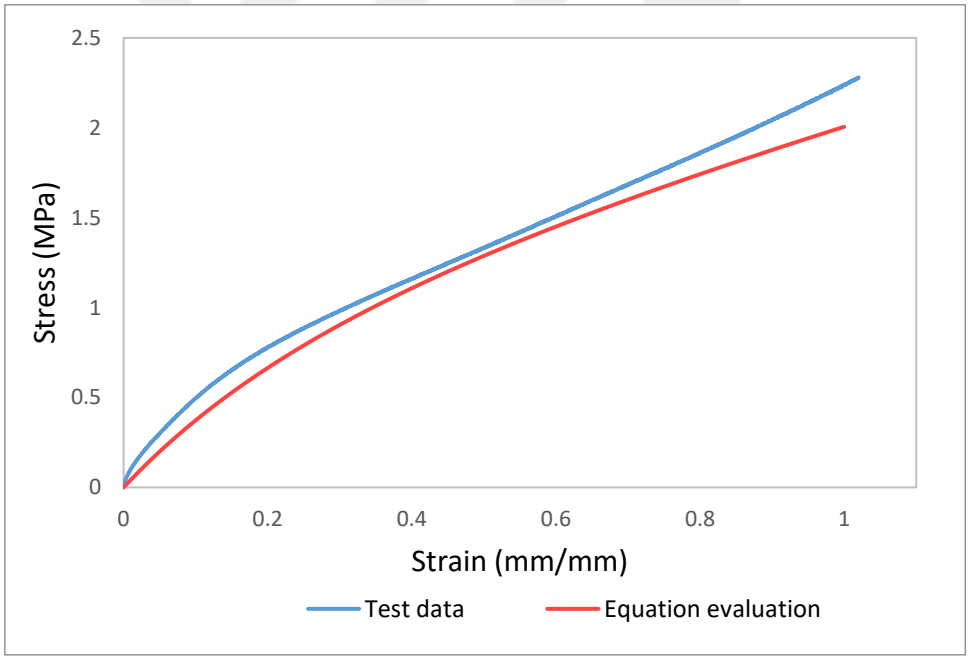

Figure 4.18 Mooney-Rivlin planar results for H100044

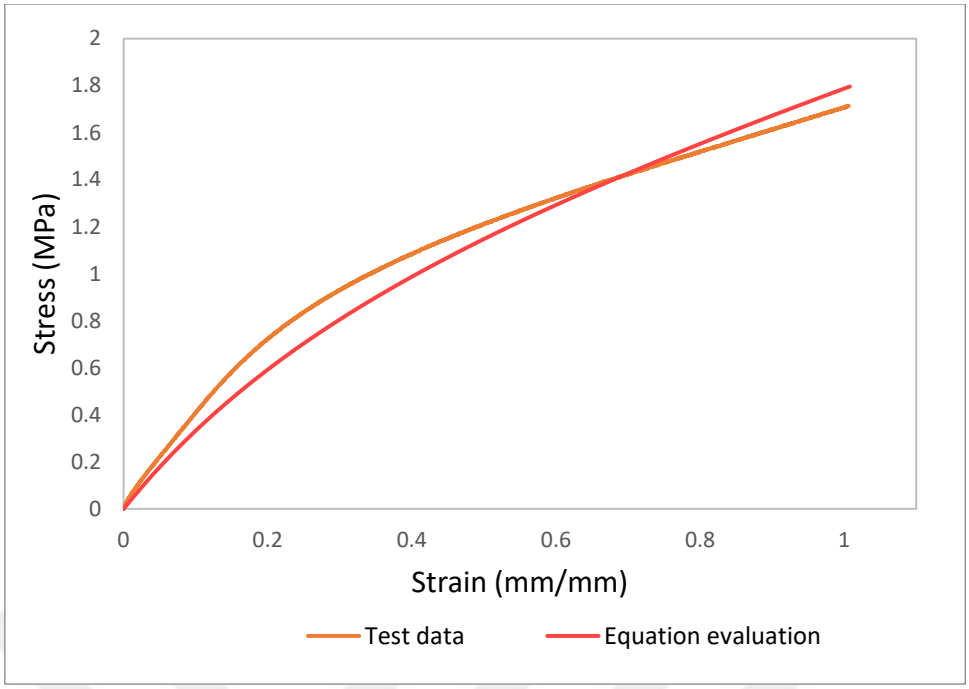

Figure 4.19 Mooney-Rivlin planar results for H400010

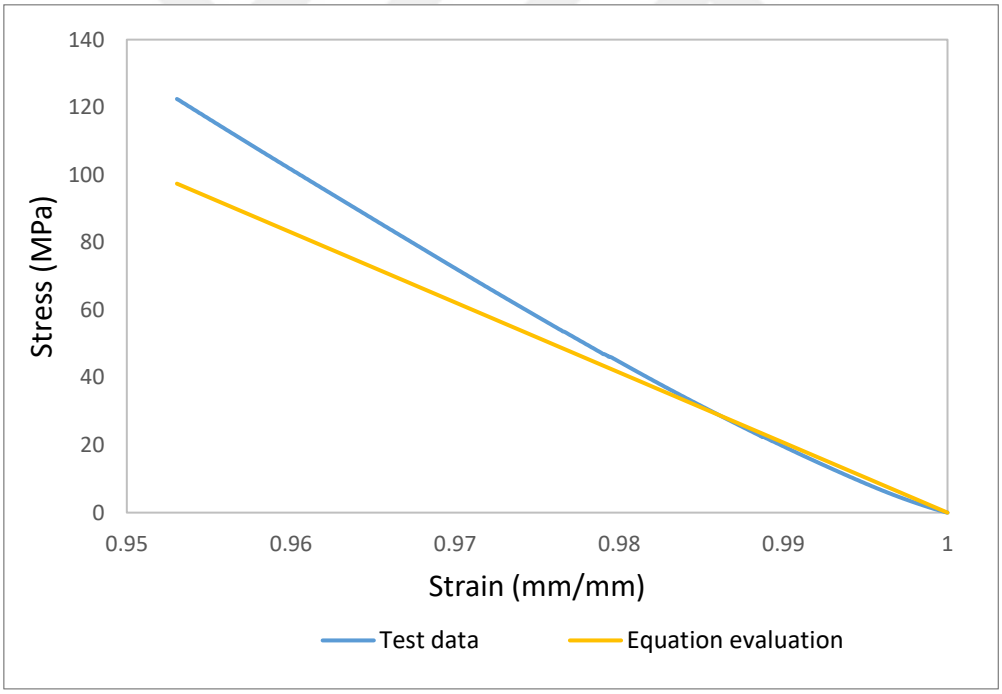

Figure 4.20 Moony-Rivlin volumetric test result for H100044 specimen

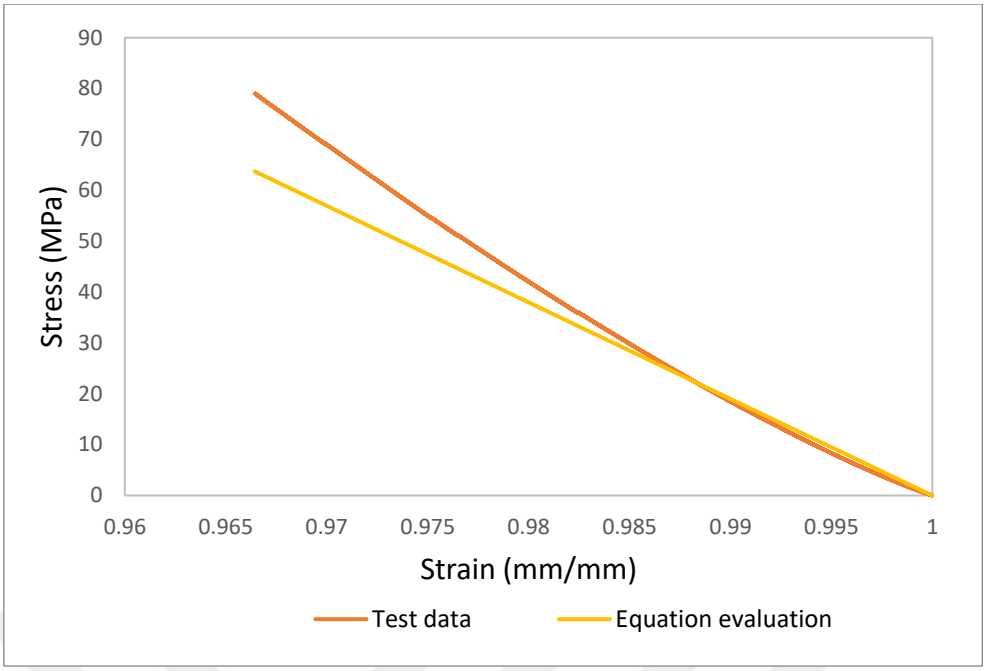

Figure 4.21 Moony-Rivlin volumetric test result for H400010 specimen

4.2.4 Reduced Polynomial Model

This model does not contain I2 dependency. Generally, Strain energy function is less sensitive to the change in I2 compared to the sensitivity for variation in I1. The elimination of I2 term from energy function appears to improve the ability to predict complicated strain behavior in case of limited test data available. The form is represented in equation 4.5 below,

$$U = \sum_{i=1}^{N} C_{i0} \left(\bar{I}_1 - 3\right)^i + \sum_{i=1}^{N} \frac{1}{D_1} \left(J^{e\ell} - 1\right)^{2i} \tag{4.5}$$

U is the strain energy per unit volume;

N is a material parameter;

C_{i0} *and* D_i: are temperature dependent material parameters.

$\bar{I}_1$ are the first deviatoric strain invariants.

Table 4.7 Reduced polynomial parameters for H100044

C10	0.618000436
C20	-2.929612005E-02
D1	9.747434790E-04
D2	1.310381215E-05

Table 4.8 Reduced polynomial parameters for H40001

C10	0.541545978
C20	-4.266347466E-02
D1	1.097620614E-03
D2	7.273682241E-06

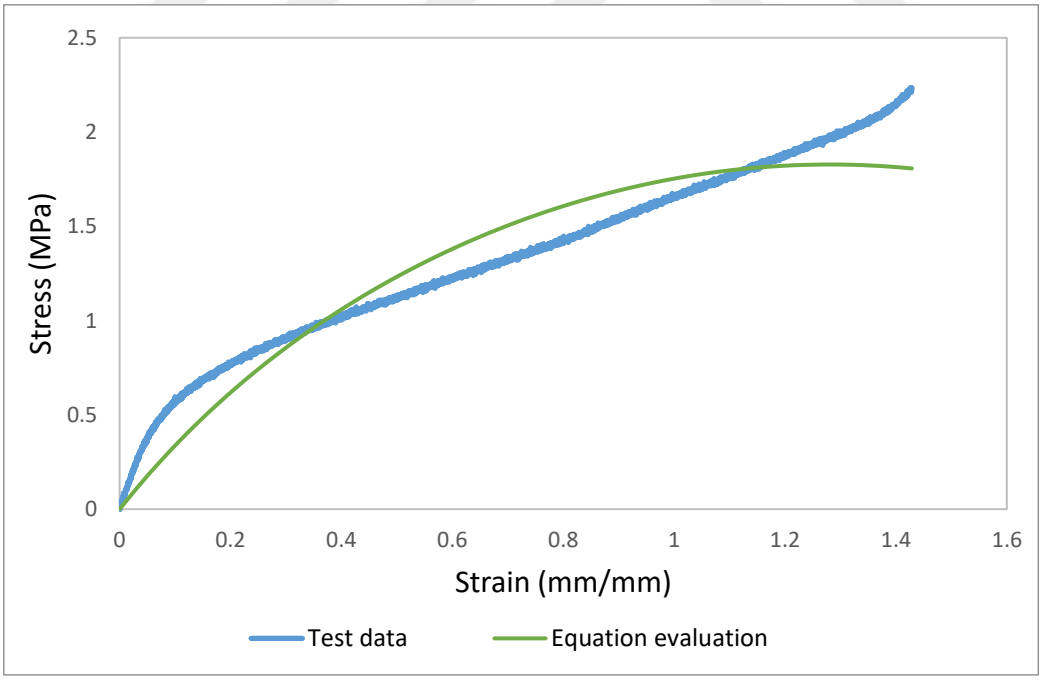

Figure 4.22 Reduced polynomial Uniaxial modeling for 100044

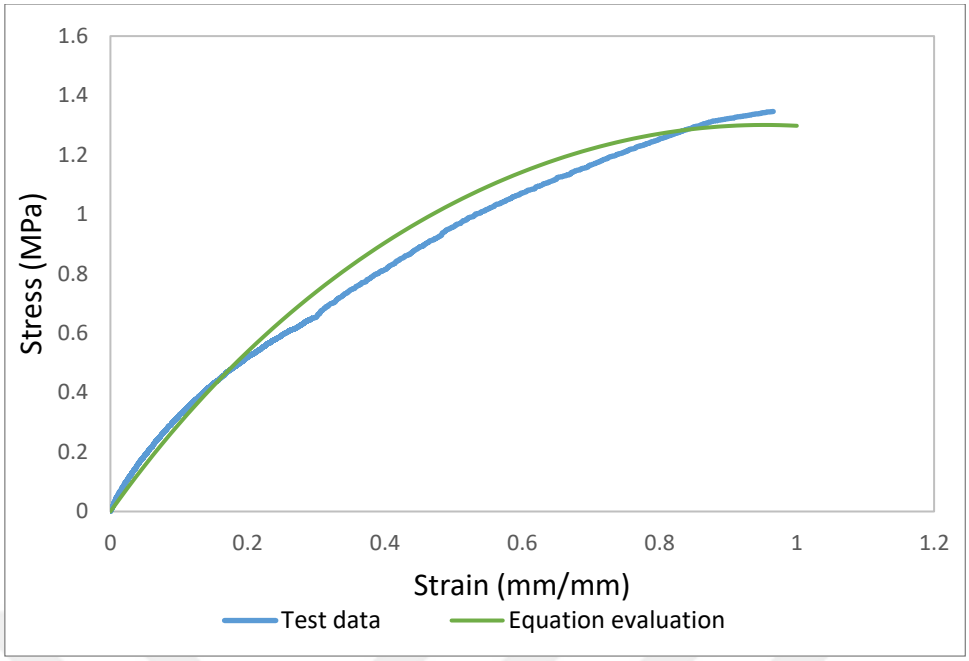

Figure 4.23 Reduced polynomial Uniaxial modeling for 400010

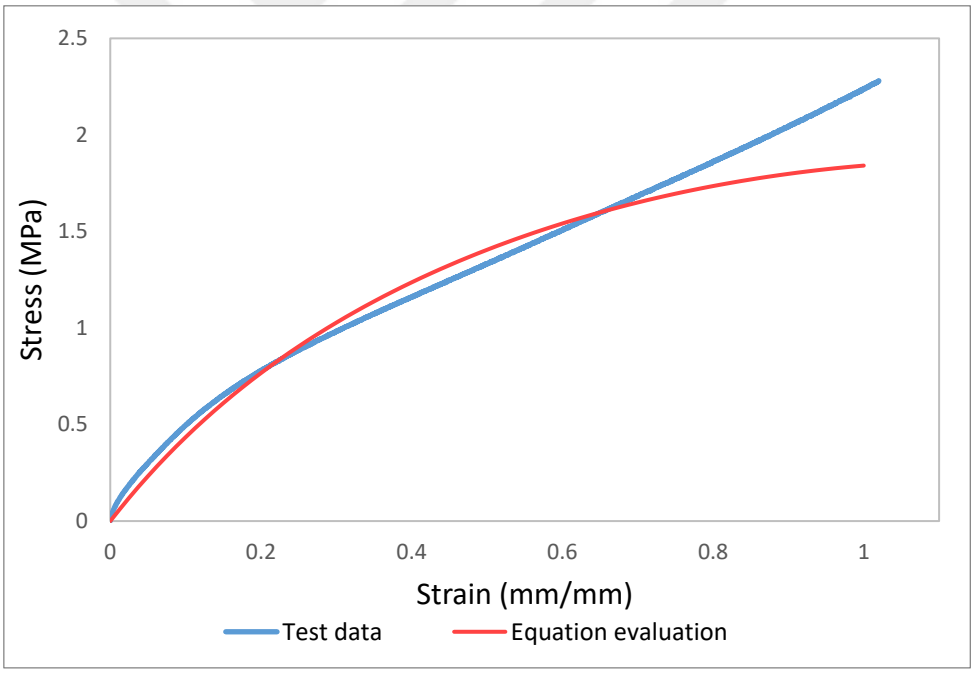

Figure 4.24 Reduced polynomial planar results for H100044

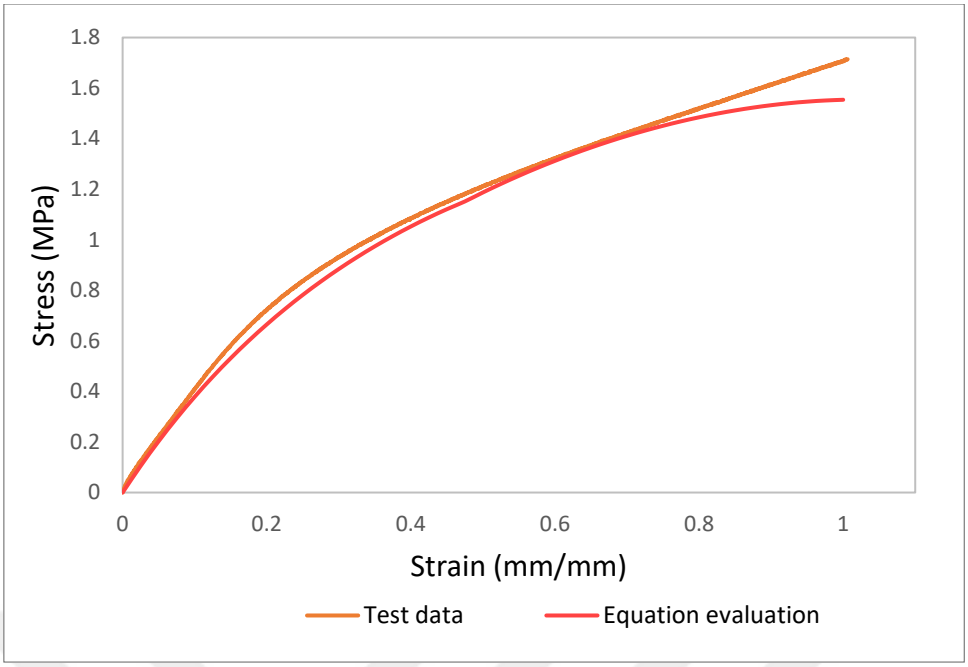

Figure 4.25 Reduced polynomial planar results for H400010

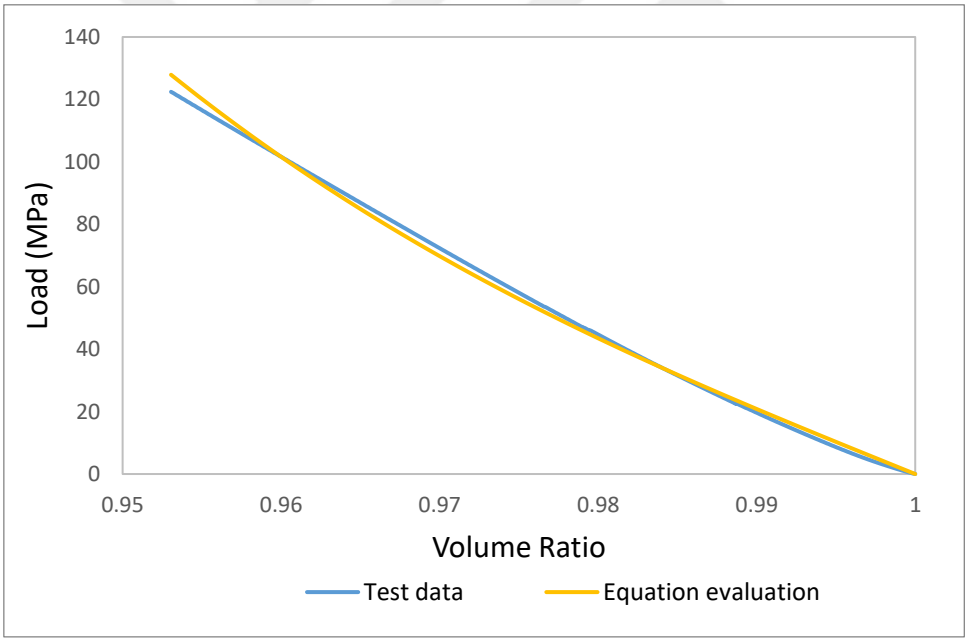

Figure 4.26 Reduced polynomial Volumetric modeling for 100044

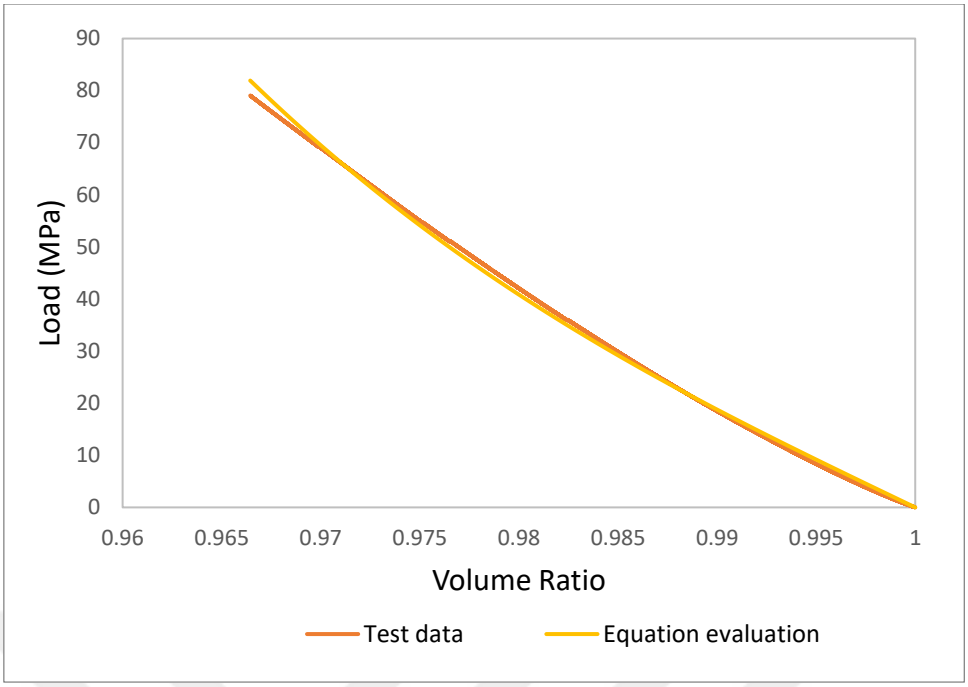

Figure 4.27 Reduced polynomial Volumetric modeling for 400010

4.2.5 Neo-Hookean Model

This model represents the first order Reduced polynomial model, it based on phenomenological descriptions for material. Form is shown in equation 4.6 below.

$$U = C_{10}\left(\bar{I}_1 - 3\right) + \frac{1}{D_1}\left(J^{el} - 1\right)^2 \tag{4.6}$$

U is the strain energy per unit volume;

C_{10}, D_1: Temperature-dependent material parameters;

$\bar{I}_1$: The first deviatoric strain invariant

Table 4.9 Neo-Hooke N1 10001

C10	0.520784316
D1	8.428745339E-04

Table 4.10 Neo-Hooke N1 40001

C10	0.476655153
D1	9.450181728E-04

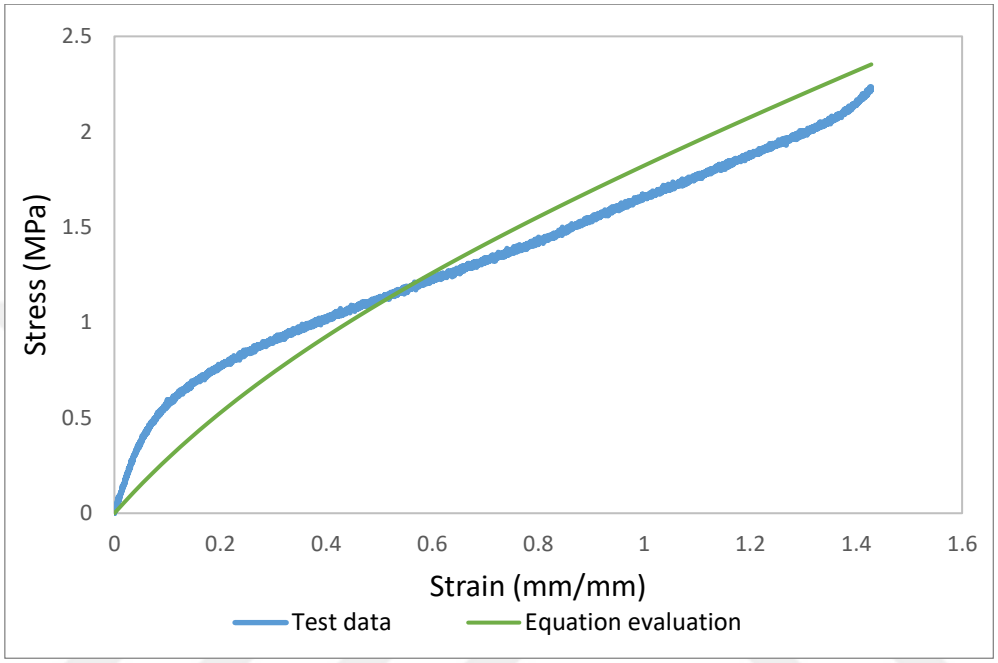

Figure 4.28 Neo-Hooke uniaxial model for H100044

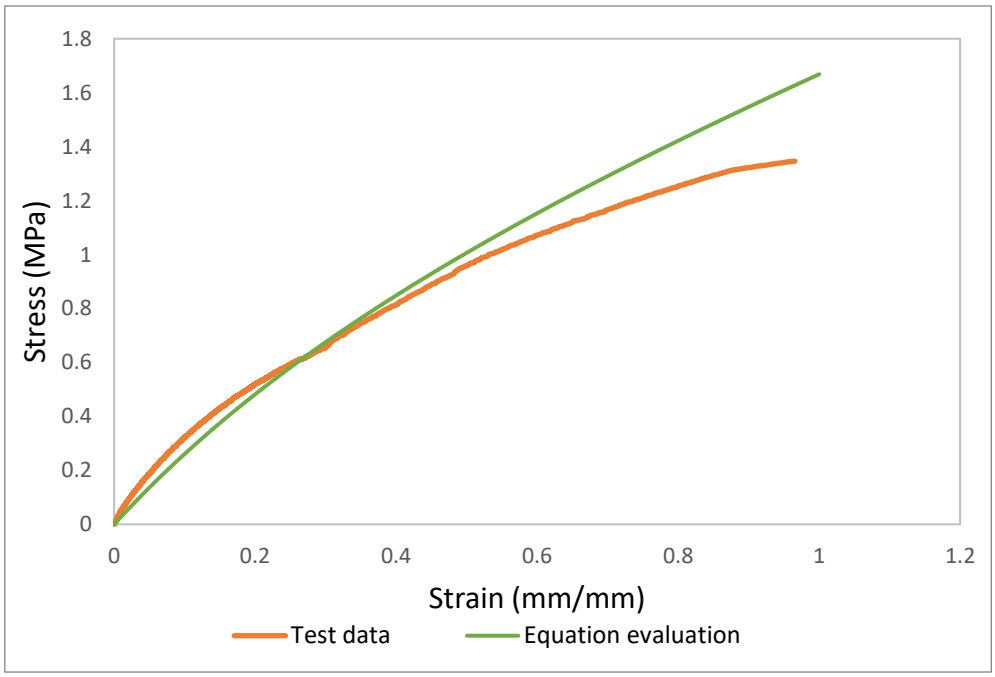

Figure 4.29 Neo-Hooke uniaxial model for H400010

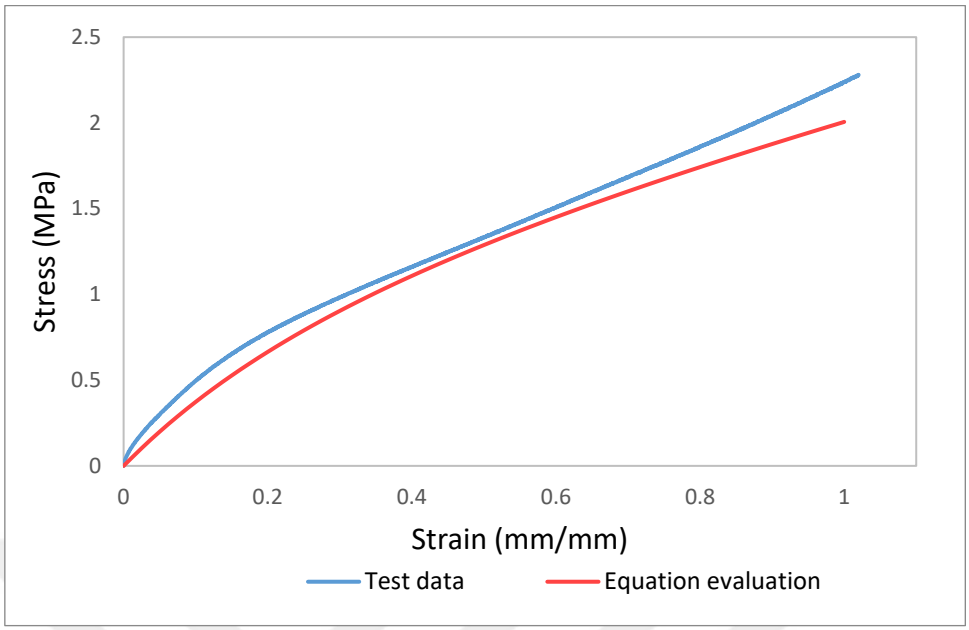

Figure 4.30 Planar results for H100044

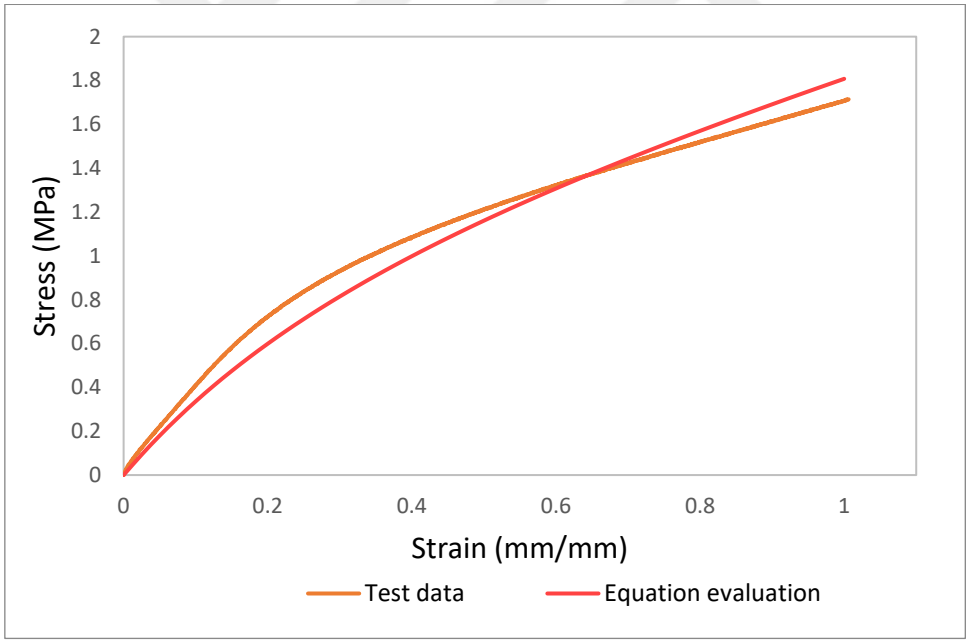

Figure 4.31 Planar results for H400010

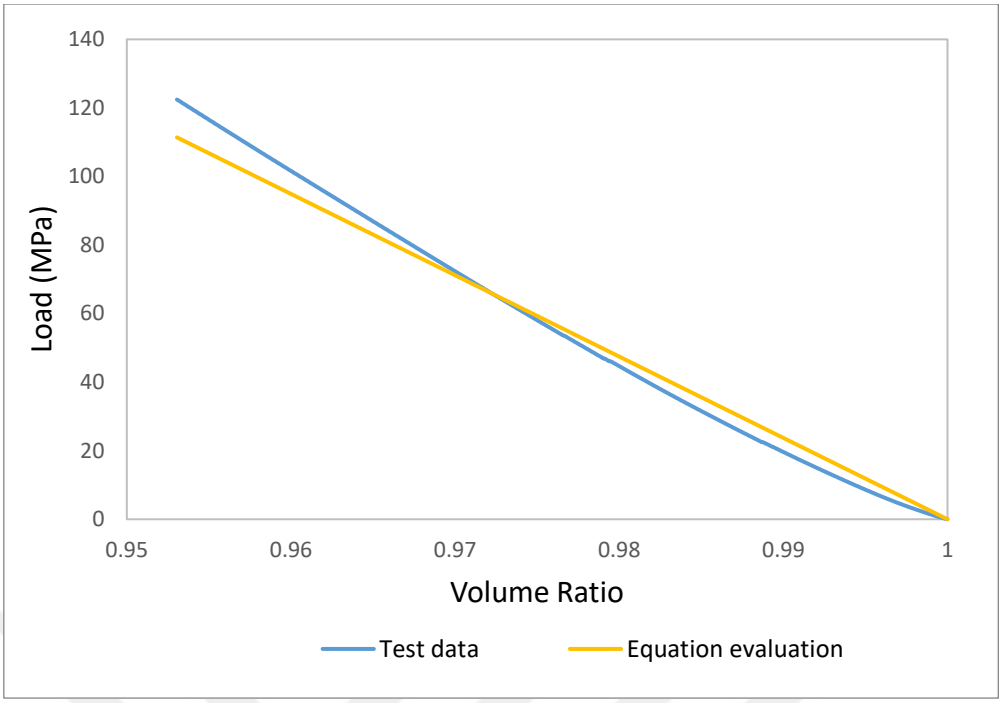

Figure 4.32 Neo-Hooke volumetric model for H100044

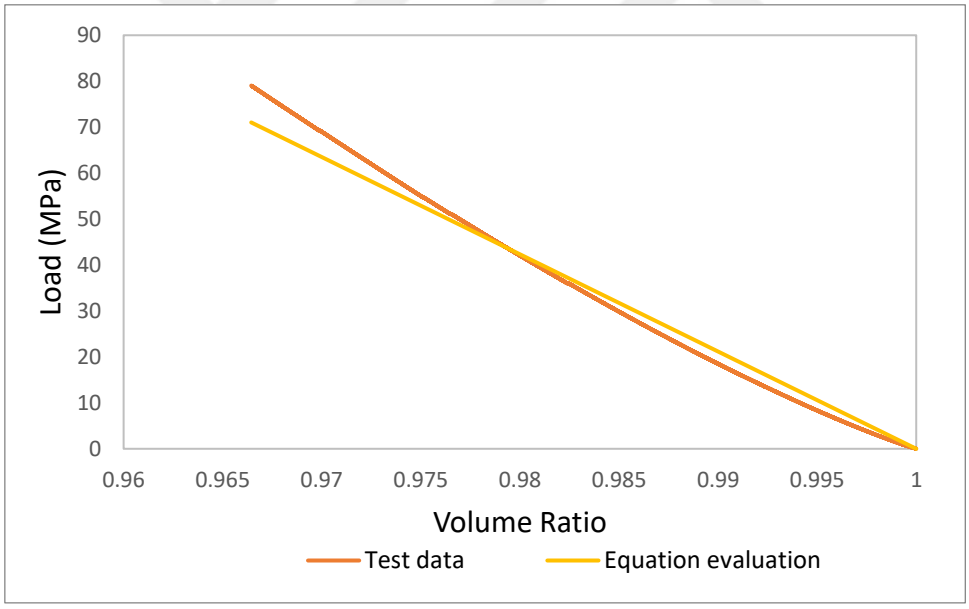

Figure 4.33 Neo-Hooke volumetric model for H400010

4.2.6 Yeoh Model

Yeoh model can be derived from third-order reduced-polynomial form, it was first introduced by [23], equation 4.7 is represented below.

$$U = C_{10}(\bar{I}_1 - 3) + C_{20}(\bar{I}_1 - 3)^2 + C_{30}(\bar{I}_1 - 3)^3 + \frac{1}{D_1}(J^{el} - 1)^2 + \frac{1}{D_2}(J^{el} - 1)^4 + \frac{1}{D_3}(J^{el} - 1)^6 \quad (4.7)$$

U is the strain energy per unit volume;

C_{i0} *and* D_i: are temperature-dependent material parameters.

$\bar{I}_1$ *is the first deviatoric strain invariants.*

Table 4.11 Yeoh Model parameters for H100044

C10	0.737681807
C20	-0.134273200
C30	1.964328727E-02
D1	1.058086406E-03
D2	5.169864694E-06
D3	-2.765533078E-08

Table 4.12 Yeoh Model parameters for H40001

C10	0.564529642
C20	-9.916937295E-02
C30	1.785868489E-02
D1	1.171157101E-03
D2	3.339201482E-06
D3	-1.018970646E-08

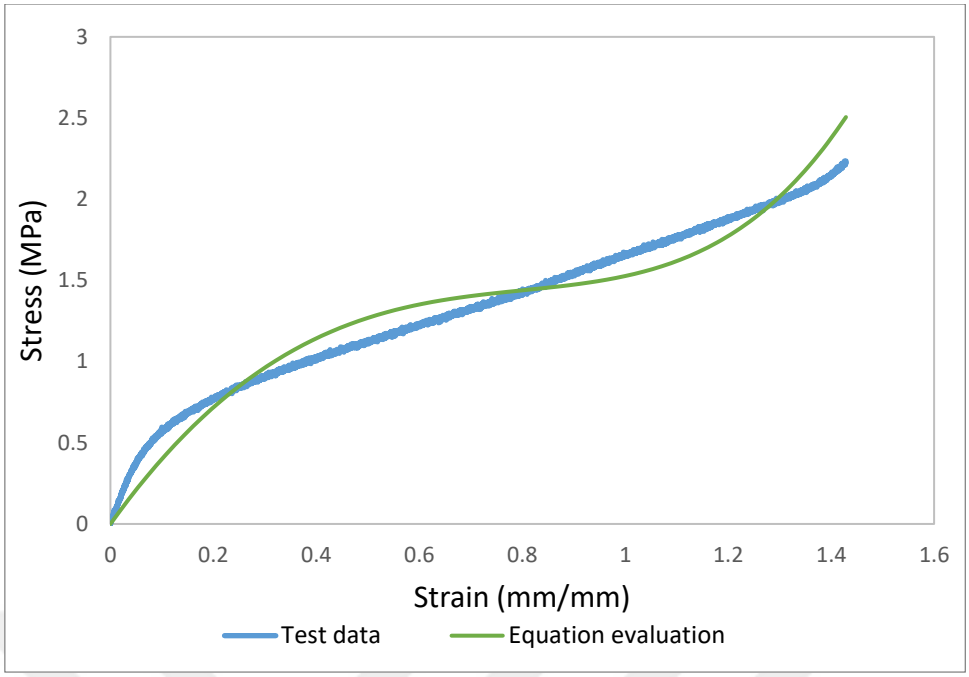

Figure 4.34 Yeoh Uniaxial model for H100044

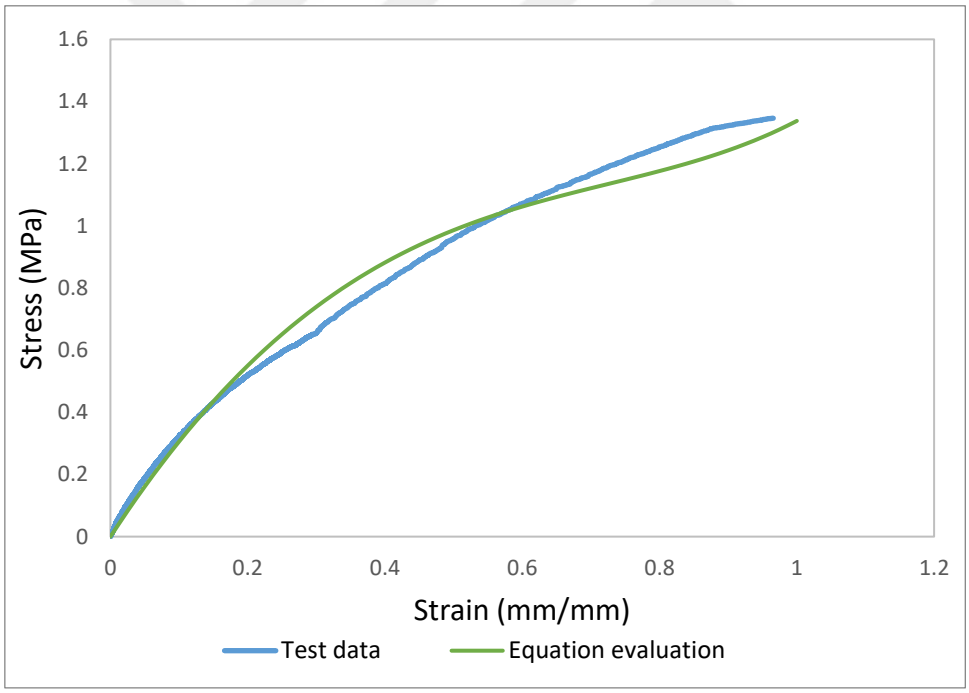

Figure 4.35 Yeoh Uniaxial model for H40001

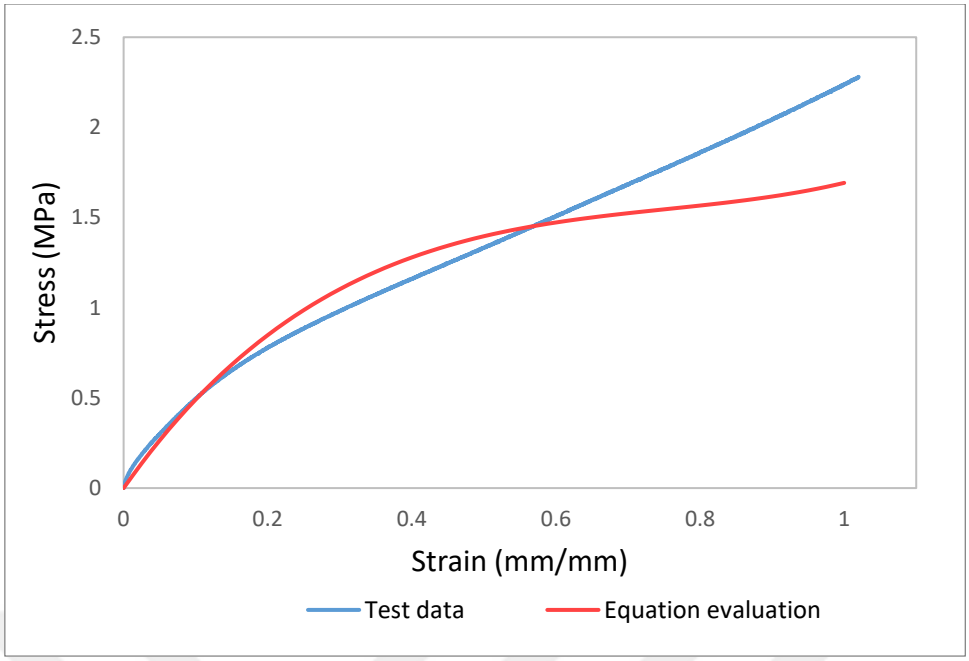

Figure 4.36 Planar results for H100044

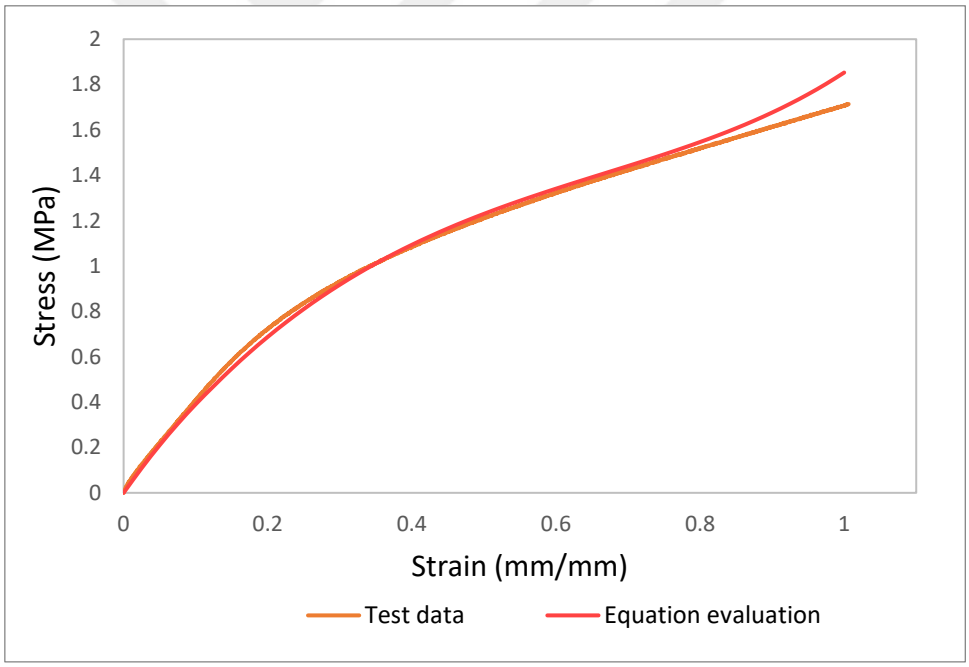

Figure 4.37 Planar results for H400010

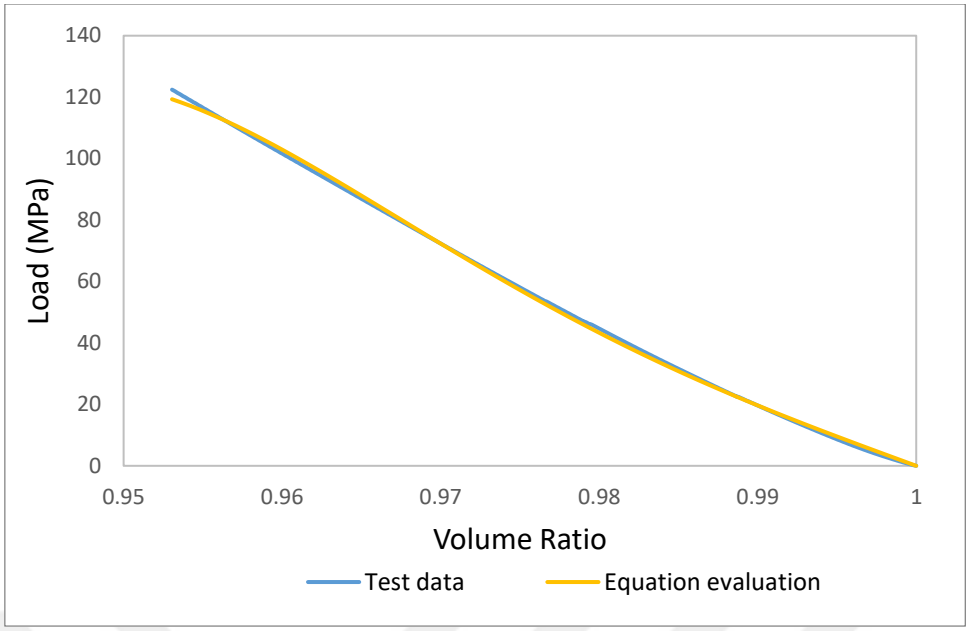

Figure 4.38 Yeoh volumetric model for H100044

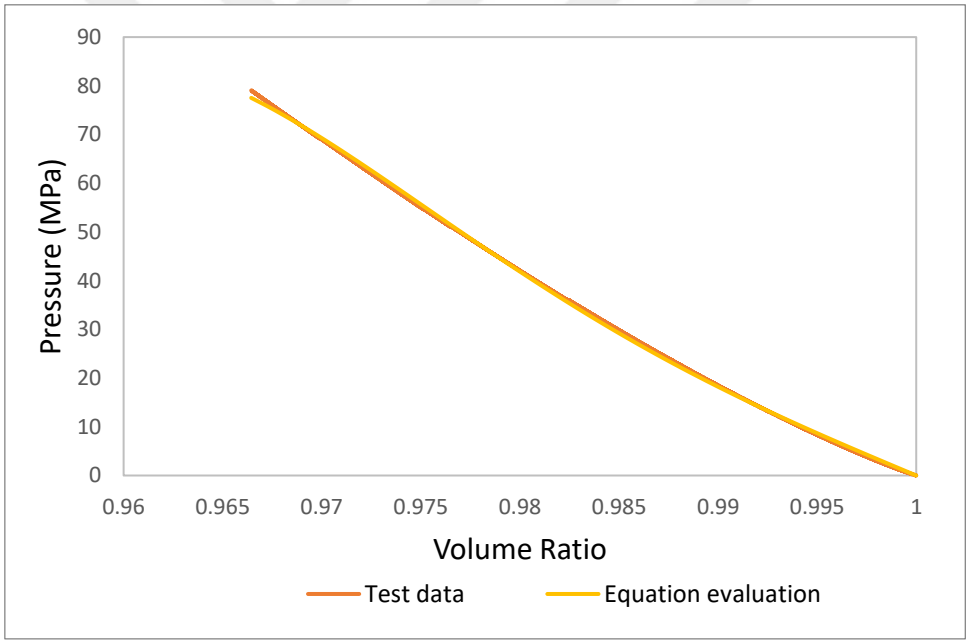

Figure 4.39 Yeoh volumetric model for H40001

4.2.7 Ogden Model

The Ogden model was first proposed in 1972 by [24]. Coefficients for the first and second orders have been evaluated. The general equation is shown in equation below.

$$U = \sum_{i=1}^{N} \frac{2\mu_i}{\alpha_i^2} \left(\lambda_1^{-\alpha_i} + \lambda_2^{-\alpha_i} + \lambda_3^{-\alpha_i} - 3\right) + \sum_{i=1}^{N} \frac{1}{D_1} \left(j^{e\ell} - 1\right)^{2i} \quad (4.8)$$

$\overline{\lambda}_i$ are the deviatoric principal stretches $\overline{\lambda}_i = J^{-\frac{1}{3}} \lambda_I$, $\lambda_I$are the principal stretches;

N is a material parameter;

$\mu_i, \alpha_i \; and \; D_i$: are temperature dependent material parameters.

The initial shear modulus and bulk modulus for Ogden are represented by Mooney-Rivlin and neo-Hookean forms can also be found from this general Ogden energy potential for particular μ_i, α_i.

Table 4.13 First order Ogden parameters for H100044

μ	1.56942683
α	4.841725165E-02
D	8.428745339E-04

Table 4.14 First order Ogden parameters for H40001

μ	1.19978779
α	0.137054314
D	9.450181728E-04

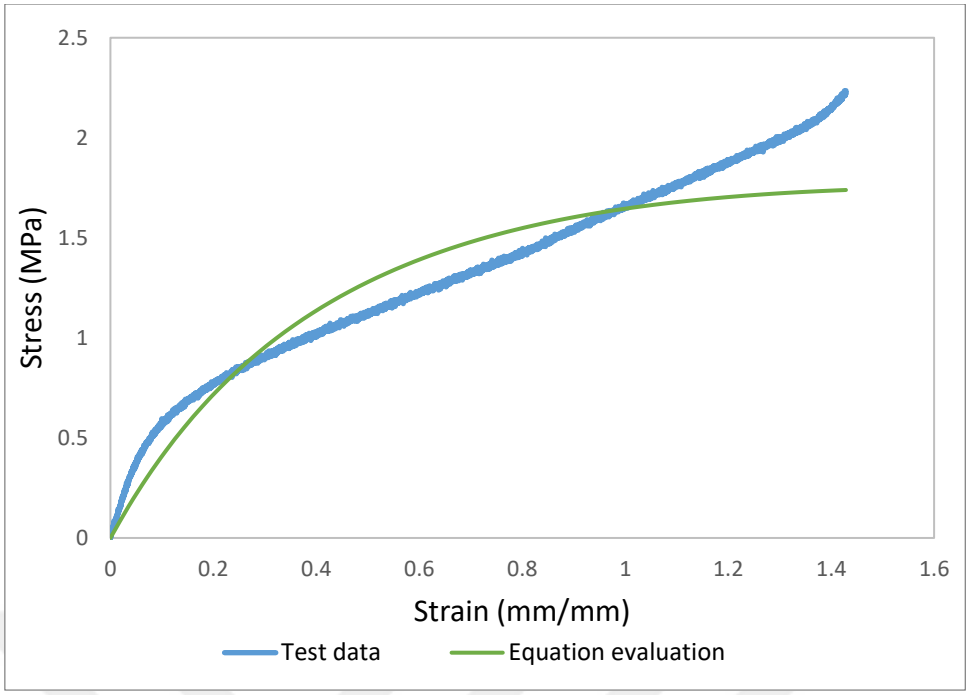

Figure 4.40 First order Ogden uniaxial test results for H100044

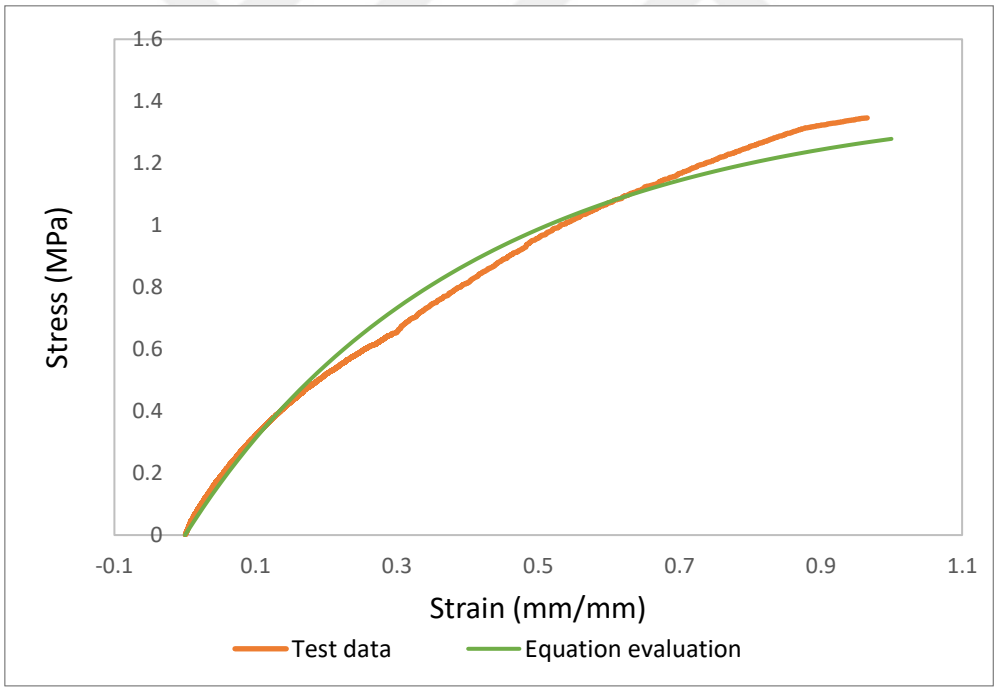

Figure 4.41 First order Ogden uniaxial test results for H400010

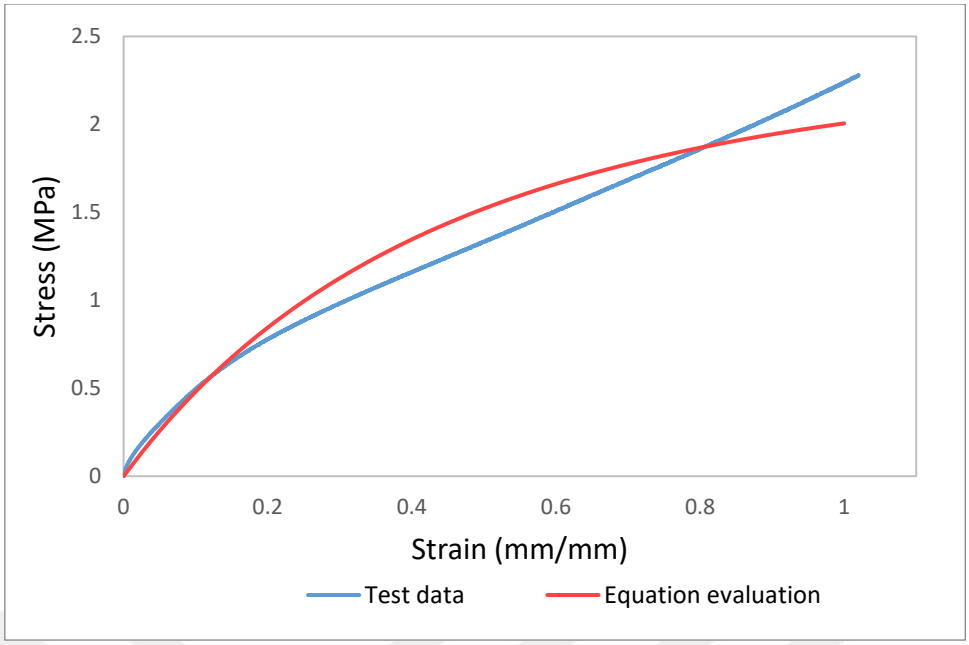

Figure 4.42 First order Ogden planar results for H100044

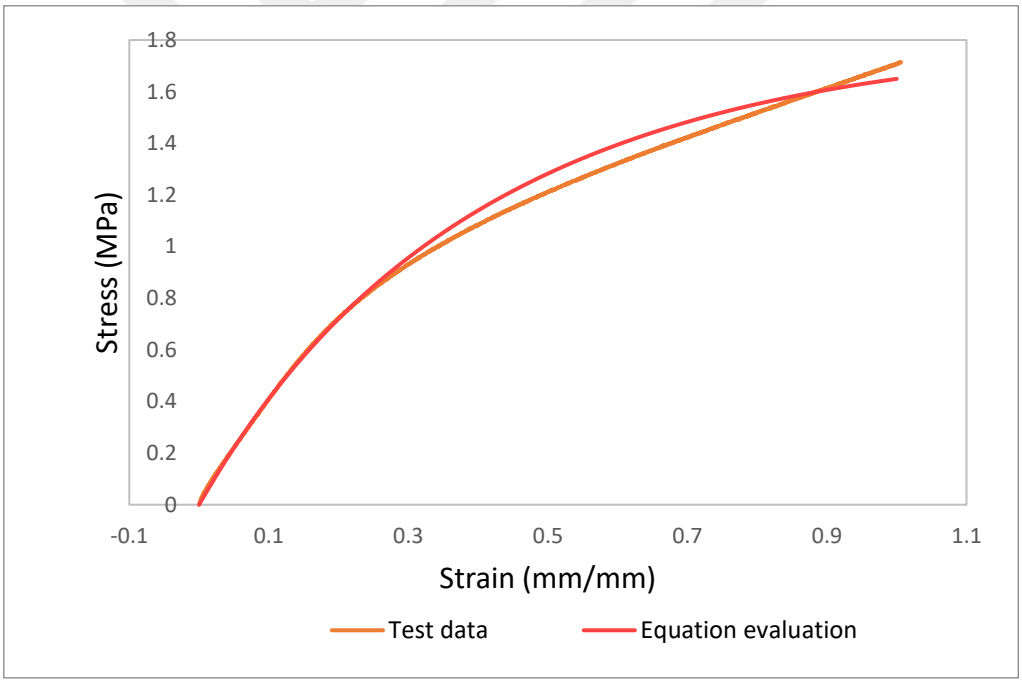

Figure 4.43 First order Ogden planar results for H400010

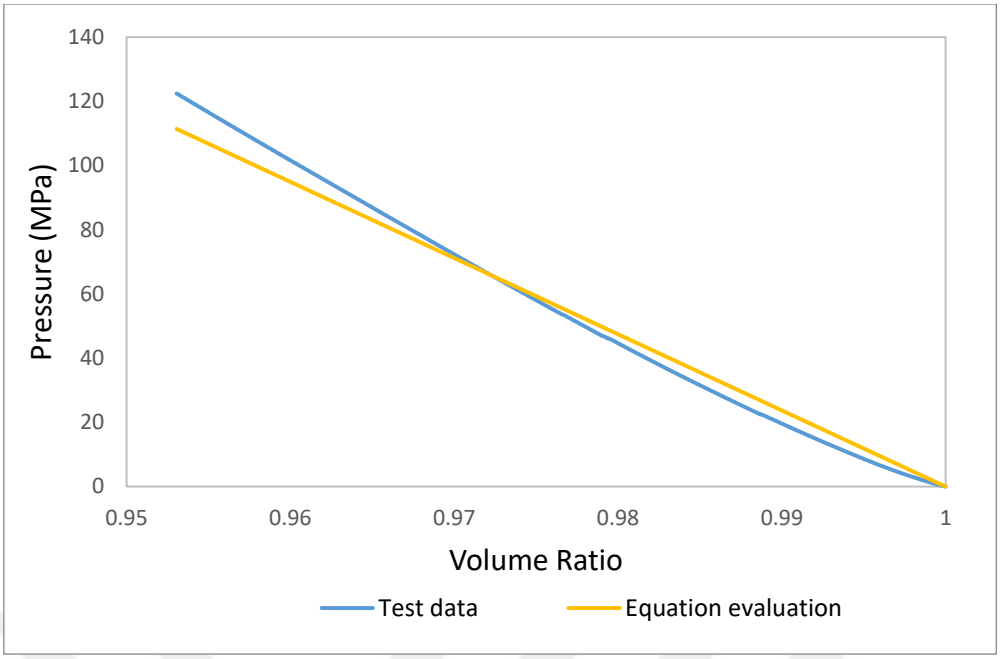

Figure 4.44 First-order Ogden volumetric test results for H100044

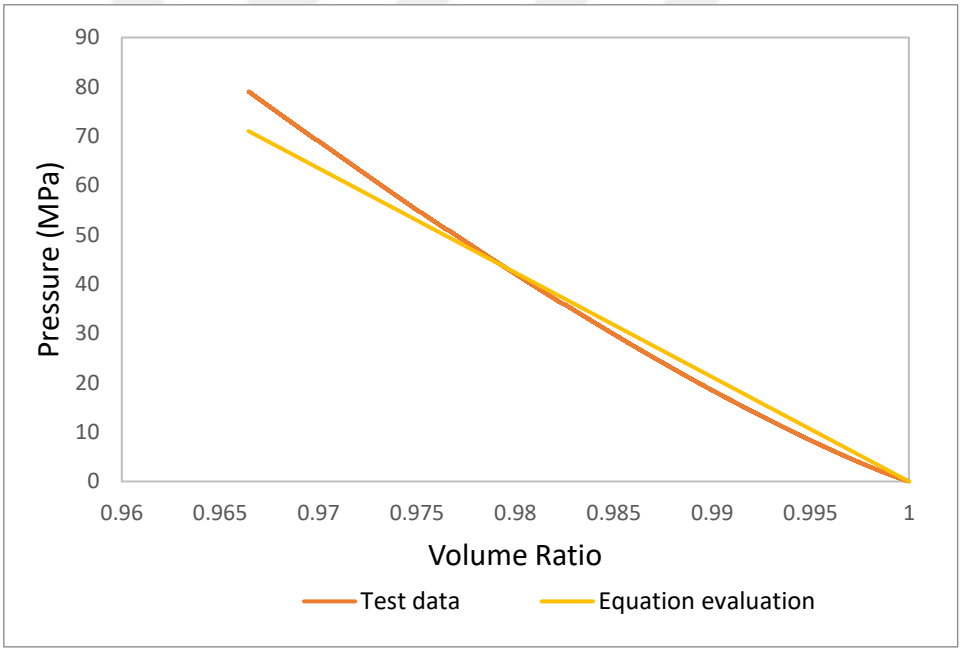

Figure 4.45 First-order Ogden volumetric test results for H400010

Table 4.15 Ogden parameters for H100044

$\mu 1$	1.56942683
$\mu 2$	4.74099315
$\alpha 1$	4.841725165E-02
$\alpha 2$	-7.94335790
D1	8.428745339E-04
D2	1.310381215E-05

Table 4.16 Ogden parameters for H400010

$\mu 1$	-0.325083366
$\mu 2$	1.90047934
$\alpha 1$	5.82183916
$\alpha 2$	-8.75920670
D1	1.097620614E-03
D2	7.273682241E-06

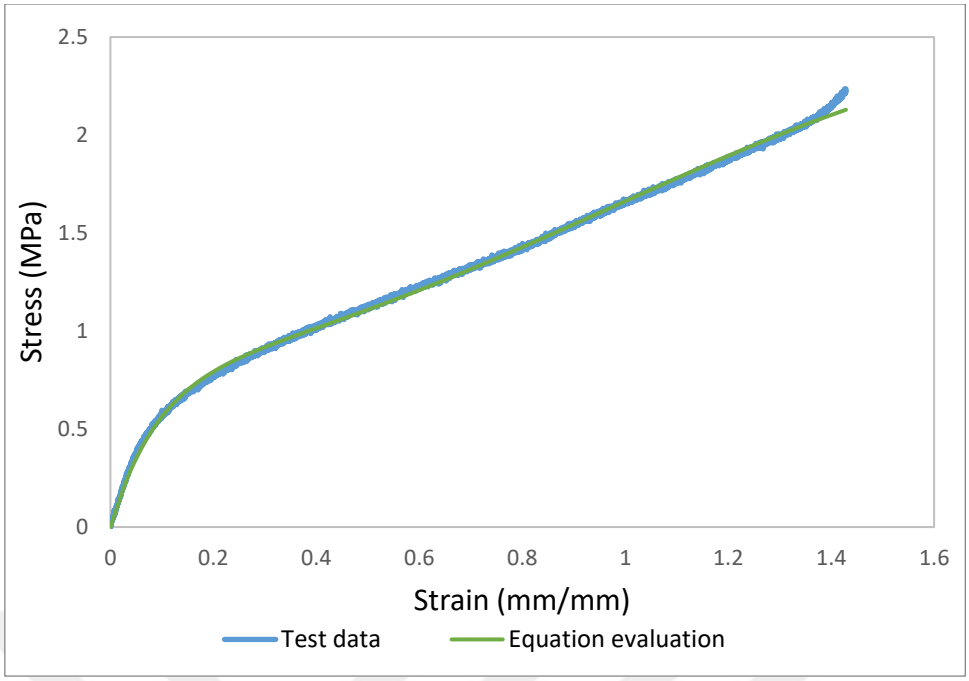

Figure 4.46 Second order Ogden uniaxial test results for H100044

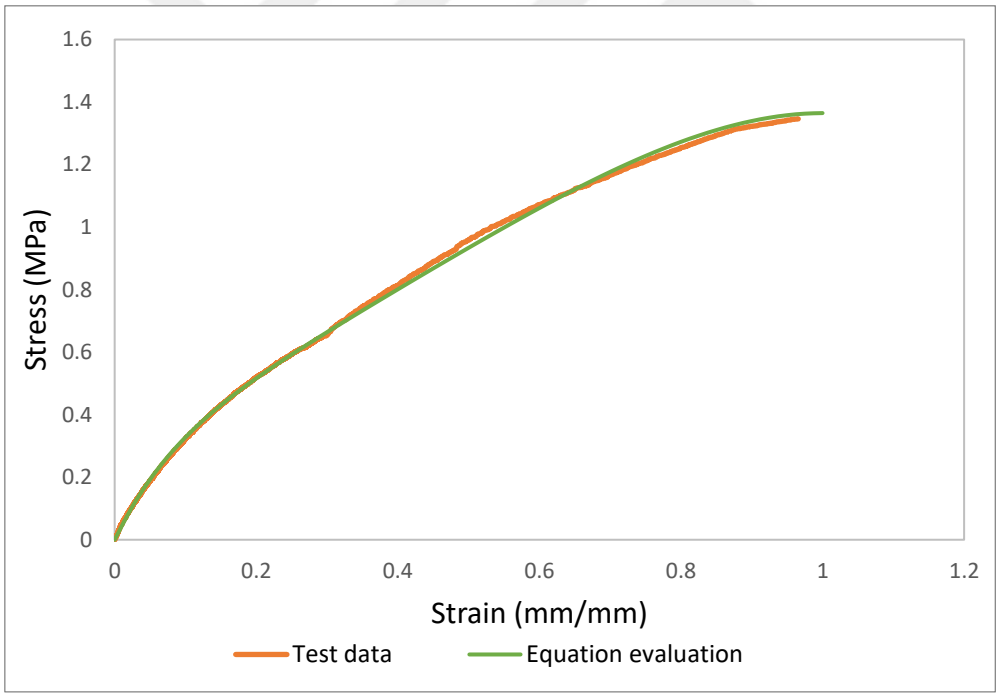

Figure 4.47 Second order Ogden uniaxial test results for H400010

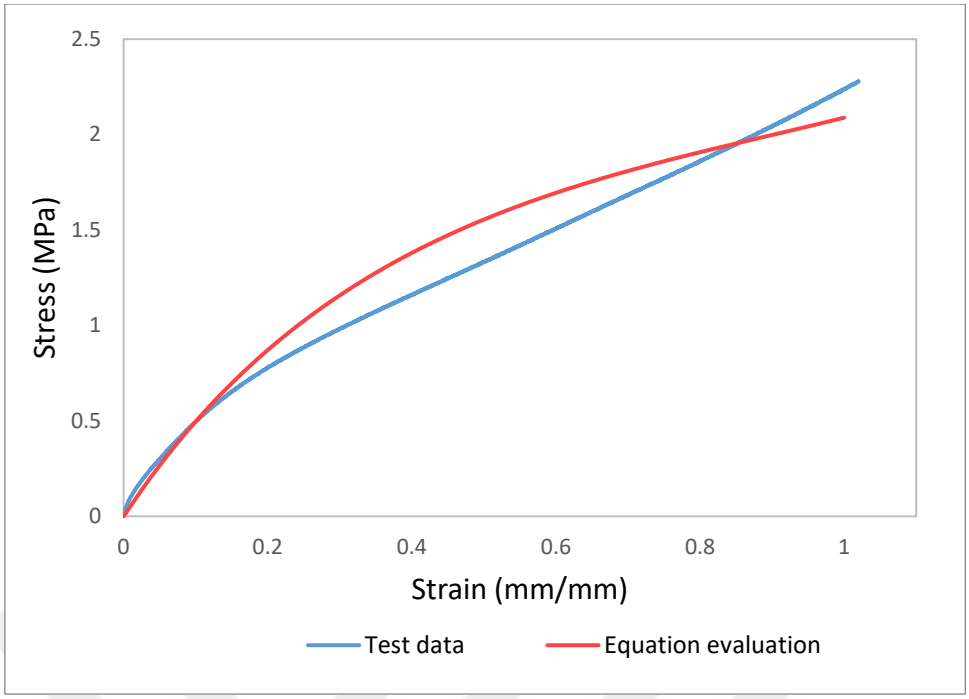

Figure 4.48 Second order Ogden planar results for H100044

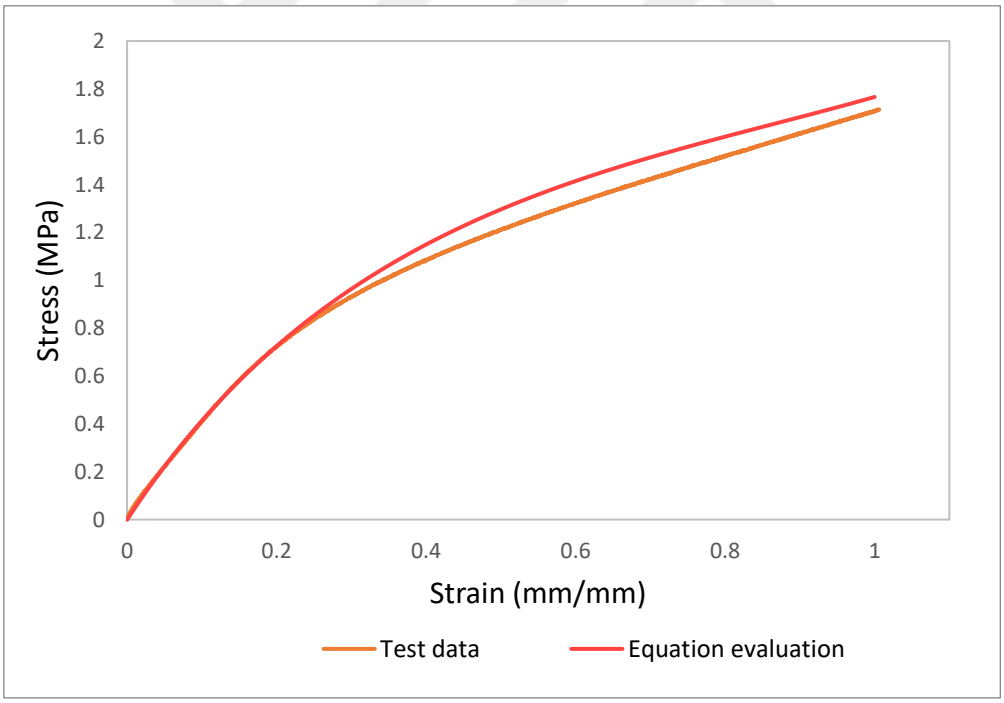

Figure 4.49 Second order planar results for H400010

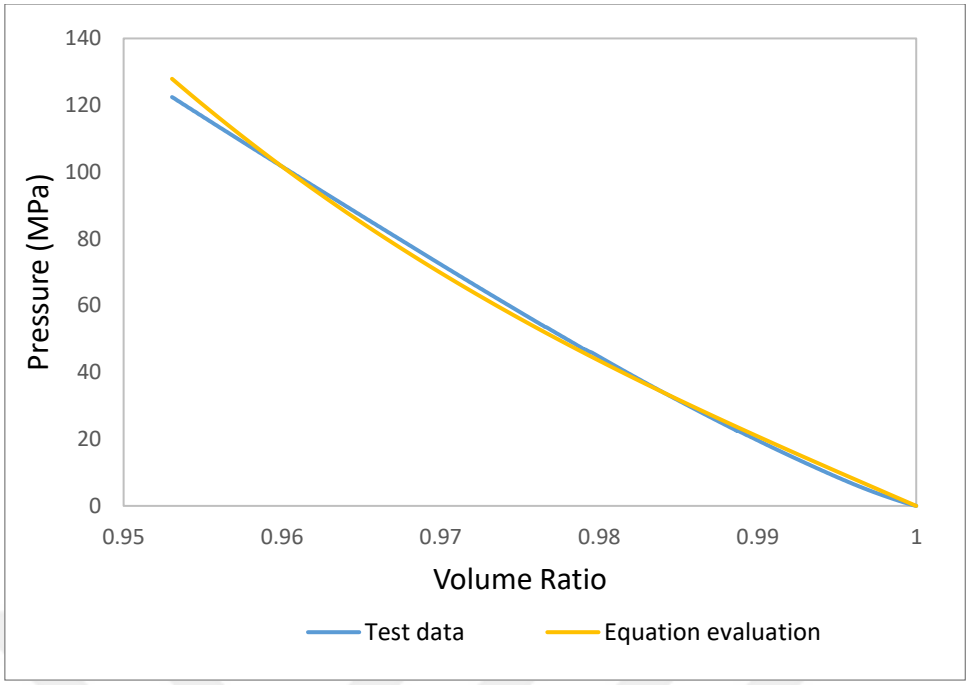

Figure 4.50 Second order Ogden volumetric test results for H100044

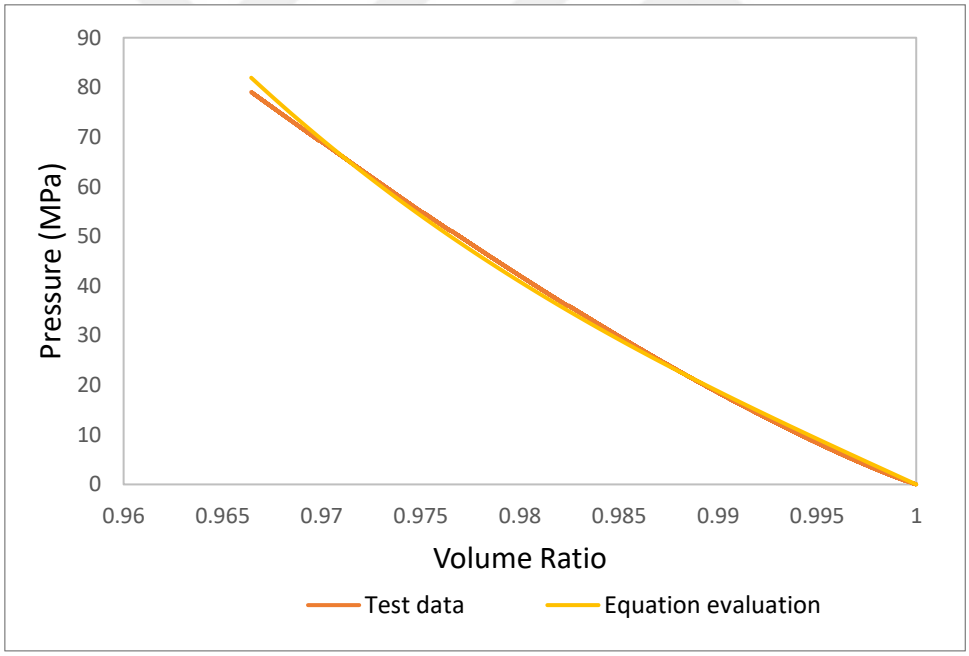

Figure 4.51 Second order Ogden volumetric result for H400010 specimen

Table 4.17 Ogden parameters for H10001

$\mu 1$	0.968723983
$\mu 2$	-2.44135445
$\mu 3$	4.54376110
$\alpha 1$	2.69903966
$\alpha 2$	4.76585312
$\alpha 3$	-9.63695049
D1	1.058086406E-03
D2	5.169864694E-06
D3	-2.765533078E-08

Table 4.18 Ogden parameters for H400010

$\mu 1$	0.907220012
$\mu 2$	-0.765854852
$\mu 3$	1.52915437
$\alpha 1$	1.90005970
$\alpha 2$	8.81171161
$\alpha 3$	-17.6132608
D1	1.171157101E-03
D2	3.339201482E-06
D3	-1.018970646E-08

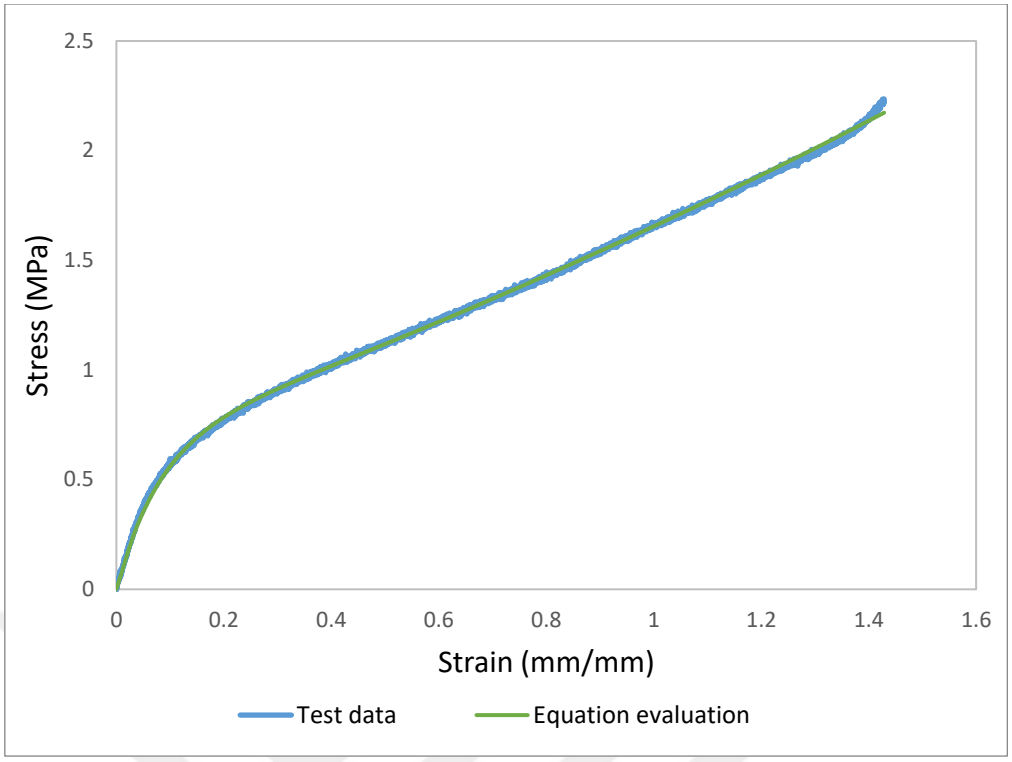

Figure 4.52 Third order Ogden uniaxial test results for H100044

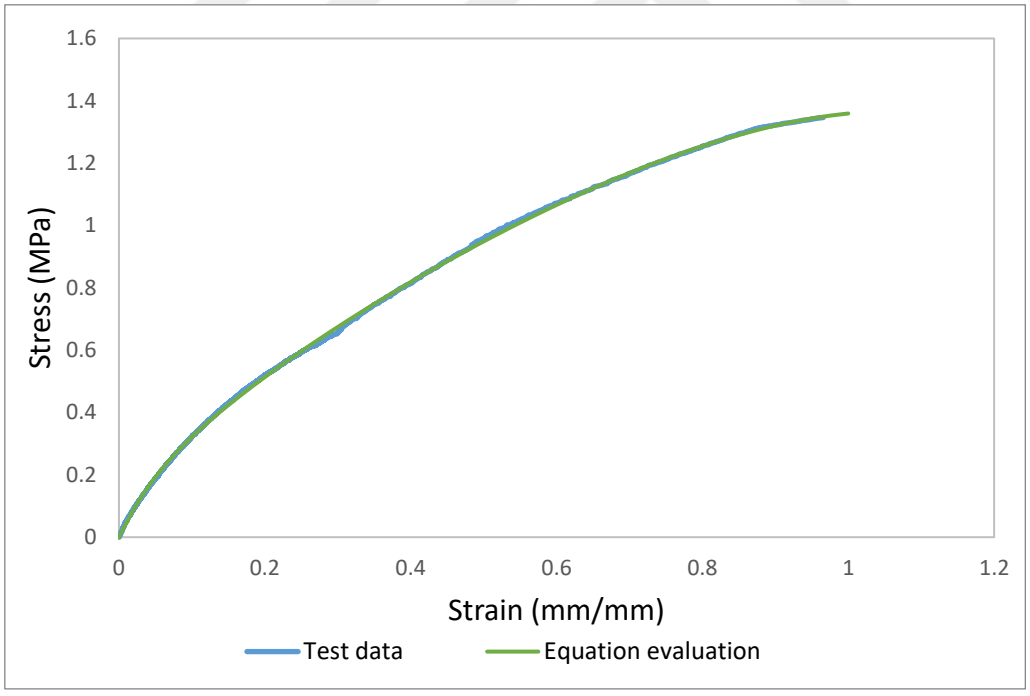

Figure 4.53 Third order Ogden uniaxial test results for H400010

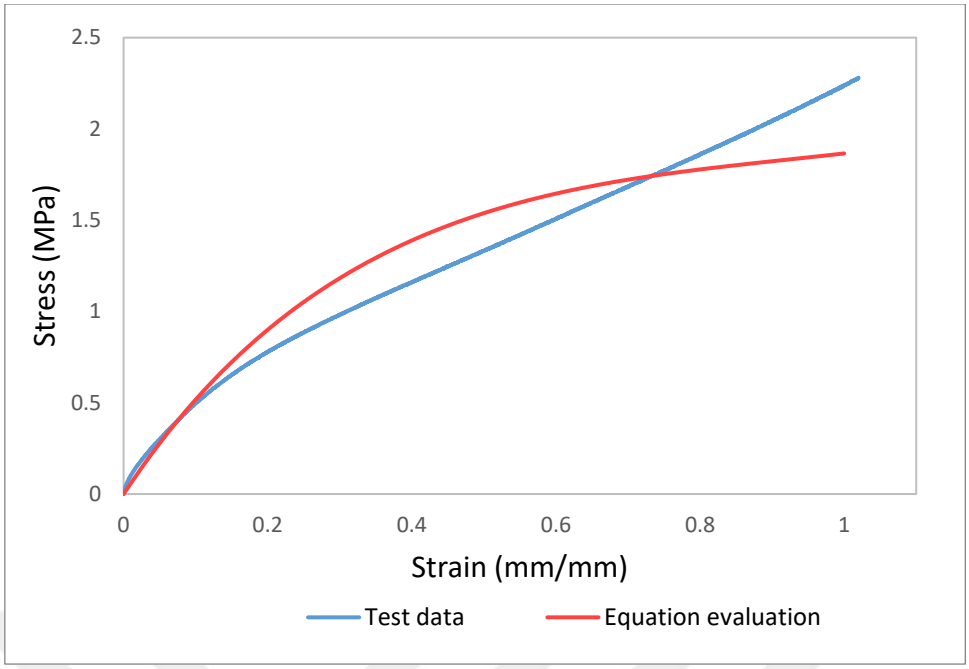

Figure 4.54 Third order planar results for H400010

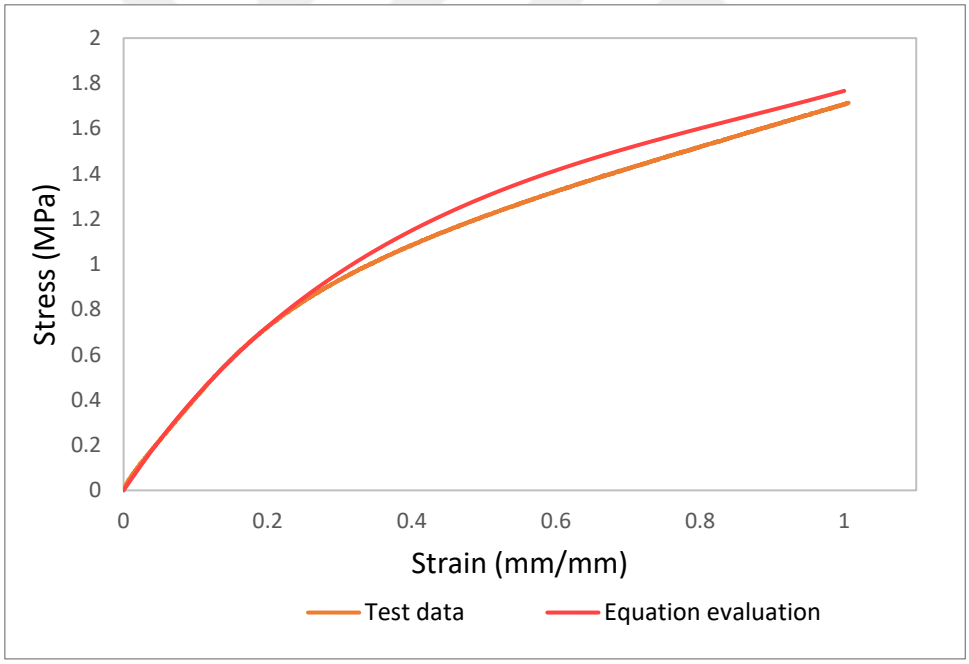

Figure 4.55 Third order planar results for H400010

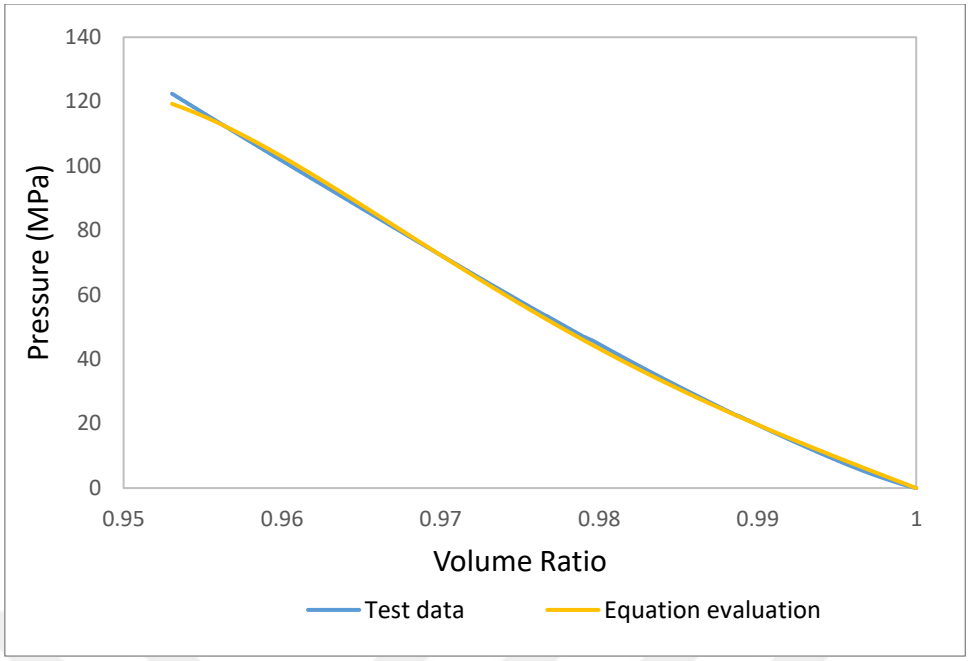

Figure 4.56 Third order Ogden volumetric result for H100044 specimen

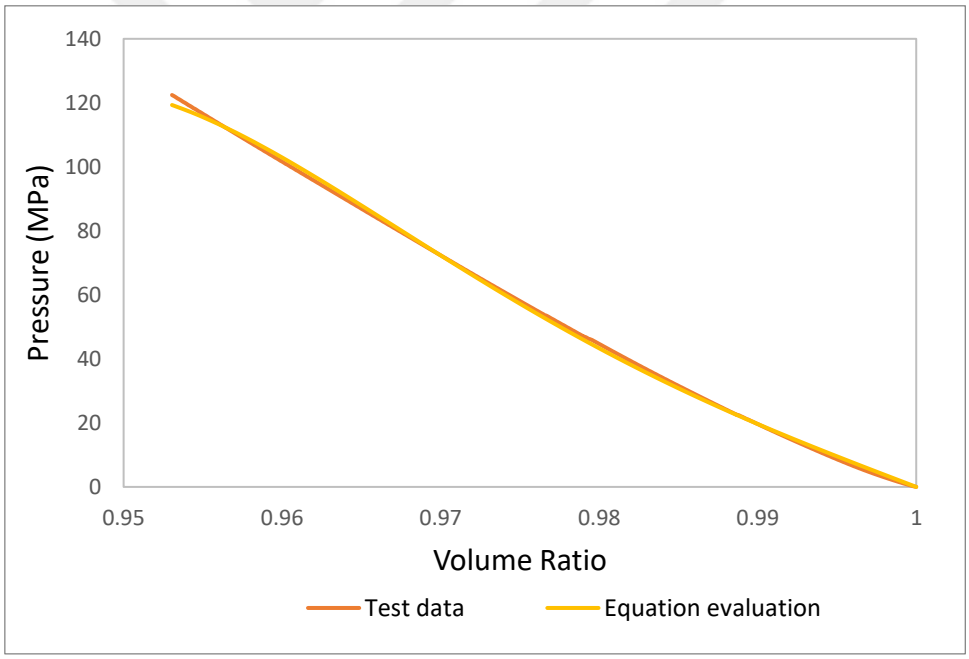

Figure 4.57 Third order Ogden volumetric result for H400010 specimen

4.2.8 Marlow Model

In the Marlow hyperelastic model [27], it's assumed that the strain energy density is independent of the second invariant. as discussed in the material definition, either by providing uniaxial, biaxial, or planar test data is required to determine the deviatoric

part, while the volumetric test data is required to define the volumetric part in equation 4.9 below. The model failed to predict samples for 400010 due to instability.

$$U = U_{dev}\left(\bar{I}_1\right) + U_{vol}\left(J_{el}\right) \tag{4.9}$$

U is the strain energy per unit volume;

U_{dev}: eviatoric part;

U_{vol}: Volumetric part;

$\bar{I}_1$: The first deviatoric strain invariant

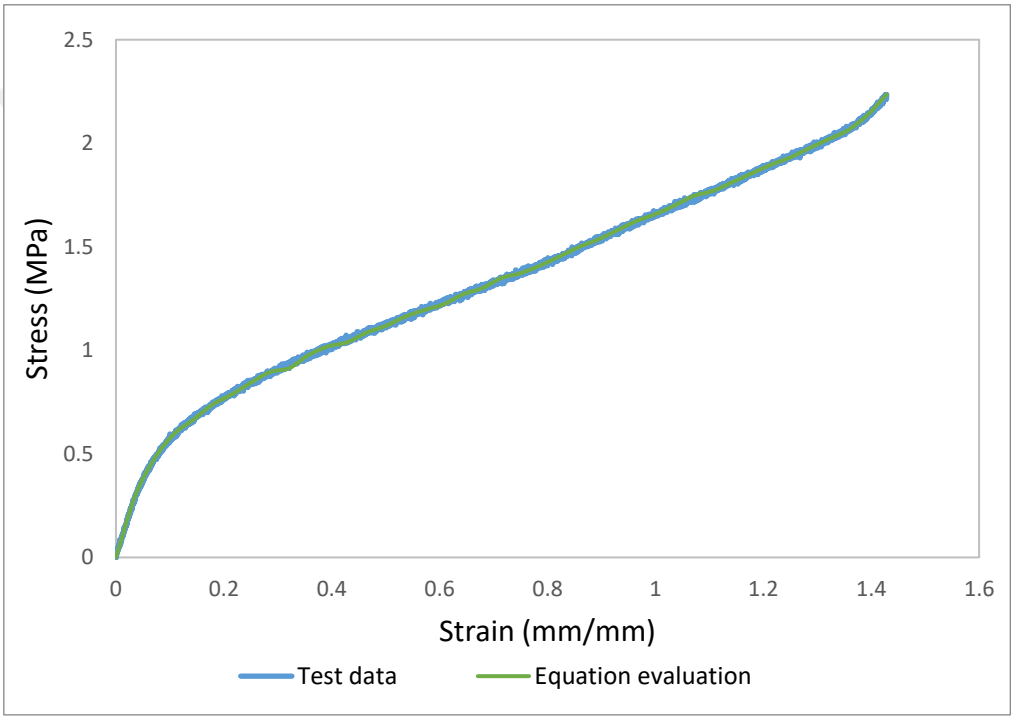

Figure 4.58 Marlow uniaxial result for H100044 specimen

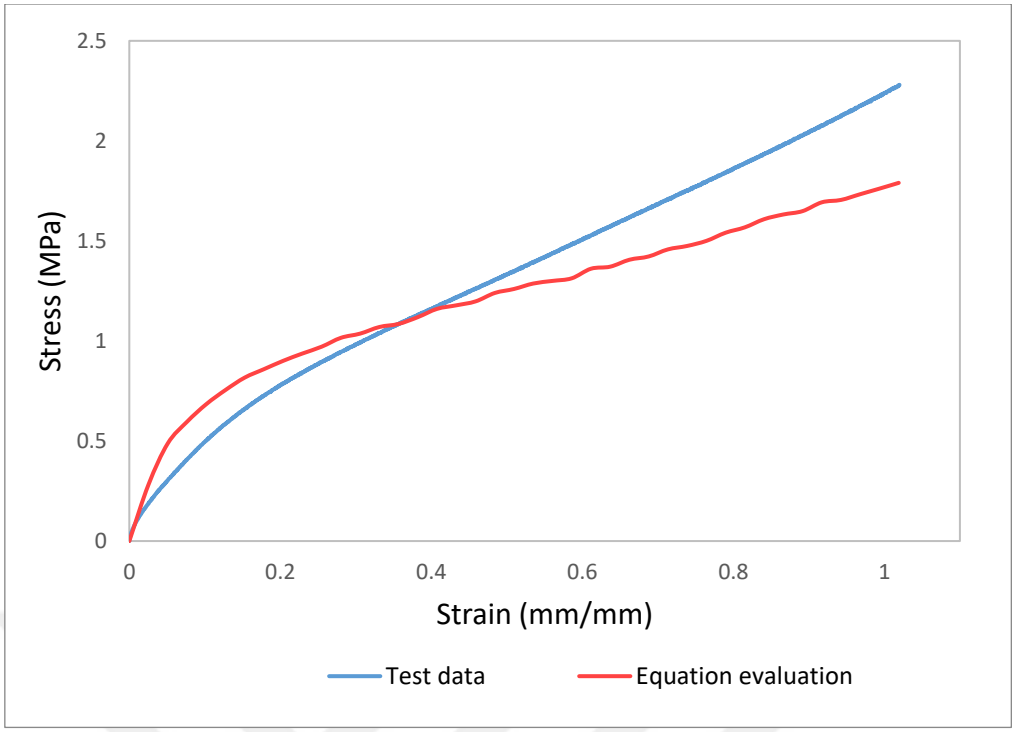

Figure 4.59 Marlow planar results for H100044

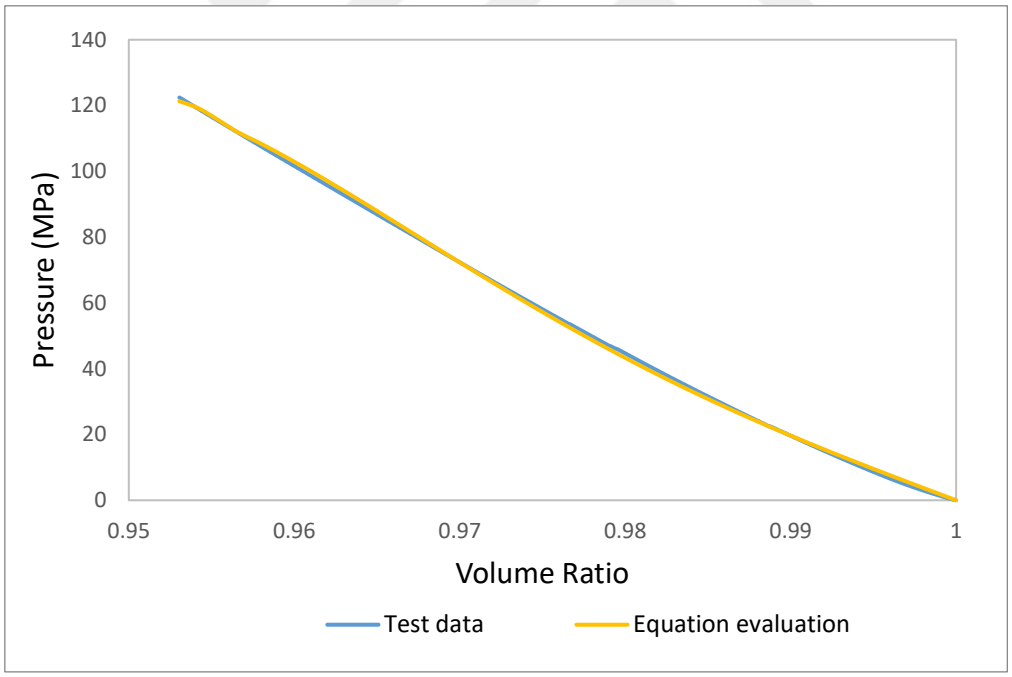

Figure 4.60 Marlow volumetric result for H100044 specimen

4.2.9 Van Der Waals Model

The strain energy potential of the Van der Walls equation is presented below.

$$U = \mu \left\{ -(\lambda_m^2 - 3)\left[\ln(1-\eta) + \eta\right] - \frac{2}{3}\alpha\left(\frac{\bar{I} - 3}{2}\right)^{\frac{3}{2}} \right\} + \frac{1}{D}\left(\frac{J_{e\ell}^2 - 1}{2} - \ln J_{e\ell}\right) \quad (4.10)$$

U is the strain energy per unit volume;

μ *is the initial shear modulus*;

λ_m *is the locking stretch*;

α *is the global interaction parameter*;

β *is an invariant mixture parameter*;

D *governs the compressibility*.

$\bar{I}_1$ *and* $\bar{I}_2$ *are the first and second deviatoric strain invariants*.

Table 4.19 Van Der Waals parameters for H100044

μ	1.71906175
λ_m	9.77477687
α	0.290955347
β	0.778379530
D	9.723752396E-04

Table 4.20 Van Der Waals parameters for H400010

μ	1.25703258
λ_m	9.70219777
α	0.242823994

Table 4.20 Van Der Waals parameters for H400010 (continued)

β	0.726934363
D	1.060178162E-03

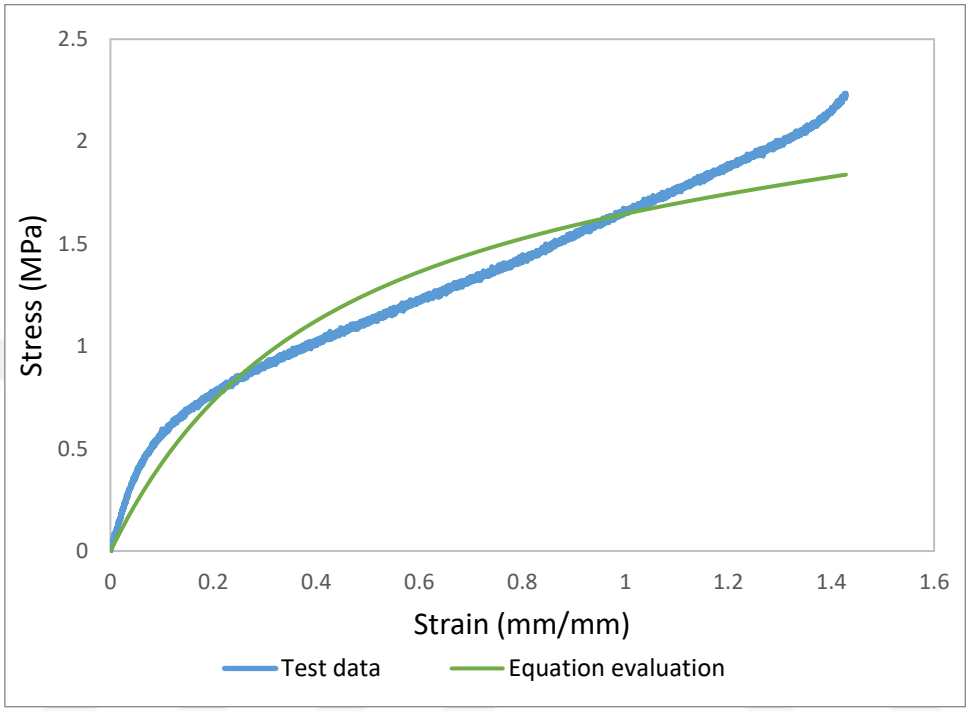

Figure 4.61 Van Der Waals uniaxial result for H100044 specimen

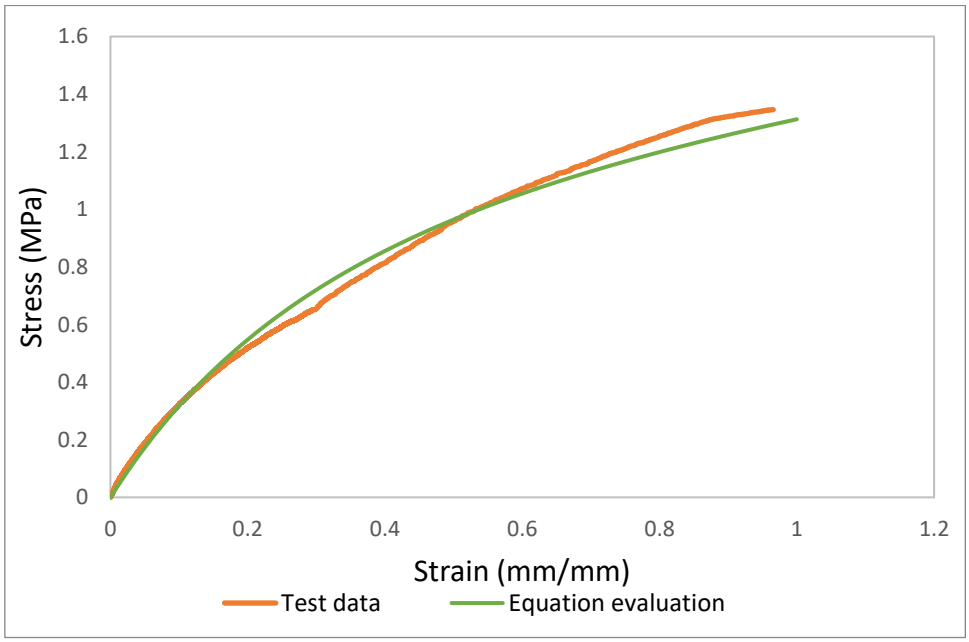

Figure 4.62 Van Der Waals uniaxial result for H400010 specimen

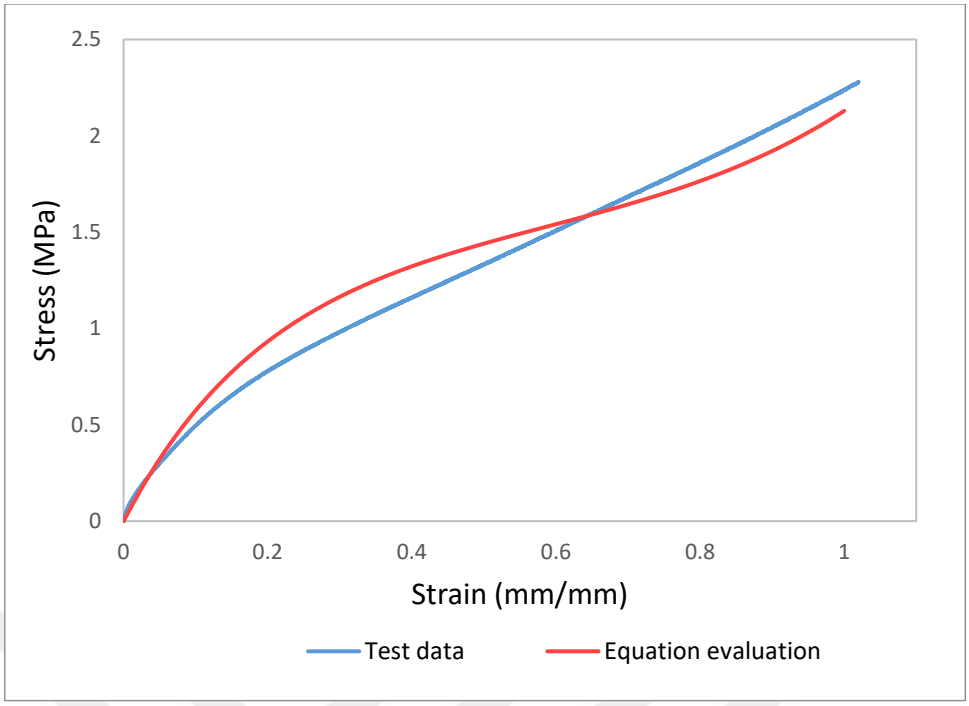

Figure 4.63 planar results for H100044

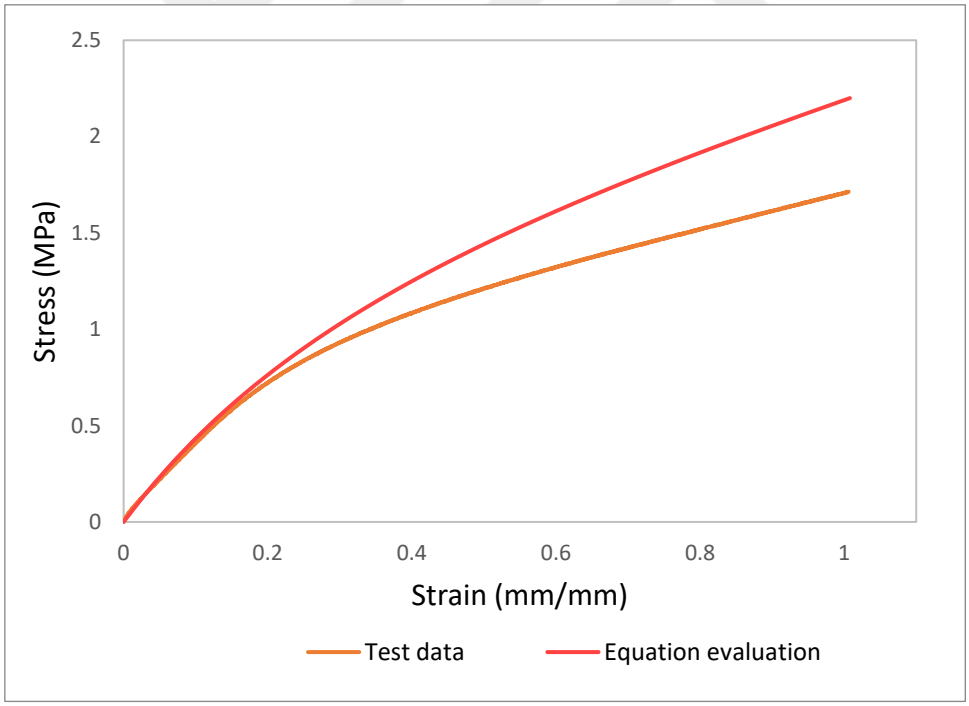

Figure 4.64 planar results for H400010

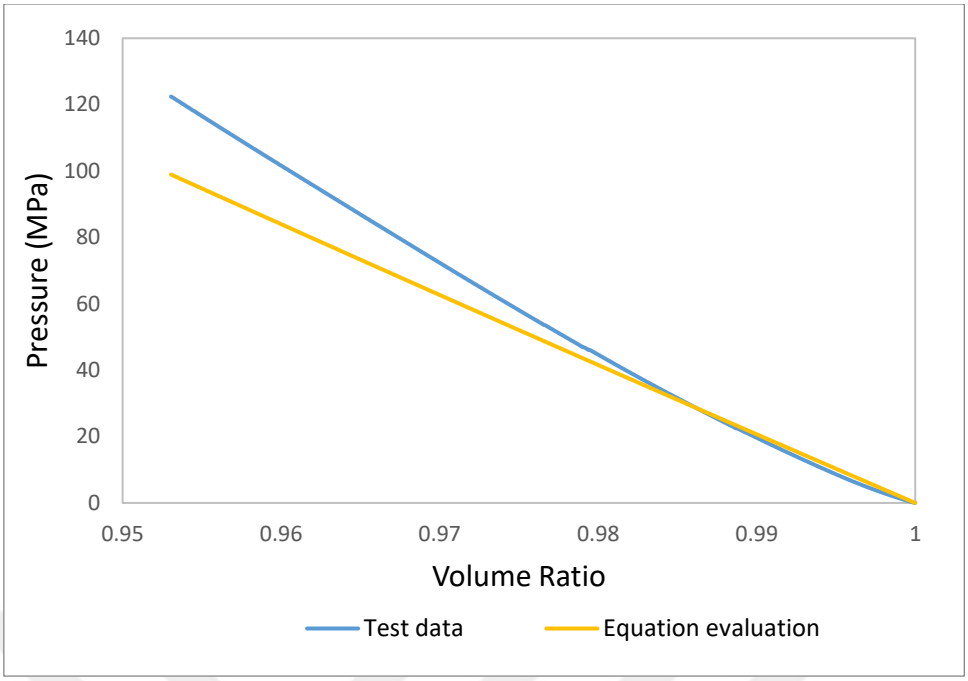

Figure 4.65 Van Der Waals volumetric result for H100044 specimen

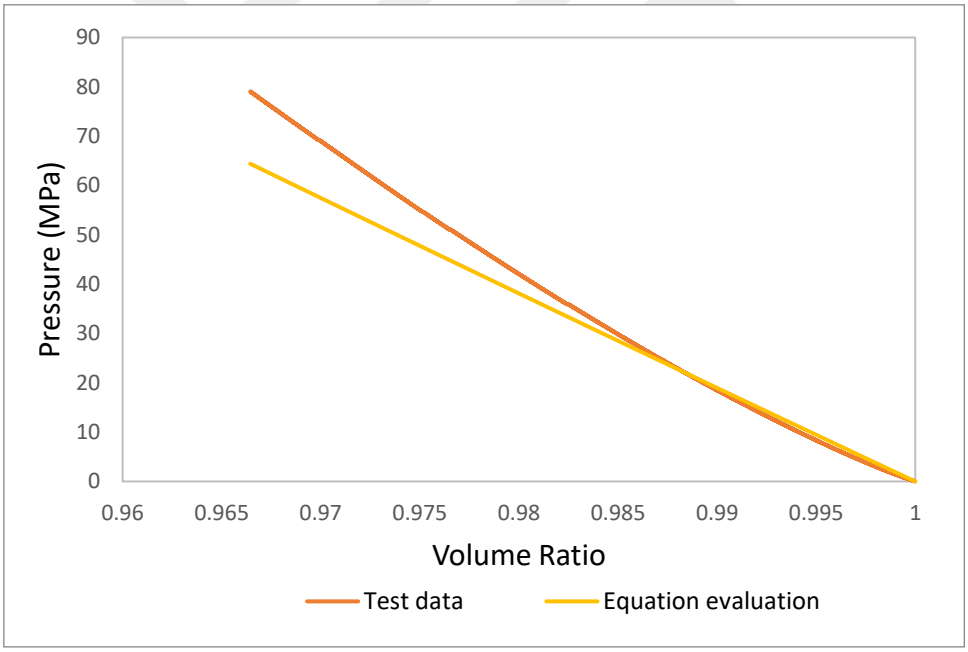

Figure 4.66 Van Der Waals volumetric result for H400010 specimen

4.3 Validation of Results

ABAQUS CAE 2017 software was also used in the modeling process [11]. Polynomial and Ogden models seem to be the best hyperelastic model that represented the behavior of the material in these two tests for both materials specimens, however,

selected models were used in modeling the double shear elastomeric specimen in finite element to make the final decision. Finite element validation aims to find the best model that can correctly predict the element behavior in various specimens and different loads values and directions. After finding the most suitable model, the other behaviors of this structural element can be predicted. There is several finite element software that can solve and model a hyperelastic material. ABAQUS software is one of the best programs that can be used in FE modeling. All of the hyperelastic models used to define strain energy function (SEF) to characterize the material behavior are pre-defined in the software as evaluated previously. To validate the evaluated models, double shear specimen was modeled in the software and double shear test were simulated.

4.4 Double Shear Test Modeling

A digital model was created to simulate the double shear test and compare the result with the physical test, all details will be described as follow. The exact dimensions for experimental specimen have been modeled and coefficients evaluated before defining it in the material property. All parts have been linked together in a single instance for better performance analysis. **Figure 4.67** represents the three-dimensional view of the specimen.

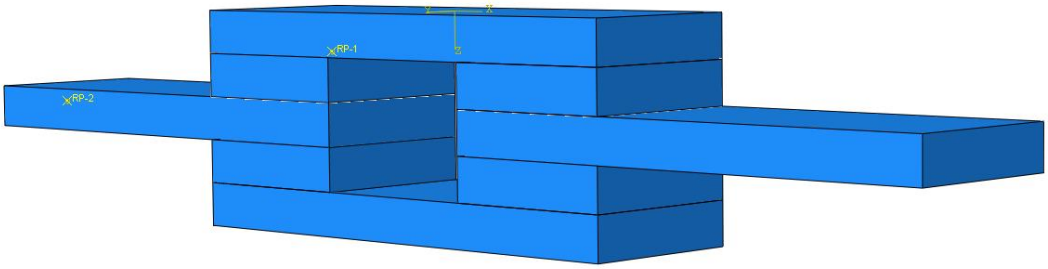

Figure 4.67 3d model for double shear specimen

4.4.1 Mesh Size

After several analyses using different mesh sizes, a 4mm mesh size was used in the simulation process. This mesh size can give more accurate results. The total number of

elements is 300 for each rubber part and the elements are distributed as shown in **Figure 4.68**.

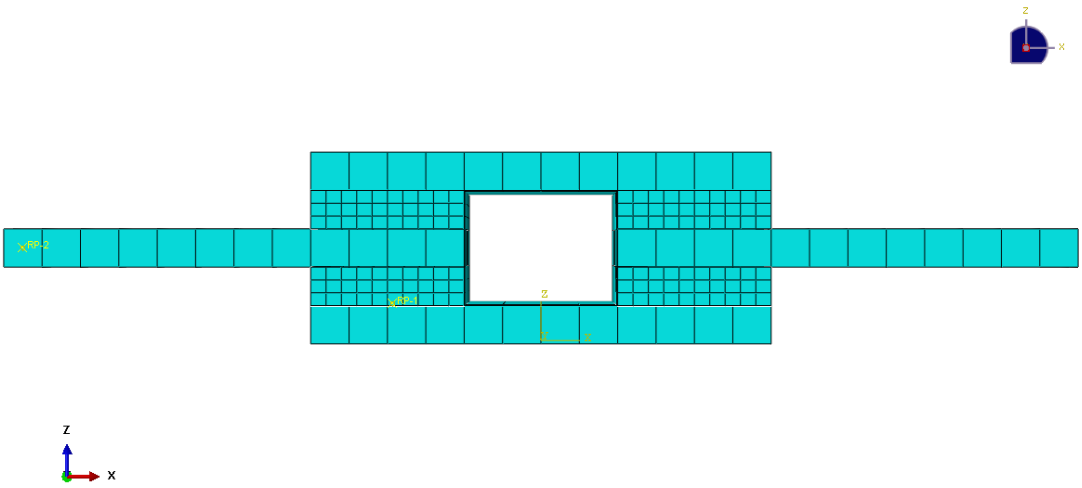

Figure 4.68 Mesh distribution for model assembly

4.4.2 Boundary Conditions

The boundary conditions were defined to simulate the physical test environment which undergoes several cycles in compression and tension in the longer direction. Constraints are added to the right side of the double shear specimen in the initial step to prevent the movement in any direction (U1 = U2 = U3 = UR1 = UR2 = UR3 = 0). Displacement of ±100 mm is applied to the left handle side of the specimen to simulate the physical experiment, while the displacement in other directions was restricted (U1 = ±100, U2 = U3 = UR1 = UR2 = UR3 = 0). Force-displacement and stress-strain results were recorded at the top surface to compare with the test results. **Figure 4.69** shows the loading steps in the FE model simulation. After finishing all the required setup, the model has been run for all seven different material models. Output history data has been observed similar to the physical test.

4.4.3 Test Simulation:

Simulation job has made for one cycle in tension and compression in three steps, displacement was applied to one side of the specimen similar to the physical test. Output request has been created to collect stress and strain data at load point. Damping factor is also added at each step to simulate cycles damping since the viscoelastic effect

is not a part of our study. The behavior and load distribution at different displacements is shown in **Figure 4.69** below.

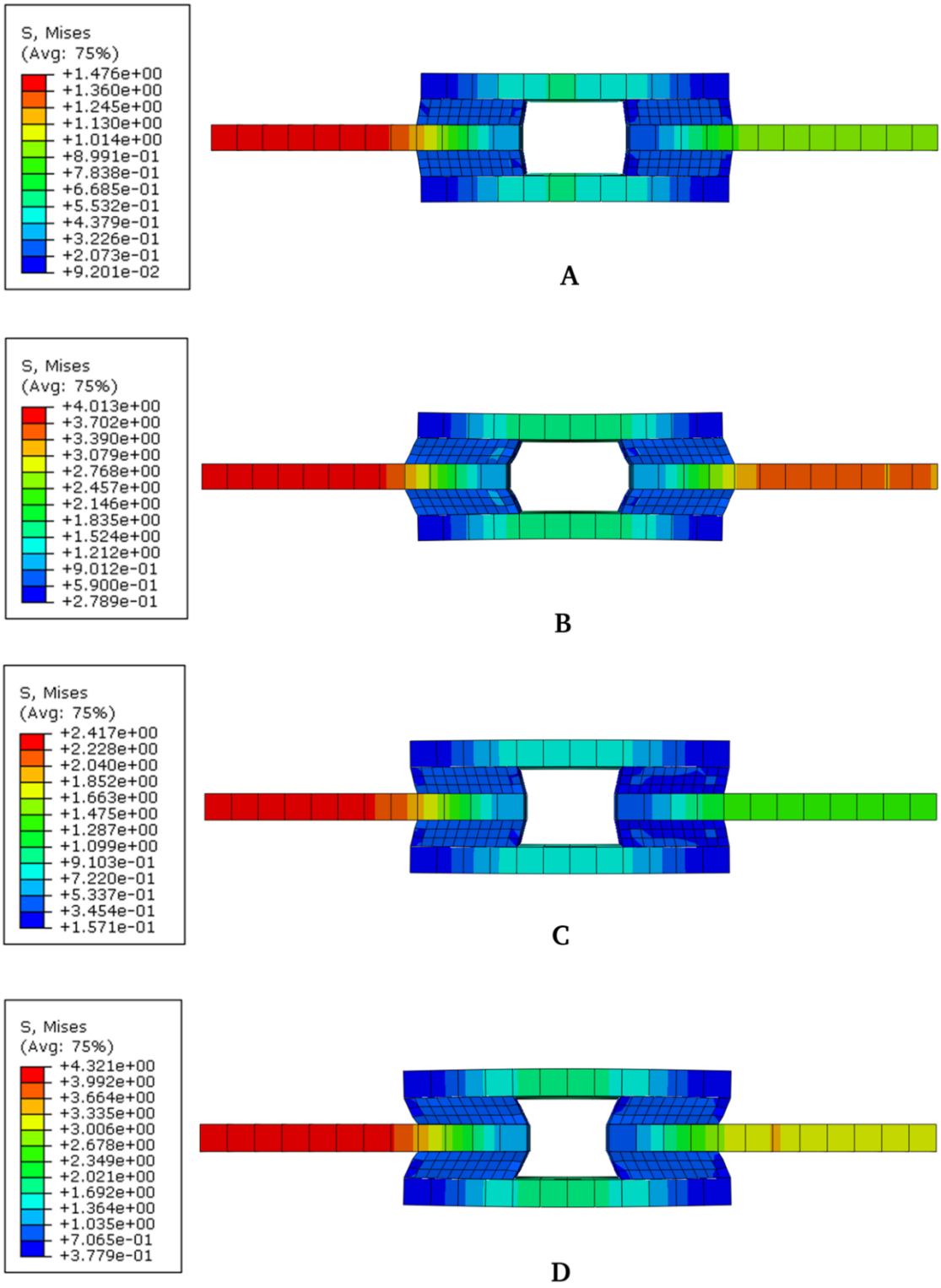

Figure 4.69 Double shear test simulation

Results for both types of hyperelastic material are shown in **Figure 4.70**, **Figure 4.71**, **Figure 4.72**, and **Figure 4.73** below.

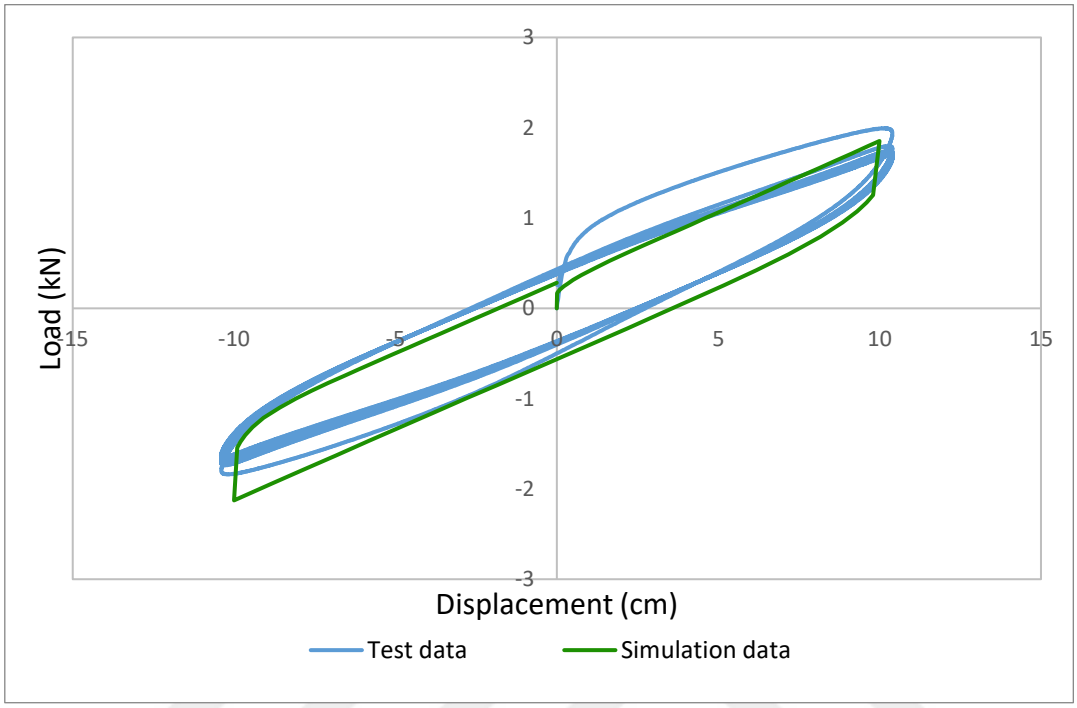

Figure 4.70 Double shear Polynomial modeling result for H100044

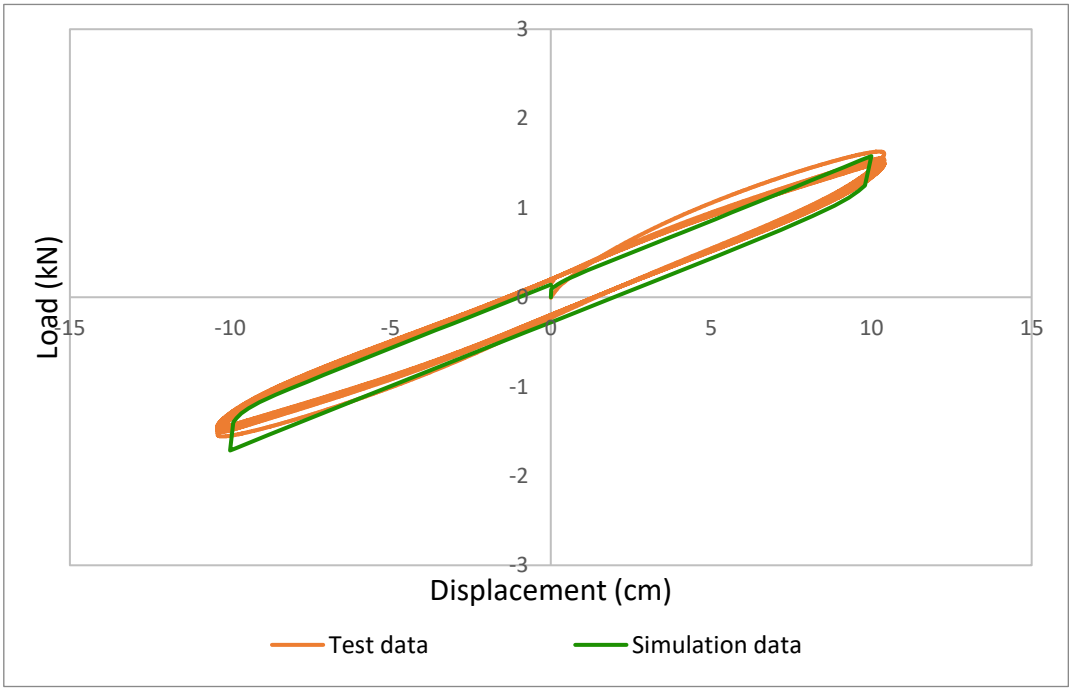

Figure 4.71 Double shear Polynomial modeling result for H400010

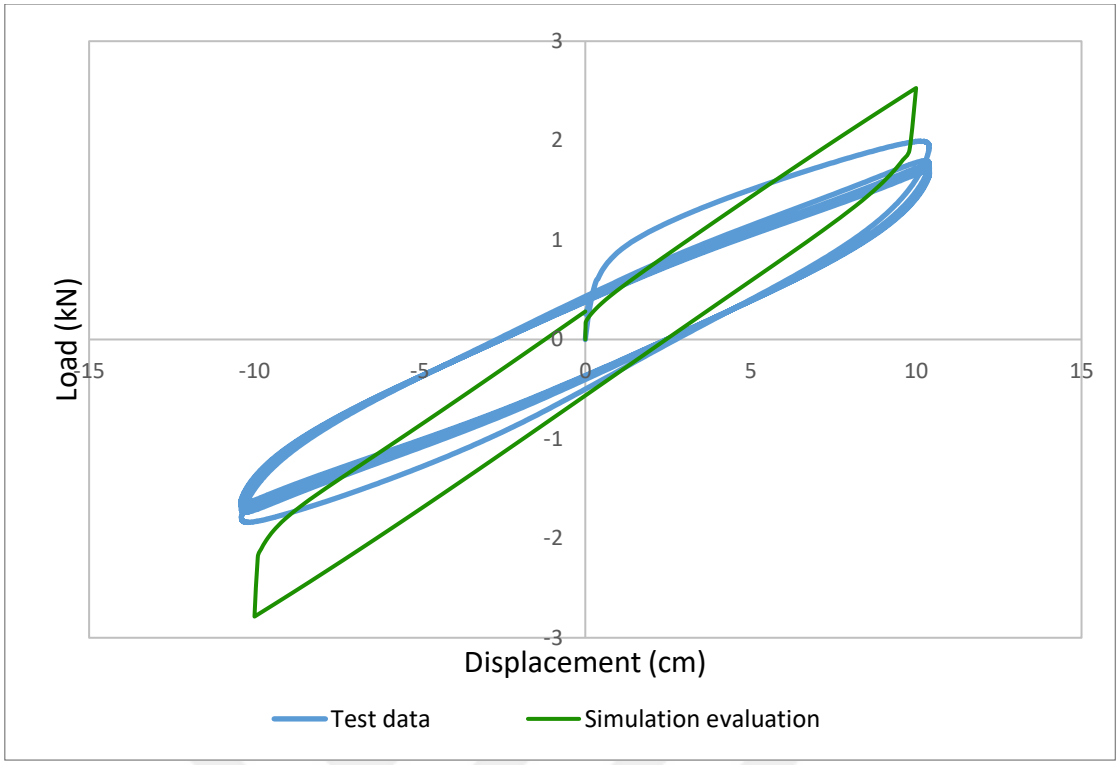

Figure 4.72 Double shear Ogden modeling result for H100044

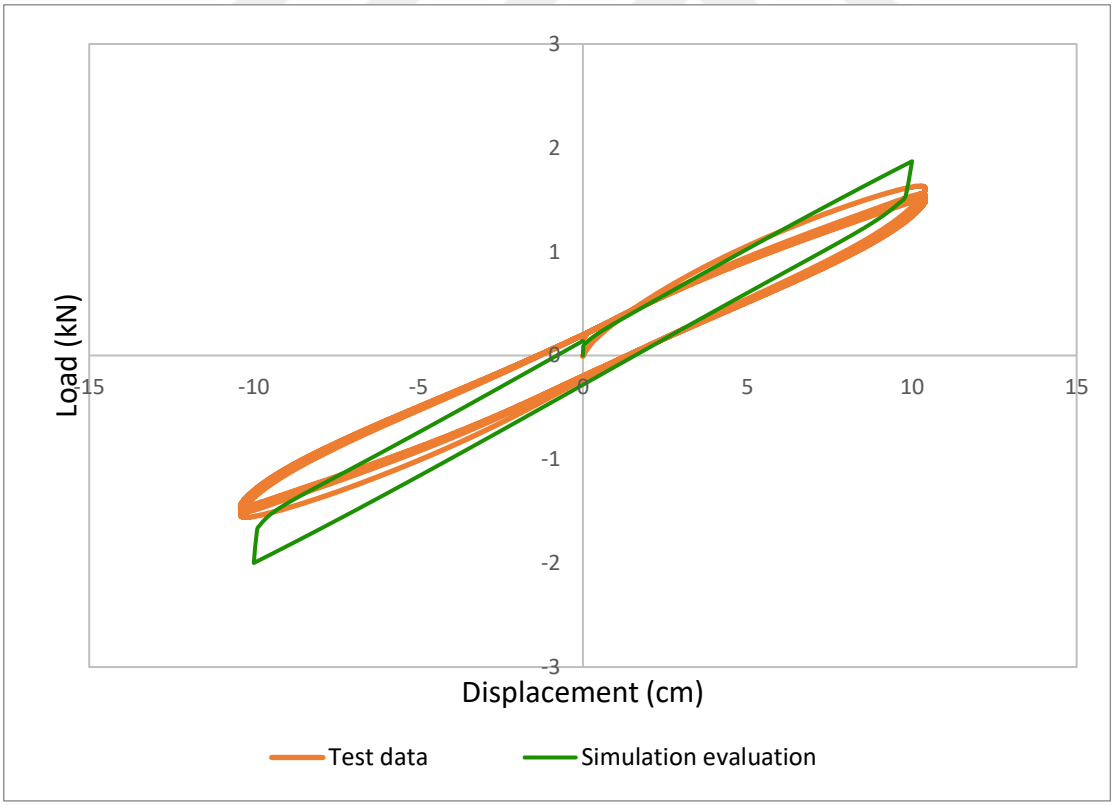

Figure 4.73 Double shear Ogden modeling result for H400010

5
DISCUSSION

Six experiments were performed (uniaxial, planar, and volumetric) for two different materials (H100044 and H400010) to define hyperelastic models, followed by two experiments on an elastomeric double shear specimen to validate hyperelastic models. Curve fitting was used to select the best model that predicted definition tests. More than one model gave acceptable results in fitting with test data and low error.

Arruda-Boyce, Van Der Walls, and Reduced couldn't give an accurate prediction for both material types and the curve couldn't be fitted in the test result. Although Marlow's model succeeded in predicting H1 material behavior, it couldn't complete analysis for H4 material and it was unstable. First-order Ogden model unsuccessfully predicted the behavior especially for the H100044 uniaxial test, while the other material and tests gave acceptable results. while Ogden's second and third orders were perfectly evaluated. Also, first order polynomial model (Moony Rivlin) couldn't give an acceptable result while the second order was able to predict it perfectly for both materials and tests.

Polynomial and Ogden models were used to simulate the double shear test in order to validate it since both had the best curve fit with the experimental result. However, Ogden model failed to give an accurate prediction while Polynomial model succeeded. Curves data were added for polynomial model and error percentage is listed in the next section.

5.1 Compression Model Error

Test simulations made with the selected hyperelastic models and. To compare these models with physical test results, error percentages were calculated using the following equation.

$$\%Error = \frac{Test\ Results - Finite\ Element\ Results}{Test\ Results} * 100 \qquad (5.1)$$

Validation results are listed in **Table 5.1**, Polynomial was selected to model the material for shear tests since it has the lowest error and had the best fit with the experimental curve. However, Ogden model shows a high error value in predicting the load value, with a maximum error of 40% for H1 and 21% for H4 material specimen. Polynomial results show acceptable convergence from the physical test for both materials, maximum error percent also was less than 19% for H1 and 16% for H4 material specimen as shown in **Table 5.1**, Curve fitting results show a very satisfactory convergence from the physical results as shown in **Figure 4.70** and **Figure 4.71**. However, the curve is not fitted in some points especially during unloading points due to viscoelastic behavior.

Table 5.1 Maximum and minimum error for the selected models

Material	Model	Min Error %	Max Error %
H100044	Polynomial	<1	19
H100044	Ogden	≃1	40
H400010	Polynomial	<1	16
H400010	Ogden	≃1	21

6
CONCLUSION

Comparisons were made between six hyperelastic models to find the best model that can fit this type of rubber. Selecting the best model passed through two main steps. The first step of selecting the best model is using curve fitting from equation evaluation, two models were selected (Ogden and Polynomial). These two models were used for the second validation step, double shear tests were used to make the final decision as this test is more complex and needs an accurate model to evaluate it. In conclusion, second-order polynomial can be selected to model these two types of rubber material for further simulation experiments. However, some observations are found from the results,

- The success of equation evaluation does not guarantee that the model can predict all material behaviors, as resulted in Ogden model.
- Difficulties have been faced in performing planar test which can increase the error in results, this error can be noticed during the comparison of equations evaluation with test result for planar test.
- To predict the cyclic load behavior, Viscoelastic or damping properties should be included in the model to give precise results. If viscosity didn't encloud in the simulation process the loading and unloading results will be identical. As mentioned in this research damping factor is used during analysis, this can explain why double shear result curves are not identical with simulation curves.
- Some models can succeed in predicting the behavior only for small displacement values, when strain value increases the error will increase. as shown in the results of Neo-Hooke and Ogden (N2) forms.
- Abaqus gives a warning for specific strain values, as resulted in Van Der Walls model in simulating shear tests.

- Volumetric coefficients or the compressibility behavior are hard to predict by FE simulations. No difference can be noticed even when D coefficients were used as zero. Hyperelastic material has very small compressibility, it can take a long time to detect the compressed value. Therefore, it is hard to be noticed in short simulation analysis.
- The first cycle in double shear tests has a different behavior than other cycles, this can be explained by the earlier discussed behavior Mullins effect. Therefore, the first cycle is neglected in the comparison steps.

Hyperelastic models would be a glimpse of the research for future work that will match cyclic load. In order to get a perfect fitting for cyclic loads in rubbers, viscoelastic properties should be added beside the hyperelastic properties. Viscoelasticity is a time-dependent property that can be found by importing load versus time data for different modes of testing.

6.1 Suggestions to Improve Fitting Accuracy

The curve fitting of the models compared to experimental data may not be as well as expected, this condition can happen for all general models. However, for simpler models, stability can be guaranteed by using simple rules,

- The Arruda-Boyce model is always stable when the initial shear modulus, μ, and the locking stretch, λm are positive values.
- The neo-Hookean model is always stable when the coefficient C_{10} is positive.
- For Yeoh model, stability can be assured if all $C_{i0} > 0$, while C_{20} should be negative to help capture the S-shape stress-strain curve. Therefore, increasing the absolute value of C_{10} and reducing the value of C_{20} can help make Yeoh model more stable.
- For models evaluation tension and compression test data are acceptable; however, stress-strain data for compressive tests are entered as negative values.
- Experimental data points should be more than unknown coefficients.

- If the number of orders N >= 3 is used, tensile strain data for at least 100% or compressive strain for 50% experimental data should be available.
- Error messages and warnings should be noticed, especially the lack of convergence notifications in fitting test data.
- More noise can appear in higher order models N, which can lead to instability in stress-strain curves. Especially for low values of strain data available (less than 100%).

REFERENCES

[1] R. Ogden, Non-Linear Elastic Deformations, 1984.

[2] S. K. a. J. R. W. e. De, Rubber technologist's handbook, vol. 1, iSmithers Rapra Publishing, 2001.

[3] M. Fragnet, "Elastomers and Rubbers used in Civil Engineering," Organic Materials for Sustainable Construction, 2013, pp. 283-312.

[4] H. Ozkaynak, Betonarme Yapılarda Sismik Çarpışma Etkisinin Azaltılması, 2018.

[5] K. EKŞİ, Investigate Elastomeric Bearings Under Fatigue Loading, Master Thesis, Yildiz Technical University, 2019.

[6] AFAD, "T.C. İÇİŞLERİ BAKANLIĞI Afet ve Acil Durum Yönetimi Başkanlığı,". [Online]. Available: https://deprem.afad.gov.tr/depremkatalogu. (visited on 4/10/2019)

[7] M. e. a. Shahzad, "Mechanical characterization and FE modelling of a hyperelastic material.," *Materials Research 18.5*, pp. 918-924, 2015.

[8] K. Miler, "Testing elastomers for finite element analysis.," *Axel Products*, 2004.

[9] D. J. J. Y. a. K. K. T. Charlton, "A review of methods to characterize rubber elastic behavior for use in finite element analysis.," *Rubber chemistry and technology*, vol. 67, no. 3, pp. 481-503, 1994.

[10] Simscale. [Online]. Available: https://www.simscale.com/docs/simulation-setup/materials/hyperelastic-materials/. (visited on 3/4/2021)

[11] Abaqus-Docs, "Hyperelastic behavior of rubberlike materials,". [Online]. Available: https://abaqus-docs.mit.edu/2017/English/SIMACAEMATRefMap/simamat-c-hyperelastic.htm. (visited on 12/1/2021)

[12] A. e. a. Barroso, "Biaxial testing of composites in uniaxial machines: manufacturing of a device, analysis of the specimen geometry and preliminary experimental results.," *15th European Conference on Composite Materials: Composites at Venice, ECCM.*, vol. 2012, 2012.

[13] L. E. e. a. Crocker, "Hyperelastic modelling of flexible adhesives," 1999.

[14] P. Medellín, "Design of a biaxial test module for uniaxial testing machine.," vol. 4.8, pp. 7911-7920, 2017.

[15] R. e. a. Tobajas, "Visco-hyperelastic model with damage for simulating cyclic thermoplastic elastomers behavior applied to an industrial component," *Polymers*, vol. 10, no. 6, p. 668, 2018.

[16] L. Mullins, "Softening of rubber by deformation.," *Rubber chemistry and technology*, vol. 41, no. 1, pp. 339-362, 1969.

[17] R. K. e. a. Luo, "Mullins effect modelling and experiment for anti-vibration systems.," *Polymer testing*, vol. 40 , pp. 304-312, 2014.

[18] "Polymerfem,". [Online]. Available: https://polymerfem.com/all-about-the-mullins-effect/. (visited on 10/4/2020)

[19] Abaqus, "Hyperelastic behavior of rubberlike materials," [Online]. Available: https://abaqus-docs.mit.edu/2017/English/SIMACAEMATRefMap/simamat-c-hyperelastic.htm. (visited on 11/15/2021)

[20] G. a. A. M. Ferron, "Design and development of a biaxial strength testing device," *Journal of testing and evaluation*, vol. 16, no. 3, pp. 253-256, 1988.

[21] M. Mooney, "A theory of large elastic deformation," *Journal of applied physics*, vol. 11, no. 9, pp. 582-592, 1940.

[22] R. S. a. D. W. S. Rivlin, "Large elastic deformations of isotropic materials. I. Fundamental concepts," *Philosophical Transactions of the Royal Society of London. Series A, Mathematical and Physical Sciences*, vol. 240, no. 822, pp. 459-490, 1948.

[23] O. H. Yeoh, "Some forms of the strain energy function for rubber," *Rubber Chemistry and technology*, vol. 66, no. 5, pp. 754-771, 1993.

[24] R. W. Ogden, "Large deformation isotropic elasticity–on the correlation of theory and experiment for incompressible rubberlike solids.," *Proceedings of the Royal Society of London. A. Mathematical and Physical Sciences*, vol. 326, no. 1567, pp. 565-584, 1972.

[25] E. M. a. M. C. B. Arruda, "A three-dimensional constitutive model for the large stretch behavior of rubber elastic materials," *Journal of the Mechanics and Physics of Solids*, vol. 41, no. 2, pp. 389-412, 1993.

[26] Abaqus, Analysis User's Manual 6.12, Volume II, 2012.

[27] R. S. Marlow, "A general first-invariant huperelastic constitutive model," *Constitutive Models for Rubber*, pp. 157-160, 2003.

[28] H. T. T. a. Y. L. Sugihardjo, "FE Model of Low Grade Rubber for Modeling Housing's Low-Cost Rubber Base Isolators.," *Civil engineering journal*, pp. 24-45, 2018.

[29] C. G. a. J. M. K. Koh, "A simple mechanical model for elastomeric bearings used in base isolation.," *International journal of mechanical sciences*, vol. 30, no. 12, pp. 933-943, 1988.

PUBLICATIONS FROM THE THESIS

Papers

1. Ahmed, F. & Alemdar, F. (2021). Validation of an elastomeric bearing characterized with finite element hyperelastic models. European Journal of Science and Technology, (27), 471-478